ASSESSMENT OF THE VARIABILITY OF SPATIAL INTERPOLATION METHODS USING ELEVATION AND DRILL HOLE DATA OVER THE MAGMONT MINE AREA, SOUTH-EAST MISSOURI

A Thesis

presented to

the Faculty of the Graduate School

at the University of Missouri-Columbia

In Partial Fulfillment

of the Requirements for the Degree

Master of Arts

---

by

Madi Linglingue

Dr. Michael A. Urban, Thesis Supervisor

December 2017

Approval Page

The undersigned, appointed by the dean of the Graduate School, have examined the thesis entitled

ASSESSMENT OF THE VARIABILITY OF SPATIAL INTERPOLATION METHODS USING ELEVATION AND DRILL HOLE DATA OVER THE MAGMONT MINE AREA, SOUTH-EAST MISSOURI

presented by Madi Linglingue,

a candidate for the degree of Master of Arts

and hereby certify that, in their opinion, it is worthy of acceptance.

Professor Michael A. Urban

Professor Blodgett Clayton

Professor Hong He

D**edication**

To my family

Acknowledgements

I would like to take this opportunity to say thank you to all who helped me take this step: the administration, the teachers, my class mates and friends from who I gained experience both scholarly and about the American culture. My special thanks go to Blodgett Clayton who adopted me earlier in the program as “a member of his family”, to Dr. Mike Urban my adviser who has always been there to subtly guide me to take control of my thesis, to Timothy Healcoath who mentored me on GIS and facilitated contacts and infrastructure for my work and to Dr. Hong He who accepted to be part of my committee.

Thank you to my family which, despite distance was always there to give me the courage to continue.

I also thank the Missouri Geological Service in Rolla, especially Cheryl Seeger for providing me with the Magmont mine area data set.

My final thanks go to the government of the United States of America through the Fulbright program which gave me the opportunity to fulfill this program.

Table of Contents

List of Tables

List of Figures

Abstract

Spatial interpolation methods are widely used in fields of geoscience such as mineral exploration. Interpolation methods translate the distribution of discrete data into continuous field over a given study area. Many methods exist and operate differently. Choosing judiciously the best interpolation method calls for an understanding of the algorithm, the intent or goal of the investigation and the knowledge of the study area. In the field of mineral exploration, accurate assessment is important because both overestimation and underestimation at spatially defined variables result in varied consequences.

Assessment of methods' variability can be used as an additional criterion to help make an informed choice. Here, eight interpolation methods were tested on two spatial data sets consisting of topographic surface elevations and subsurface elevations of the top and the bottom of lead orebody at the Magmont mine area, in South-east Missouri. Variability between the interpolation methods was assessed based on statistical paired t-test of each method against a reference value, geometric analysis the map algebra tool in Arcmap 10.4.1 and comparison of their algorithms. Two of the methods returned values not significantly different from the reference value while the others were less robust. In testing model variability a second time on a reduced sample size, results suggest that interpolation methods are sensitive to sample size. Similarly, building the orebody top and bottom surfaces from information on the depths across the mineralized intersection showed dissemblance among methods.

Key words: spatial interpolation, GIS, Magmont mine area, variability, math algebra, paired t-test

Chapter 1. INTRODUCTION

1. Background

Mineral exploration is a process aiming ultimately at the discovery of economically viable ore resources in which only a few companies succeed (Marjoribanks, 2010). It involves strategic decisions and actions, huge financial investments, socio-economic and environmental issues, as well as scientific knowledge. Mining companies rely on primary data collected on the field and/or secondary data acquired from remotely sensed information to identify and develop potential targets. Throughout the exploration process, investigations are progressively narrowed to circumscribed targets: activities are scaled down from regional to local scale and from surface to subsurface level. Sample design is often a grid oriented perpendicular to the trend of identified anomalies. Samples are taken at discrete locations as points (e.g., soil samples) or as continuous intervals (e.g., drill holes, trench). Those samples are then sent to the laboratory for assaying; the returned results are interpreted to understand the 2-D and 3-D distributions of the mineralization and to serve for the estimation of ore resources.

Accuracy of resource estimate is of capital importance in mineral exploration, as confirmed by Shahbeik et al (2013): “estimation of mineral resources and reserves with low values of error is essential in mineral exploration”. Inaccurate estimation can lead to various consequences ranging from the loss of investment to legal pursuits and in extreme circumstances, to death. For example, the Bre-X scandal in 1997 following a willingly overestimate of gold resources to 6 million ounces in Indonesia resulted in a 200-million-dollar stock market bubble, the discredit of the mining

company, judiciary pursuits after the board and most importantly, the suicide of the chief geologist on a monitoring trip to the field (Groia et al, 2008).

Mineral exploration is an imperfect science because there are many uncertainties involved in the process; any way to decrease the overall uncertainty in the exploratory process can lead to greater success rates, compliance with ethical rules and standards and ultimately greater profitability. Various factors both at the field and laboratory levels can account for these uncertainties (Marat, 2011). In the field, grid design, rock type, geomorphology, sample size, sample recovery and sampling method are examples of factors that can influence the estimated pattern of mineralization. Variation in any of these parameters will result in a significant difference on estimates. Similarly, at the laboratory level, sampling technique, analytical methods, sample preparation quality or protocol are among other factors influencing assaying results.

Another source of uncertainty, which is the interest of the current thesis, is about the spatial interpolation method used to translate discrete data into continuous distribution. Many interpolation methods are available for geospatial applications like mineral exploration, each one having its specific strengths and weaknesses. Li and Heap (2014) and Zimmerman et al. (1999) pointed out that the specificity of the different methods make them unique to a point that it is difficult to determine which one is the best.

Li and Heap (2014) proposed a decision tree to help select the appropriate method based on their features, the data available, the nature of the data and the expected estimations. They also remarked that the methods are usually “data specific or data driven and their differences are inconsistent.” Moreover, many factors related to the data

themselves affect the performance of the interpolation methods, including: sampling design, sample spatial distribution, data quality, correlation between primary and secondary variables, and interaction among all these factors. In other words, the interpolation functions of the different methods differ from one another by their algorithm, the type of data, the source of the data, the uncertainties involved in their collection and treatment as well as their spatial distribution. For example, the number of neighbors considered in the estimation of a location's attribute influences the outcome of the estimation (Campbell and Wynne 2011, Isaaks and Srivastava 1989, Goovaerts 1997). Along the same lines, Trauth (2012), Isaaks and Srivastava (1989) and Goovaerts (1997) argue the nearness and sample distribution around the estimated location influence the ultimate assignment of weight. Nearest neighbors have the greatest weights and contribute most to the estimation. Anderson et al. (2015) introduce other factors influencing the development such as the model goal, the time allotted to its development, or the level of certainty required. More generally, Isaaks and Srivastava (1989) mention that variability in data distribution affects the accuracy of prediction, independently of the interpolation method used.

2. Research question

Given the diversity and variability associated with interpolation methods and the uncertainties involved in sampling and assaying, we decided to answer the question: how does one judiciously choose an interpolation method to assess a given mineralization? In other words, does it make a significant difference to use a given interpolation method instead of another? There is a debate on the appropriateness of the interpolation method

among the scientists' community as reminded by Zimmerman et al. (1999). The answer to this question is given through the investigation of three specific objectives.

3. Objectives

The first specific objective is based on the description of the mathematical functions behind each interpolation method to understand how they work. The purpose of the method, its assumptions, weaknesses and strengths are explored. These descriptions allow us to understand the intrinsic variabilities among the methods.

The second specific objective is to test the sensitivity of each method to sample density and sample size. Geographic analysis can be utilized to reduce the overall level of systematic uncertainty by guiding the sampling process as well as interpolating the data once they have been collected and sent to the laboratory for chemical analysis. The significance of any assay result must be contextualized within the pattern of the geographic location, the representability of the material sampled within the population and the total number of samples collected on the media, among others. Sample size and sample density are important in analyzing the distribution pattern because they directly determine the relationship with the neighboring samples and therefore the correlation with them. Testing the selected methods with a different sample size and sample density offered an additional way to appreciate the way they differ.

The third specific objective is to compute the magnitude of the differences between the different methods. These differences are determined both qualitatively and quantitatively by means of statistical tools: a paired t-test was used to measure the likelihood of the methods to return similar estimates at given locations while the by

"Math Algebra" tool in Arcmap was used to assess the magnitude of the differences among those estimates. In each case, one method was chosen as a reference to which the others were compared.

The initial selection of interpolation methods to be used this thesis was based on a review by Li and Heap (2014). This review classified and quantified the features of the 25 most commonly used interpolation methods in geoscience to show the similarities and relationship among them. Among the features were the integration of the method into a GIS platform and the number of variable used by the function. Our selection focused on the integration of the method into an ArcGis platform (table1 and table2 below) and the category of univariate functions because our dataset had only one variable.

Table 1: availability of interpolation methods in common software packages (source: Li and Heap, 2014)

Method/package	ArcGIS[a]	GS+	R											S-PLUS[b]	SURFER
			stats	akima	deldir	fields	geoR	geoRglm	GRASS	Gstat	spatial	Sgeostat	RandomFields	Tripack		
NN	Yes				Yes					Yes				Yes		Yes
TIN	Yes				Yes									Yes	Yes	Yes
NaN	Yes															Yes
Cl		Yes	Yes												Yes	
TSA	Yes										Yes				Yes	
IDW	Yes	Yes								Yes						Yes
LM	Yes		Yes							Yes					Yes	Yes
TPS	Yes		Yes	Yes		Yes				Yes					Yes	
SK	Yes					Yes?	Yes			Yes		Yes?	Yes			
OK	Yes	Yes					Yes		Yes	Yes			Yes		Yes	Yes
UK	Yes					Yes	Yes			Yes	Yes				Yes	Yes
SCK	Yes									Yes						
OCK	Yes	Yes								Yes						
Universal CK	Yes									Yes						
SCCK										Yes						
KED							Yes			Yes						
StOK/StSK		Yes								Yes						
IK	Yes									Yes						
MBK							Yes	Yes								

[a] Including ArcGIS Geostatistical Analyst, an extension to ArcGIS.

Table 2: classification of the selected methods by geostatistical and non-geostatistical category and by number of variables (source: Li and Heap, 2014)

Non-geostatistical	Geostatistical (kriging)		Combined methods
	Univariate	Multivariate	
Nearest neighbours (NN)	Simple kriging (SK)	Universal kriging (UK)	Classification combined with other interpolation methods
Triangular irregular network related interpolations (TIN)	Ordinary kriging (OK)	SK with varying local means (SKlm)	Trend surface analysis combined with kriging
Natural neighbours (NaN)	Factorial kriging (FK)	Kriging with an external drift (KED)	Lapse rate combined with kriging
Inverse distance weighting (IDW)	Dual kriging (DuK)	Simple cokriging (SCK)	Linear mixed model (LMM)
Regression models (LM)	Indicator kriging (IK)	Ordinary cokriging (OCK)	Regression trees combined with kriging
Trend surface analysis (TSA)	Disjunctive kriging (DK)	Standardised OCK (SOCK)	Residual maximum likelihood-empirical best linear unbiased predictor (REML-EBLUP)
Splines and local trend surfaces (LTS)	Model-based kriging (MBK)	Principal component kriging (PCK)	Regression kriging (RK)
Thin plate splines (TPS)		Colocated cokriging (CCK)	Gradient plus inverse distance squared (GIDS)
Classification (Cl)		Kriging within strata (KWS)	
Regression tree (RT)		Multivariate factorial kriging (MFK)	
		IK with an external drift (IKED)	
		Indicator cokriging (ICK)	
		Probability kriging (PK)	

Based on the tables, eight methods were selected for the comparisons: nearest neighbor, natural neighbor, inverse distance weighting, thin plate spline, regular spline, triangulated irregular network, simple kriging and ordinary kriging.

4. Data

Two datasets were used for the comparison of the performance of the different methods. The first contains surface elevation values extracted from LiDAR scenes and the second dataset consists of lead assays from exploration drill holes. LiDAR data are part of a state-wide survey aiming at providing fine resolution spatial information for public use. They were conjointly hosted by the Missouri Spatial Data and Information Service (MSDIS) at the University of Missouri; Department of Geography and Washington University in Saint Louis Missouri. The study area extends over

approximately 30Km^2 of the old Magmont Lead Mine district near Rolla in South east Missouri (Figure 1). Survey data were acquired at <1ft spatial resolution and stored in LAS format (Log ASCII Standard). Five tiles, containing approximately 64-million-point data were used to cover the entire study area: 2412.las, 2413.las, 2515.las, 2516.las and 37091f2_SE.las. To reduce computation, a subset of 2 million points was randomly generated using the "resampling tool" which is an added-in of Arcmap.

The second dataset consists of assay data for lead collected during exploration drilling over the western part of the Magmont Mine area. They were pulled from the database of the Missouri Geological Service in Rolla and provided by Cheryl Seeger, Chief of the Geological Investigations Unit, on 08/11/2016. Those assay data were used within Arcmap to the build 3-D models of the top and bottom surfaces of the ore body. In addition to the lead assay, USGS also provided a geological description file of the corresponding assays and a scanned map of the Magmont Mine area showing the locations of the drill holes (Figure 1).

Understanding the variability inherent in the different methods can provide critical guidance for those involved in mineral exploration. Immediate benefits will be the minimization of the estimation errors of subsurface mineral resources, the preservation of ethical values and better decision making support.

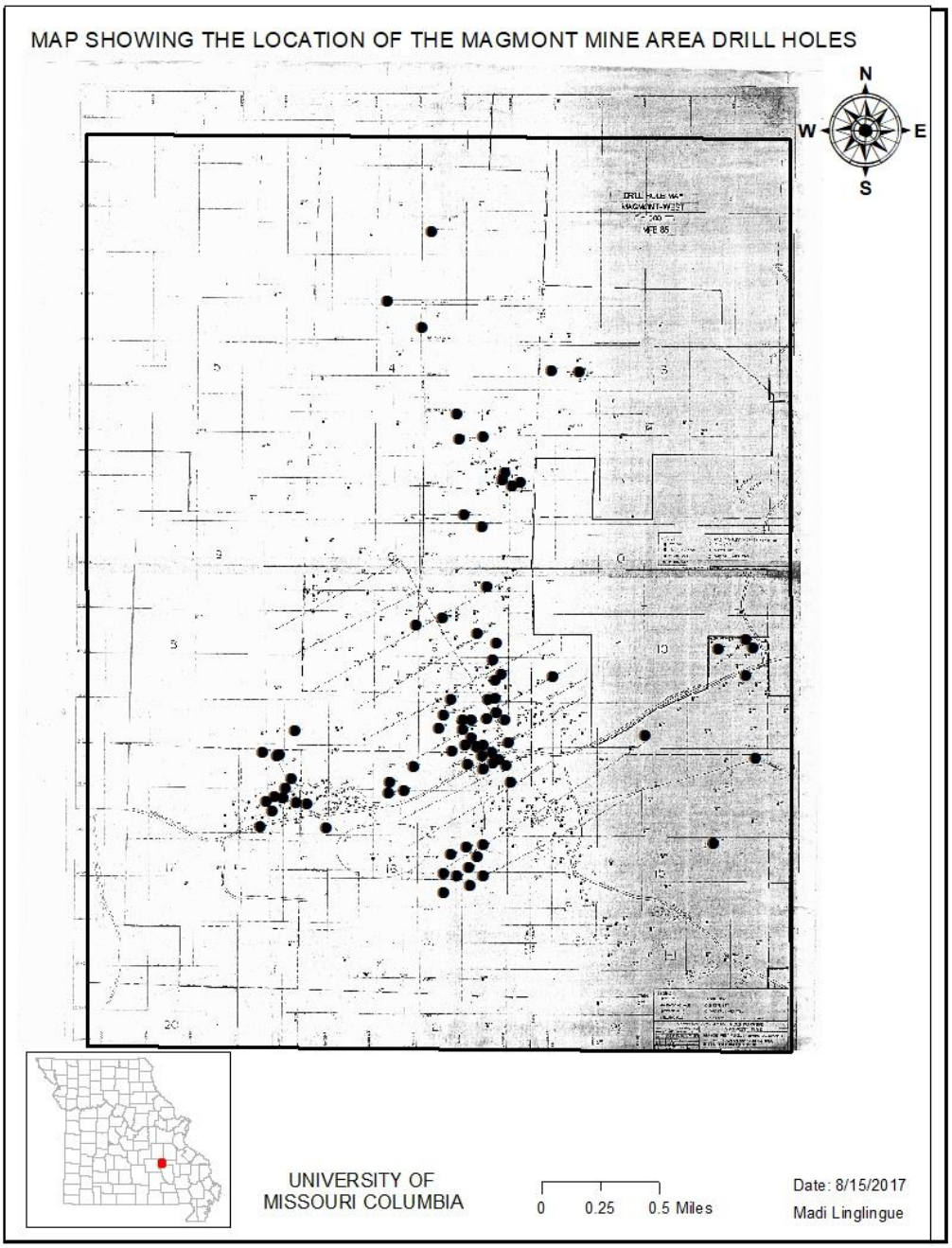

Figure 1: map of the study area showing the location of drill holes

5. Functional definitions

The term “resources” and “reserves” are used interchangeably to indicate the quantity of lead, independently of the volume of work involved in the assessment methods. Technically, the term ‘resources’ refers to the amount of ore estimated in an area following a detailed completion of exploration activities, giving a high confidence on the spatial distribution of the mineralization. “Target” refers to a piece of land with potential to host ore, for which further exploration efforts are justified.

The following sections will deal with the literature review in which knowledge and applications of the selected methods will be described. The methodology chapter will relate how the different theories were used to answer the research question. The results’ chapter will present the results obtained, which will be commented in the discussion chapter before the conclusion raps up the document.

Chapter 2. Literature review

1. Definition of some interpolation properties and parameters

This section presents the different interpolation methods used in this thesis. It presents what their purpose is, how they perform and how other people used them. Various factors affect the variability of different interpolation methods. Li and Heap (2014) enumerate among others: *exactness*, *convexity*, the *number of variables* involved in the assessment, the *size of the region* involved in the estimation, the *smoothness* of the surface generated between the observed points, the *linearity and the uncertainty* involved in the assessment.

Deterministic methods are intended to determine the exact value of an independent variable for any known dependent variable. They do not explicitly incorporate error in their assessment and only produce estimations. Furthermore, deterministic methods always return the same result for the same dependent variable. Stochastic methods however incorporate the concept of randomness and provide both estimations (i.e., deterministic part) and errors associated with the estimation (stochastic part, i.e., uncertainties represented as estimated variances) (Li and Heap, 2014).

Interpolation models also differ by purpose. Anderson et al. (2015) distinguish basically three main purposes for models: generic models, interpretive models and predictive models. Generic models are general in scope but not specific to any localized area. Therefore, they have the potential to generate more uncertainties in locations with specific features. Interpretive models on the other hand are site specific and therefore integrate more local features. Finally, in addition to being site specific, predictive models

are much more sensitive to the parameters involved in the prediction of the dependent variable.

Linearity is an important property of interpolation methods related to how they make estimates from observed values. Linear methods derive values directly from observed data while non-linear methods transform the observed data before predicting the value of the independent variable. In the latter case, a back transformation is required to restore the transformed estimate to an estimate of the original value (Isaaks and Srivastava, 1989). For example, simple kriging (SK), ordinary kriging (OK) and universal kriging (UK) are linear methods which derive the estimation using observed values given the data are normally distributed. However, Disjunctive kriging (DK), indicator kriging (IK), lognormal OK and model-based kriging (MBK) are non-linear methods (Li and Heap, 2014). Nonlinear kriging methods are thought to be more advantageous over linear kriging, by giving an estimate of the probability distribution based on observed data. Such estimations should theoretically be more precise when a Gaussian random process is inappropriate to model the observations (Li and Heap, 2014).

The number of variables involved in the estimation distinguishes univariate from multivariate functions. In geostatistics, spatial interpolation methods which only use samples of the primary variable in deriving the estimation are referred to as “univariate” methods and those which also use secondary variables as “multivariate” (Li and Heap 2011). These variables can be associated with number of parameters and conditions such that more or less complex functions and algorithms are required to find the solution. For example, Trauth (2012) highlighted how the presence of a single outlier changed the type of distribution from normal to skewed and subsequently imposed the fitting function to

change from a simple regression definable by the Pearson correlation coefficient to a more complex function.

Exactness measures the similarity between the predicted and the derived values; in other words, exactness measures how far the predicted value is from the observed one. A method that generates an estimate that is the same as the observed value at a sampled location is called an exact method. All other methods are inexact, which means that their predicted value at the point differs from its known value (Li and Heap 2011).

Convexity measures the fitness of the predicted value about the range of the observed values. Some methods constrain the predicted values to lie within the range of the observed ones whereas others do not. For example, inverse distance weighting (IDW) is a convex method whereas kriging is a non-convex method (Li and Heap, 2014).

The *size of the region* involved in the estimation differentiates global methods from local methods. Global methods use all available data in the region of interest to derive the estimation and capture the general trend(s) whereas local methods operate within a small area around the point being estimated and capture the local or short-range variation (Li and Heap, 2014). Isaaks and Srivastava (1989) explain that global estimations are used at early stages of most studies to get some characteristics of the distribution of data values over the whole area of interest. Local estimates however give detailed information about the distribution at specific locations of the study area.

Within the scale of the study area, sample density and sample distribution also influence the estimate because the estimate should reflect the sample density and

distribution. For example, clustered data should be managed in such a way that they don't create bias in the resulting map.

Smoothness is a criterion discriminating aspects of the surface generated between the observed points. For Li and Heap (2014), some methods (e.g., nearest neighbors) produce a discrete and abrupt surface, while other methods (e.g., distance based weighted averages) produce a smooth and gradual surface. They relate it to the way the interpolation method assigns weight to the reference data as distance relations criteria (e.g., IDW), minimization of variance (e.g., kriging methods) and minimization of curvature and enforcement of smoothness (e.g., splines).

2. Interpolation methods

All interpolation methods presented make estimates based mostly on the contribution of the neighboring data. Therefore, the nearest neighbor search plays an important role in the estimation process and is worth looking at. The nearest neighbors account for the estimation of the weight each sample is given. Davis (1985) describes briefly a few neighbors search methods.

2. 1 The nearest neighbor method

A widely-used version of the weighting process assigns a function whose exact form depends upon the distance from the location being estimated and the outer limits of the neighborhood.

The simplest selection of neighbors is called the "nearest-neighbor search", which locates some specified number of control points. The search concerns all data points that fall within a Euclidian distance which is calculated between the control points and the

point being estimated (figure 2). Boots and Getis (1988) explain that this distance is obtained by computing an average distance to all nearest neighbors, the distances being Euclidian. For the sake of a reasonable application of the nearest neighbor method, Getis and Boots (1978) suggest that a test for the existence of a Poisson generated pattern be conducted; such a test will inform if patterns like clustering exist, in which case further testing should be necessary. The mean spacing of the samples in a Poisson process is determined by the formula $\frac{1}{2\sqrt{n/A}}$ where *A* is the area being estimated and *n* is the total number of samples of the area. In practice, the algorithm makes this value coincide with that of one of the observed nearest neighbor's value. Then, the algorithm sorts the computed distances to choose the closest points. This method is alert to objections, one of which being that the method may find that all nearby points lie in a narrow wedge on one side of the grid node that is to be estimated.

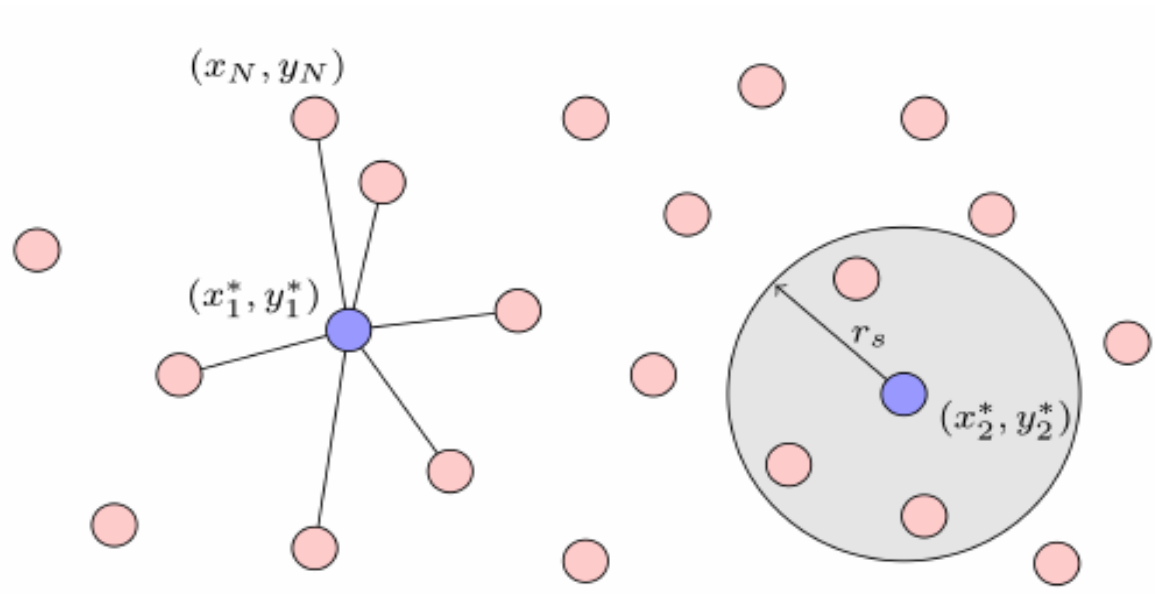

Figure 2: nearest neighbor search: a radius is defined and the control points falling inside it account for the estimation (source: Arcmap documentation)

The resulting estimate is essentially unconstrained, except in one direction. One way to avoid such a constraint is to restrict the search in some way that ensures that the control points are equitably distributed about the estimated point. This can be done by using a quadrant search or the more elaborate form, an octant search. The quadrant search implies the division of the search area into four sectors of 90 degrees each while the octant method requires the division of the same space into eight sectors of 45 degrees. In either case, the method must find a specific number of control point in each of the sectors to satisfy the determined total number of neighbors (figure 3).

Boots and Getis (1988) discussed some problems associated with nearest neighbors. One of them is about the inability of nearest neighbors to correctly reflect the pattern of the spatial distribution when "the pattern under study is the result of the operation of more than one distinct process". In an example of a regularly clustered pattern, the nearest neighbor method (NN) was unable to reflect the spacing between clusters because in each cluster, the samples are mutually next the ones to the others but not to other clusters'. In other words, NN does not account for clustering (Isaaks and Srivastava, 1989).

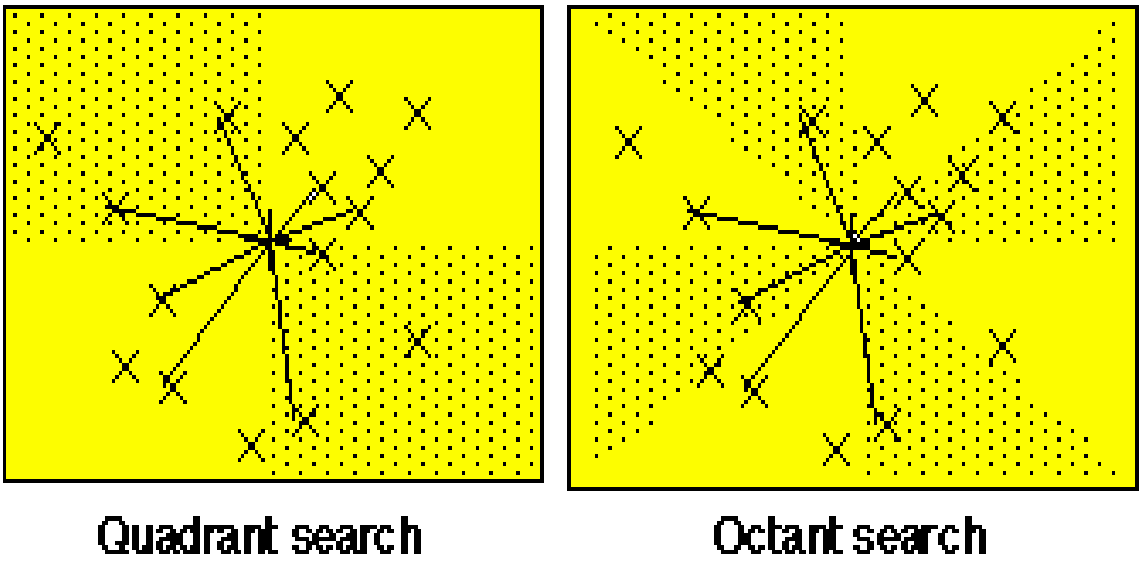

Figure 3: quadrant (4 sectors involved in the search) and octant (8 sectors involved) search methods (source:Arcmap documentation)

Another point about NN is the edge effect of the outcome, which causes distortions. One situation that can create distortions is illustrated in Getis and Boots (1978): the nearest neighbors of the data close to the edge may lie outside the study area in which case they will not considered in the estimation. Rather, the closest points within the study area are considered, despite not really being the closest neighbors. One solution would be to convert the study area into a 'torus' if it is rectangular or square by adding identical points beyond the boundaries of the area. Other solutions include the disregarding of points close to the edge, the creation of a buffer inside the outer perimeter or the assignment of a weight to the parameters in the calculations.

2. 2 Natural neighbor method

Ledoux and Gold (2005) define the natural neighbor interpolation as a weighted average technique based on the Voronoi diagram (VD) for both selecting the set of neighbors of the interpolation point x and determining the weight of each. The neighbors used in an estimation are selected using the adjacency relationships of the VD, which results in the selection of neighbors that both surround and are close to x (figure 4 and figure 5). The idea of a natural neighbor is closely related to the concepts of the Voronoi diagram and the Delaunay triangulation (DT). Let S be a set of n points in d-dimensional space. The Voronoi cell of a point $p \in S$, defined Vp, is the set of points x that are closer to p than to any other point in S. The union of the Voronoi cells of all generating points p in S form the Voronoi diagram (VD) of S. The geometric dual of VD(S), the Delaunay triangulation DT(S), partitions the same space into simplices—a simplex represents the simplest element in a given space, e.g. a triangle in 2D and a tetrahedron in 3D— whose circumspheres do not contain any other points in S. The vertices of the simplices are the points generating each Voronoi cell. The natural neighbors of a point p are the points in S sharing a Delaunay edge with p, or, in the dual, the ones whose Voronoi cell is contiguous to Vp. In other words, only cells that share a common edge are considered as neighbors.

This definition of the neighborhood makes the natural neighbors method one which makes only local estimates because restricting it to only the “real true neighbors”. The weight of each neighbor is based on the volume or the volume that the Voronoi cell of x ‘steals’ from the Voronoi cell of the neighbors in the absence of x. (Ledoux and Gold, 2005). The implementation of the natural neighbor method is technically complex

because the method requires the computation of two Voronoi diagrams (one with and one without the interpolation point) and also the computation of volumes of Voronoi cells. The concept of natural neighbors can also be applied to a point x that is not present in S. In that case, the natural neighbors of x are the points in S whose Voronoi cell would be modified if the point x were inserted in VD(S).

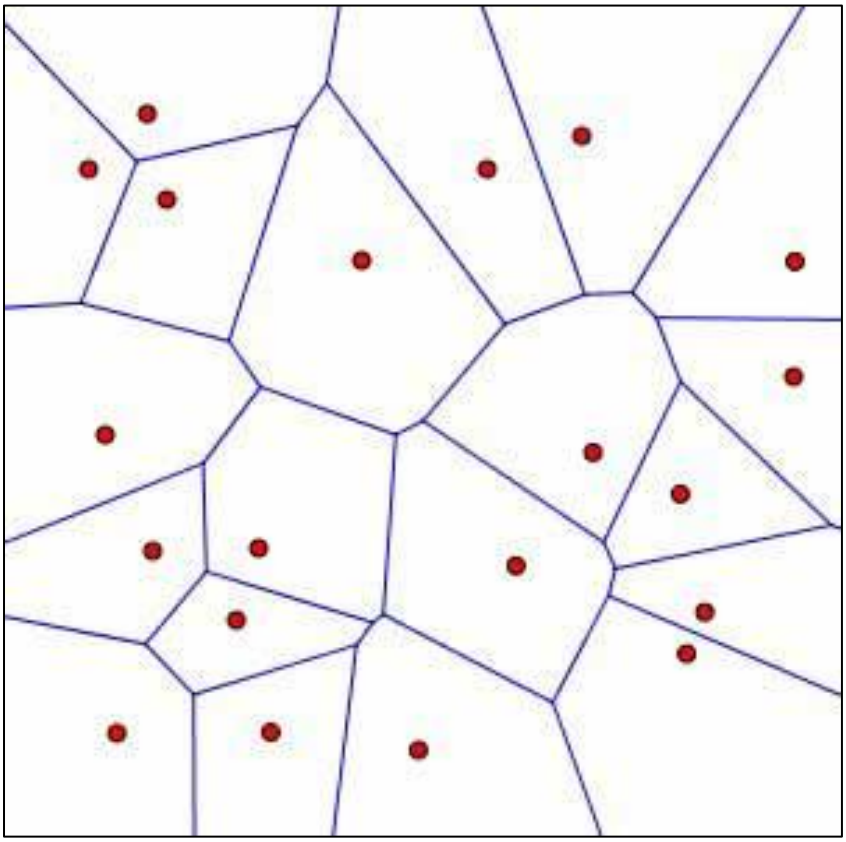

Figure 4: Voronoi diagrams (a) in 2D and (b) in 3D

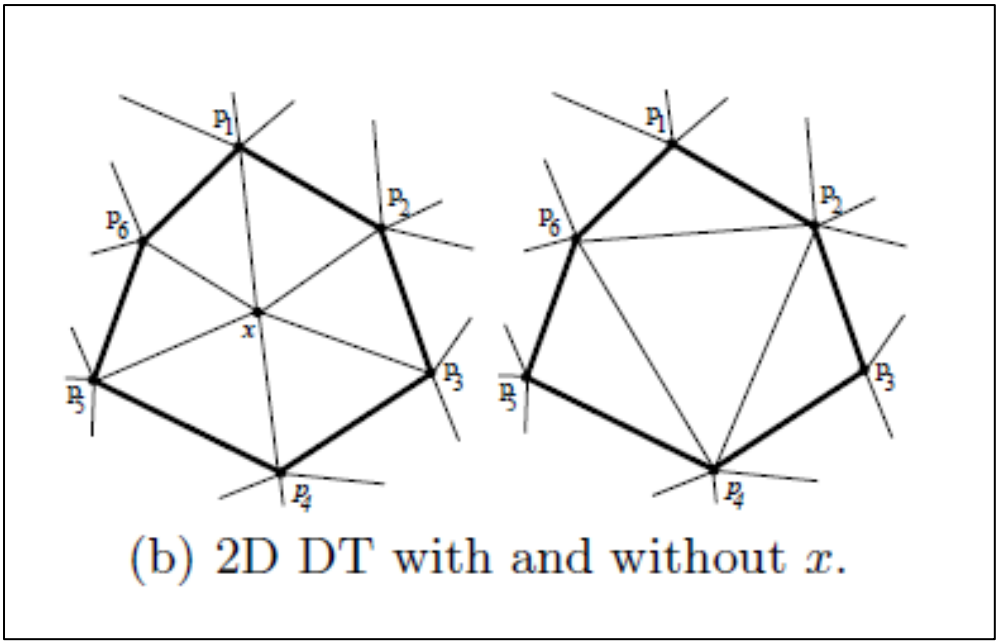

Figure 5: 2D Delaunay triangulation (DT) with and without x (source: Arcmap documentation)

The points used to estimate the value of an attribute at location x are the natural neighbors of x, and the weight of each neighbor is equal to the natural neighbor coordinate of x with respect to this neighbor. If we consider that each data point in S has an attribute a_i (a scalar value), the natural neighbour interpolation is:

$$f(x) = \sum_{i=1}^{k} w_i(x) a_i$$

where f(x) is the interpolated function value at the location x. The resulting method is exact (f(x) honors each data point), and f(x) is smooth and continuous everywhere except at the data points.

Removing the discontinuity is a challenging issue to which many authors proposed some solutions (Ledoux and Gold, 2005).

2. 3 Inverse distance weighted method

Inverse distance weighted is also referred to as inverse distance weighting and designated by the acronym IDW. According to Watson and Philip (1985), it is one of the earliest computer based schemes introduced to interpolate between scattered measurements. Because the surface generated honors the values of all of the original data, it is still widely used and integrated in many software packages. For example, it is used to generate contours of most aeromagnetic maps in the mineral exploration field. Basically, the IDW expresses the Tobler's first law in geography by attributing more influence to closer points of a point under estimate than to furthest points. The influence is computed as a weight, which is related to the distance separating the estimated point to a given reference point.

Robinson and Metternicht (2006) define inverse distance weighting as an exact interpolator which assumes that the value of an attribute at an unsampled location is a weighted average of known data points within a local neighborhood surrounding the unsampled location:

$$\hat{z}\,(x_0) = \frac{\sum_{i=1}^{n} z(x_i) d_{ij}^{-r}}{\sum_{i}^{n} d_{ij}^{-r}}$$

where x_0 is the estimation point and x_i are the data points within a chosen neighborhood. Watson and Philip (1985) use the term "linear combination of the observed values" to define the method. In the mathematical expression, the term $\frac{d_{ij}^{-r}}{\sum_{i}^{n} d_{ij}^{-r}}$ refers to the weight and involves the whole set of data points. The weights (r) are related to distance by d_{ij}, which is the distance between the estimation point and the data points. The IDW formula has the effect of giving data points close to the interpolation point relatively large weights

whilst those far away exert little influence. Each point is weighted by the inverse of the distance separating it from the reference point or by a more sophisticated function (Mesnard, 2012): the higher the weight used the more influence points close to x_0 are given. However, the interpolation can also be applied to projection of planes passing through the control points, to derivatives or to nodal points functions (Watson and Philip, 19850). The strength of the weights is expressed by assigning an arbitrary exponent to the distance function.

Mesnard (2012) thinks of the power as "exogenous with respect to the data". Watson and Philip (1985) emphasis on the high dependence of IDW on the power parameter. It has the power to contract the estimation scale from local to global because it can reflect differently on the distribution. For example, the effect can vary from highly bias in favor of the nearest data point to being nearly equal for all data points. Moreover, they highlighted a 'misunderstanding' according to which many authors thought that the function of the distance had to tend to infinity as the distance approaches zero because it is an inverse power. Rather, there is room for the function to tend to a constant as the distance approaches zero.

The effect of the exponent on the weight is made evident if expressed mathematically. Let the index i denote a point to be estimated, j the index of a reference point and n_j be the number of neighboring stations that relate to the reference point j. Each measurement is multiplied by the inverse of distance $d_{ij} \geq 0$ from the station i to the reference point j with the exponent α, i.e., $1/d_{ij}^{\alpha}$. As this would change the magnitude of the final result, each product is divided by the sum of the terms $1/d_{ij}^{\alpha}$ over all stations. This amounts to defining the weights as:

$$W_{ij} = \frac{\frac{1}{d_{ij}^{\alpha}}}{\sum_{k=1}^{n_j} \frac{1}{d_{kj}^{\alpha}}}$$

for any ij. Therefore, measurement at the reference point j equals

$$\bar{P}_j = \sum_{i=1}^{n_j} W_{ijP_{ij}}$$

which becomes after substitution of the expression of the weight:

$$\bar{P}_j = \frac{\sum_{i=1}^{n_j} \frac{1}{d_{ij}^{\alpha}} P_{ij}}{\sum_{k=1}^{nj} \frac{1}{d_{kj}^{\alpha}}}$$

such that all weights sum to 1: $\sum_{i=1}^{n_j} W_{ij} = 1$

The weight assigned to the interpolator depends on the value assigned to the power, α. Mesnard (2006) and Watson and Philip (1985) discuss some common problems related to the IDW interpolation including the judicious choice of the power for the distance as the power chosen affects the shape of the outcome, the behavior of the weight close to the reference, the inability of IDW to estimate values higher than the range of the observed values. For the choice of the power for example, Mesnard (2006) mentioned several problems related to the arbitrary choice of the exponent. The first on is the absence of an unequivocal value of α for which the inverse distance weighting performs best. Most authors take the value of 1 while others consider the square to be the best option; other even choose α =3 or α =4.

For Davis (1973) the most popular functions used for distance weighting in the contouring programs are inverse distance-powered functions ($\frac{1}{D}, \frac{1}{D^2}, \frac{1}{D^4}, \frac{1}{D^6}$) and scaled

inverse distance-squared function. Watson and Philip (1985) also contributed to the discussion on the choice of the power. For p >1, IDW observations interpolation provides an arbitrarily close approximation to classical Voronoi proximal polygonal interpolation in which the observed value at a control point is applied to all locations with the surrounding polygon. With p >>1, a dominating weight approaching unity is applied to the nearest control point for all locations closer to that control point than to any other. For p<1 on the other hand, all weights tend to be more nearly equivalent except, immediately adjacent to a control point where the weight for that point still approaches unity.

IDW method usually requires at least the choice of the power parameter and the radius but more complex variants of the method often have more than two parameters (Watson and Philip, 1985). The problem of selecting parameter values involves the variation in the density of sampling.

The choice of the search method for the neighbors is another determinant factor in the performance of inverse distance method. The number of neighbors involved in the estimation of an attribute value depends on the search method used as discussed previously. Isaaks and Srivastava (1989) give some rules to choose the convenient number of neighbors.

- On a pseudo regular grid, the minimum number of nearby samples is 12 (as in ArcMap)
- On an irregular grid, the search neighborhood should be slightly larger than the average spacing between the sample data.

For technical reasons, the appropriateness of the sample seize is crucial.

- The computation time is proportional to the cube of the sample seize, so too big a sample seize is not relevant.
- As farther samples are included, the appropriateness of a stationary random function model becomes doubtful

2. 4 Regular splines and thin plate splines

Davis (1986) gives a description of splines as follow: splines are one of a large class of piecewise functions used to represent curves in two or three dimensions. The curves result from the interconnection of sequence of points with continuous and smooth lines. One of the most used functions is the cubic polynomial. The curve defined by a cubic polynomial can pass exactly through four points, but in order to fit a longer sequence it is necessary to use a succession of polynomial segments. To ensure that there is no abrupt changes in slope or curvature between successive segments, the polynomial function is not fit to four points but only to two. Each pair of points, also called span, is connected with a smooth line, which is defined by a polynomial function. The resulting segments are then joined to fit the desired feature. A mathematical spline is constrained at defined points but between the points it flexes in a manner that results in a smoothly varying line. They are arbitrary and devoid of theoretical basis except that which defines the characteristics of the lines themselves. Splines are neither analytical function nor are they statistical models such as the polynomials. They are important in geological or geophysical numerical modeling. A cubic spline covers a single span at a time, which are functions of the form

$$Y = \beta_1 + \beta_2 X + \beta_3 X^2 + \beta_4 X^3$$

The determination of the coefficients of the spline function is achieved by solving differential equations.

Similarly, Robinson and Metternicht (2006) define splines as consisting of polynomials, which describe pieces of a line or surface that are fitted together so that they join smoothly. They find splines to fit well distributions for gently varying surfaces. Conversely, they find them to be not appropriate when there are large changes in the surface values within a short horizontal distance. Comparing the splines' fitting model with regard to kriging, Wikle and Cressie (2011) observe that thin-plate smoothing splines 'pre-select' a particular semivariogram or more generally a generalized covariance function without letting the data decide which semivariogram gives the best fit. Further, Splines are used as smoothers rather than predictors, meaning that there is no analogous notion to the kriging variance.

The technique for delineating the ends of a sequence is done by the division into relatively uniform segments and is known as zonation. Zonation is performed either by the procedure of 'local boundary hunting' which searches for abrupt changes in average values (the same as searching for the steepest gradients in the sequence) or by the 'split-moving window' which computes 'the generalized distance' by dividing the segment following a constant distance called window. The window is centered on i and has two radii. The window is travelled along the segment until the radii are found different; at that point, the algorithm knows the end of the segment.

2. 5 Simple, ordinary and universal Kriging

(1) Kriging approach and terminology

Kriging is a statistical methodology based on the theory of stochastic processes (Wikle and Cressie, 2011). Goovaert (1997) explains that it is a generic name adopted by geostatisticians for a family of generalized least-squared regression algorithms in recognition of the pioneering work of Danie Krige. More specifically, Goovaerts (1997) and Bohling (2005) define the kriging methods as estimators that are but variants of the basic linear regression estimator $Z^*(\mathbf{u})$ defined as:

$$Z^*(u) - m(u) = \sum_{\alpha=1}^{n(u)} \lambda_\alpha(u)[Z(u_\alpha) - m(u_\alpha)], \text{with}$$

$\mathbf{u}$, $\mathbf{u}_\alpha$: location vectors for estimation point and one of the neighboring data points, indexed by α

$n(\mathbf{u})$: number of data points in local neighborhood used for estimation of $Z^*(\mathbf{u})$

$m(\mathbf{u})$, $m(\mathbf{u}_\alpha)$: expected values (means) of $Z(\mathbf{u})$ and $Z(\mathbf{u}_\alpha)$

$\lambda_\alpha(u)$: kriging weight assigned to datum $Z(\mathbf{u}_\alpha)$ for estimation location $\mathbf{u}$.

For Davis (1986), kriging is an estimation procedure aiming at estimating the values of 'regionalized variables' at unsampled locations based on measured values at discrete locations, after a semivariogram function is found to express the spatial continuity of those scattered sampling points. The concept of regionalized variable refers to a naturally occurring property which has characteristics intermediate between those of truly random variables and deterministic variables. As such, the value of the attribute (elevation in this thesis) at location u, $Z(\mathbf{u})$, is treated as a random field (RF) with a trend component, $m(\mathbf{u})$, and a residual component, $R(\mathbf{u})$: $Z(\mathbf{u}) = R(u) + m(\mathbf{u})$. Bohling (2005b) reminds us that "all interpolation algorithms (inverse distance squared, splines, radial

basis functions, triangulation, etc.) estimate the value at a given location as a weighted sum of data values at surrounding locations" (figure 6). He defines the term 'interpolation' as "Estimation of a variable at an unmeasured location from observed values at surrounding locations".

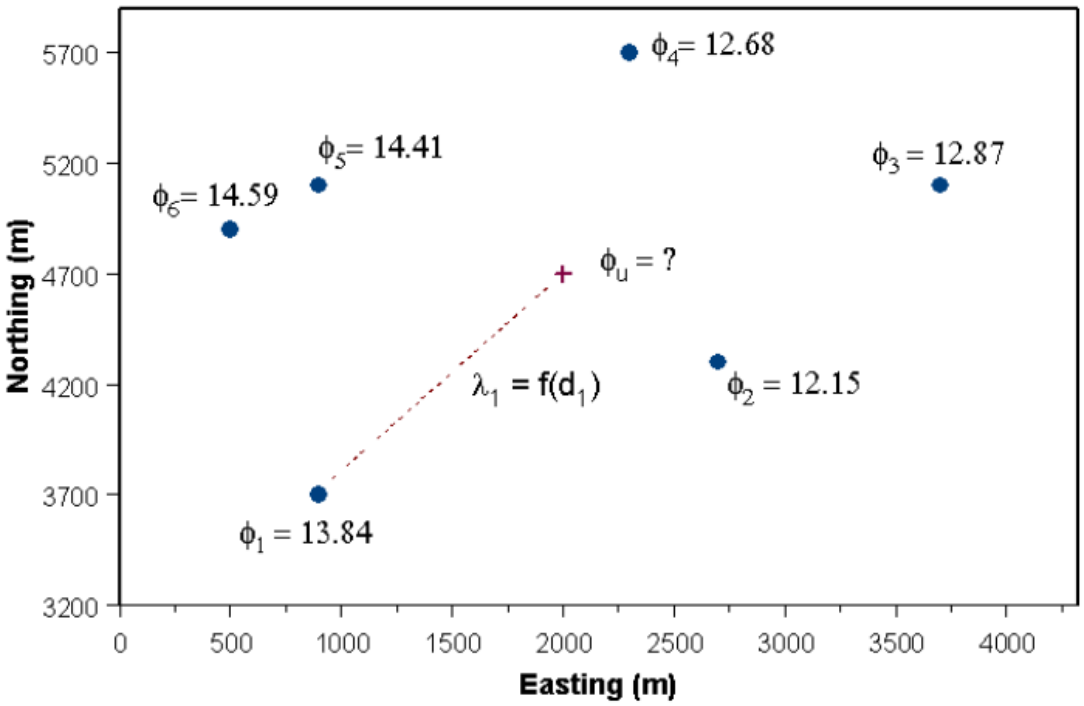

Figure 6: the assignment of weight is a function of distance (source: Bohling, 2005)

Kriging uses the notion of 'residual' in its estimates. The residual at a location **u** is a weighted sum of the residuals surrounding that point. In other words, a mean value is estimated for all point data, from which the value of each surrounding point is subtracted. This operation results in a vector stored as a residuals' matrix. Bohling, (2005b) explains that the estimated residual from the mean at u is given by the dot product of the kriging weights and the vector of residuals at the data points. This value of the residual is added back to the mean to get the value of the variable at that point. Like other geostatistical methods, kriging is optimal for normally distributed data and in stationary conditions

(Bohling, G., 2005). The residual component is treated as an RF with a stationary mean of 0 and a stationary covariance:

$$E\{R(\mathbf{u})\} = 0$$

$$\mathrm{Cov}\{R(\mathbf{u}), R(\mathbf{u}+\mathbf{h})\} = E\{R(\mathbf{u}) \cdot R(\mathbf{u}+\mathbf{h})\} = CR(\mathbf{h})$$

Therefore, the expected value of the random variable Z at a location u is thus the value of the trend component at that location: $E\{Z(u)\} = m(u)$.

That residual component is usually represented by a semivariogram model or a covariance function called covariogram. The semivariogram characterizes the correlations; it accounts for the influence of the distribution that surrounds each estimated location in the estimation (Isaaks and Srivastava, 1989). Wikle and Cressie (2011) observe that in a way, semivariogram or correlation function can be seen as parameters in the process of the kriging estimator as a whole.

There are basically two types of variogram models:

- Those that reach a plateau or transition models. They are basically the Gaussian model (linear near origin, tangent from origin cuts sill at 2/3 of range), the Exponential model (tangent to curve at origin cuts sill at 2/5 of range) and the Spherical mode
- Those that do not reach a plateau

Among the three transition models, the choice usually depends on the behavior of the sample variogram near the origin. If the underlying phenomenon is quite continuous, the sample variogram will likely show a parabolic behavior near the origin; in such situations, the Gaussian model will usually provide the best fit. If the sample variogram

has a linear behavior near the origin, either the spherical or exponential model is preferable. Isaaks and Srivastava (1989) give a few tips to help choose the best fit. Often one can quickly fit a straight line to the first few points on the sample variogram. If the line intersects the sill at about one fifth of the range, then an exponential model will likely fit better than a spherical one. If it intersects at about two thirds of the range, then the spherical model will likely fit better

As a general guideline, 'the principle of parsimony' can be used too: If a simple model fits the sample variogram as well as complex models, the simpler model is preferred. It should be noted that the RF is a function of lag, **h**, but not of position, **u.** Also, the distance involved in the computation of kriging is not geometric but statistical.

The semivariogram computes the average value of the residuals within a distribution by a process of iterative calculations based on a defined distance called lag. With the uncertainty that data points might not fall within the defined lag, the kriging process incorporates a tolerance interval to extend the search radius:

$$2\gamma z(h) = ave\{(Z(S\_i) - Z(S\_j))^2 : ||S_i - S_j|| \varepsilon\ T(h);\ i,j = 1,\ldots,m\}$$

(Wikle and Cressie, 2011) where T(h) is the tolerance region around h, Z(Si) and Z(Sj) being the elevation values at location 1 to m.

,At first, the (semi)variogram considers one point of the distribution and then defines a lag, which is a fixed radius within which all neighboring points will be included in the calculation process. The attribute of each neighbor is subtracted from that of the estimated point the difference is squared. A new estimation is made using the same estimated point, but within twice the initial lag. The process continues until the lag covers the furthest point of the distribution. A mean value is computed and assigned to the estimated point. Finally, the process starts again with another point and so on, until all points are considered (figure 7). The average points are plotted on a 'lag vs mean residual' diagram and a regression function chosen to fit the resulting distribution. The subsequent function is called (semi)variogram; it is used to continuously estimate the values at for all the points of the study area.

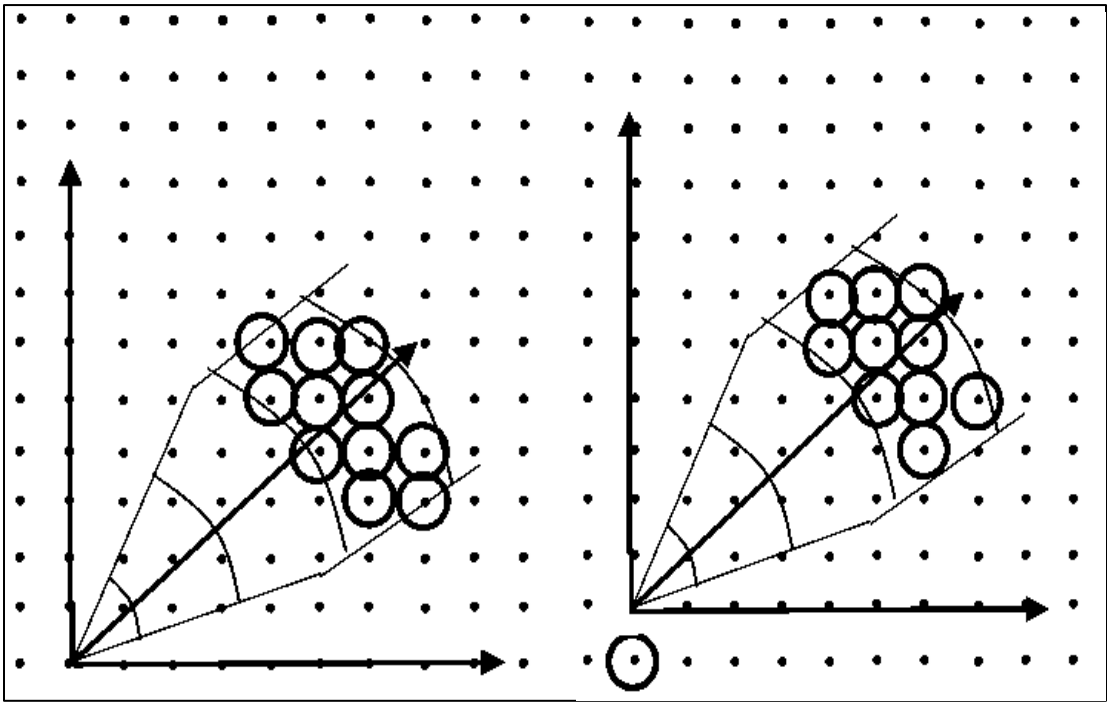

Figure 7: step 1 Left) and step 2(right) of variogram estimate for lag 4

For the sake of kriging (or stochastic simulation), the empirical semivariogram needs to be replaced with an acceptable semivariogram model. Part of the reason for this is that the kriging algorithm will need access to semivariogram values for lag distances other than those used in the empirical semivariogram. Indeed, the sample variogram does not provide any information for distance shorter than the minimum spacing between the sample data (Isaaks and Srivastava, 1989). More importantly, the semivariogram models used in the kriging process need to obey certain numerical properties in order for the kriging equations to be solvable. (Technically, the semivariogram model needs to be non-negative definite, in order for the system of kriging equations to be non-singular). In practice, geostatisticians choose from a palette of acceptable or licit semivariogram models (Bohling, 2005). The five most frequently used models are: nugget, spherical, exponential, Gaussian and power.

The (semi)variogram is a curve defined by the following parameters: the nugget effect, the sill and the range (figure 8). Bohling (2005a) gives definitions of these terms:

Sill:

The sill is the semivariance value at which the variogram levels off. The sill is also used to refer to the "amplitude" of a certain component of the semivariogram. For the plot above, "sill" could refer to the overall sill (1.0) or to the difference (0.8) between the overall sill and the nugget (0.2). the meaning depends on the context.

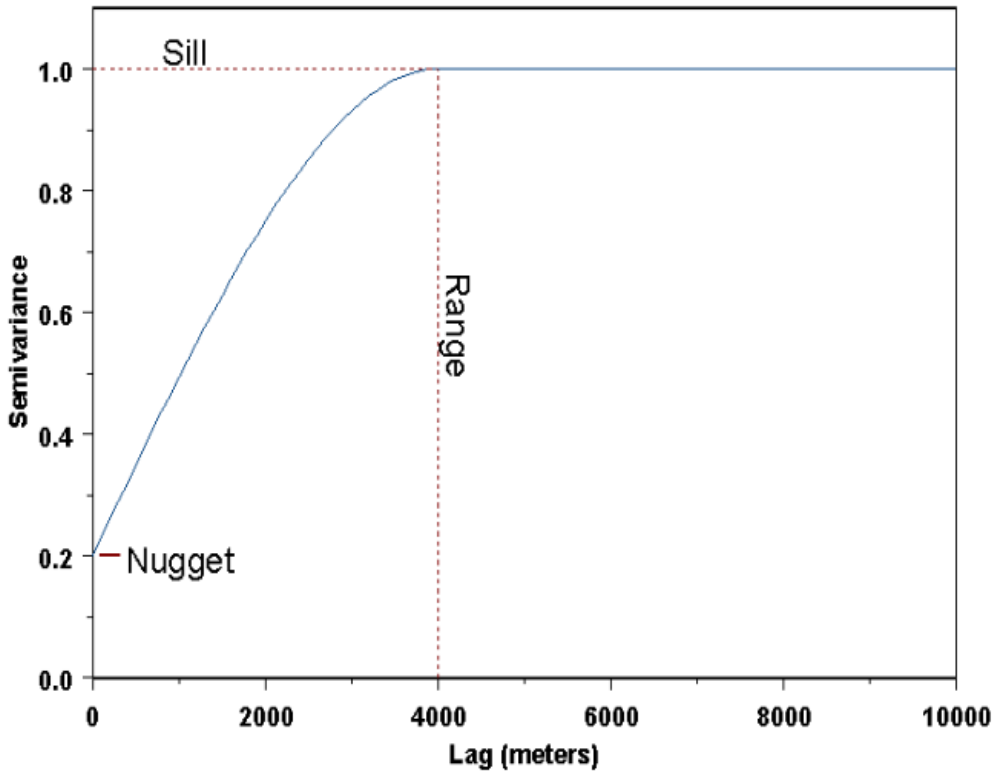

Figure 8 characteristics of a variogram (source: Bohling, 2005)

Range:

It is the lag distance at which the semivariogram (or semivariogram component) reaches the sill value. Presumably, autocorrelation is essentially zero beyond the range. That means that the influence of the contributing samples to the estimate is neglected beyond the range. The effect of range on the estimate can be summarized as follow: the smallest the range, the farther statistically the points among themselves and with the one being estimated and the lowest the weight.

Nugget:

In theory, the semivariogram value at the origin (0 lag) should be zero. If it is significantly different from zero for lags very close to zero, then this semivariogram value is referred to as the nugget. The nugget represents variability at distances smaller

than the typical sample spacing, including measurement error (Bohling, 2005a). The nugget effect tends to make the weights more similar than the absence of nugget effect. A pure nugget effect exhibits no correlation; the estimate is the average value of the neighboring values. The weights all become 1/n

In the estimation of the residual value at location u, weights, λ_{α}, are assigned to the neighboring points based on the distance of each neighbor to the estimated point. The estimation is done such a way to minimize the variance of the estimator

$$\delta_E^2 (\mathbf{u}) = \mathrm{Var}\{Z^*(\mathbf{u}) - Z(\mathbf{u})\}$$

under the unbiasedness constraint

$$E\{Z^*(u) - Z(u)\} = 0.$$

Almost all interpolation methods assign weights according to functions that give a decreasing weight with increasing separation distance, but Kriging assigns weights according to a (moderately) data-driven weighting function, rather than an arbitrary function (Isaaks and Srivastava, 1989). The number of data involved in the estimation as well as their weights may change from one location to another. In practice, only the n(u) data closest to the location u being estimated are retained, i.e., the data within a given neighborhood or window W(u) centered on u (Goovaerts, 1997).

The shape of the variogram function affects the weight of the variogram estimates through the distribution of the sample data. For example, a parabolic function involves

more samples in the neighborhood. The same, some samples behave as screen to other samples, affecting the weight of the hidden samples which can have end up having a negative weight.

Bohling (2005a) and Isaak and Srivastava (1989) made some few notes about the variogram with regard to the estimation of the weight. For Bohling (2005a):

- The use of a parabolic function can enhance the screening effect
- The advantage of negative weights or weights greater than 1 is that it allows the interpolation to generate values beyond the maximum or the minimum values of the dataset, which is reasonable
- However, if negative weight is assigned to big values, the resulting estimate can be negative, which does not make sense physically for natural phenomena. In that case, the weight is reduced to 0
- Variogram models with parabolic behavior are avoided because they tend to make the estimation very erratic

The description above assumes that the spatial correlation structure is the same in all directions, or isotropic. In this case the covariance function (or correlogram) and the semivariogram depend only on the magnitude of the lag vector, h = |h|. Such a semivariogram is described as omnidirectional. In many cases, however, Bohling (2005a) teaches us that a property shows different autocorrelation structures in different directions, and an anisotropic semivariogram model should be developed to reflect these differences. The most commonly employed model for anisotropy is geometric anisotropy, with the semivariogram reaching the same sill in all directions, but at

different ranges. The most common approach to modeling geometric anisotropy is to find ranges a_x, a_y, and a_z in three principal, orthogonal directions and transform a three-dimensional lag vector h (h_x, h_y, h_z) into an equivalent isotropic lag using:

$$h = \sqrt{(h_x/a_x)^2 + (h_y/a_y)^2 + (h_z/a_z)^2}$$

To check for directional dependence in an empirical semivariogram, we have to compute semivariance values for data pairs falling within certain directional bands as well as falling within the prescribed lag limits. The directional bands are specified by a given azimuthal direction, angular tolerance, and bandwidth (figure 9).

Bohling (2005a) remarks that the directional semivariograms are noisier due to the reduced number of data pairs used for estimation. They do not show overwhelming evidence of anisotropy.

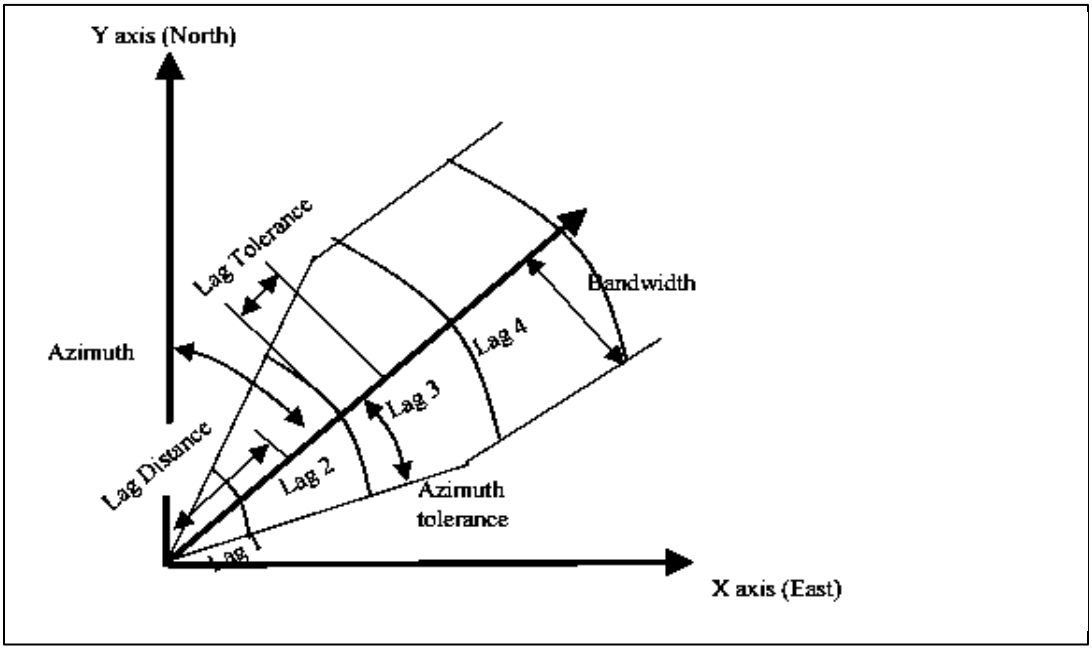

Figure 9: Characteristics of a variogram (source: Arcmap documentation)

The direction of anisotropy defines the major direction of spatial continuity, along which the maximum weight is assigned to the samples. Isaaks and Srivastava (1989) inform us that in some cases, the direction of the variogram may vary with local fluctuations. If there is not enough information to quantitatively determine the anisotropy, it is acceptable to consider an isotropic distribution. Sometimes, there is a significant spatial trend in the variable, resulting in the empirical semivariogram continuing to climb steadily beyond the global variance value. In that case, Bohling (2005) suggests three options:

- Fit a trend surface and work with residuals from the trend
- Try to find a "trend-free" direction and use the variogram in that direction as the variogram for the "random" component of the variable
- Ignore the problem and use a linear or power variogram

In the estimation, the semivariogram goes through a process called 'cross-validation' to validate the accuracy of an interpolation (Robinson and Metternicht, 2006). Cross-validation is also found to be excellent for solving the inconvenience of redundant data collection. The cross-validation technique is used to choose the best variogram model among candidate models and to select the search radius and lag distance that minimizes the kriging variance. It is also used to assist finding the best parameters from those tested for IDW and splines.

The kriging procedure uses cross validation to compare estimates and true values based on the information available in the sample data set. In a cross validation exercise, the estimation method is tested at the locations of existing samples through an iterative process where one sample is left every time and its value estimated from those of the

remaining samples. At the end, the estimated values are compared to the true values. There are some limitations of the cross validation regarding clustering. The effect of clustering reflects on the spread of the errors which in turn appear clustered and therefore a good estimate is not got.

Depending on the model considered for the trend component m(u), there are different types of kriging. Different constraints are applied to each method, especially regarding the mean value. Additionally, error estimations go along with the kriging process. For the sake of comparison, key characteristics of kriging were described by Bohling (2005b):

- **Smoothness**: Kriged surface will basically be as smooth as possible given the constraints of the data; in many cases, probably smoother than the "true" surface.
- **Bullseyes**: Because kriging averages between data points, local extremes will usually be at well locations; bullseyes are inevitable. This is true of almost all interpolation algorithms. Extreme form of this is artifact discontinuities at well locations when semivariogram model includes significant nugget.

The three most used variants of kriging methods are : simple kriging, ordinary kriging and universal kriging (also called kriging with a trend model(KT)) (Goovaerts, 1997, Bohling, 2007).

b) Simple kriging

Simple kriging (SK) considers the mean m(u) to be known and constant throughout the entire area (Isaaks and Srivastava, 1989, Bohling 2005b, Goovaerts, 1997):

$$Z^*(u) = m + \sum_{\alpha=1}^{n(u)} \lambda_\alpha^{SK}(u)[Z(u_\alpha) - m]$$

This estimate is automatically unbiased, since

$$E\{Z_{SK}^*(u) - Z(u)\} = m - m = 0$$

so that

$$[Z_{SK}^*(u)] = m = E[Z(u)]$$

. The estimation error $Z_{SK}^*(u) - Z(u)$ is a linear combination of random variables representing residuals at the data points, u_α , and the estimation point, **u**:

$$Z_{SK}^*(u) - Z(u) = [Z_{SK}^*(u) - m] - [Z(u) - m] =$$

$$\sum_{\alpha=1}^{n(u)} \lambda_\alpha^{SK}(u)R(u_\alpha) - R(u) = R_{SK}^*(u) - R(u)$$

After the math, that estimation error turns to be the difference between the residuals of the data point and the estimation point. By analogy, Bohling (2005a) concluded that the covariance function for $Z(\mathbf{u})$ is the same as that for the residual component, C(h) = C_R(h), so that it is possible to write the simple kriging system directly in terms of $C(\mathbf{h})$:

$$\sum_{\beta}^{n(u)} \lambda_{\beta}^{SK}(u)\, C(u_\alpha - u_\beta) = C(u_\alpha - u)\ \ \alpha = 1, \dots, n(u)$$

This can be written in matrix form as

$$K\lambda_{SK}(u) = k$$

,

from which the weights can be solved for:

$$\lambda_{SK} = K^{-1}k$$

Once the kriging weights are got, it is possible to compute both the kriging estimate and the kriging variance.

c) Ordinary kriging

Rather than assuming that the mean is known and constant through the entire area, ordinary kriging (OK) assumes that it is constant in the local neighborhood of each estimation point. Goovaerts (1997) expresses this invariability within the local neighborhood as is: "Ordinary kriging (OK) accounts for local fluctuations of the mean by limiting the domain of stationarity of the mean to the local neighborhood W(u) centered on the location u being estimated". In other words, $m\,(u_\alpha) = m(u)$ for each nearby data value $Z(u_\alpha)$ used to estimate Z(u). The OK estimator can be written

$$Z*(u)\ = m(u) + \sum_{\alpha=1}^{n(u)} \lambda_\alpha(u)[Z(u_\alpha) - m(u)]$$

Or

$$Z*(u)\ = \sum_{\alpha=1}^{n(u)} \lambda_\alpha(u) Z(u_\alpha) + \left[1 - \sum\nolimits_{\propto=1}^{n(u)} \lambda\alpha(u)\right] m(u)$$

The unknown local mean m(u) can be filtered out by constraining the weights' sum to be 1, leading to the expression of the ordinary kriging estimator of:

$$Z_{OK}^{*}(u) = \sum_{\alpha=1}^{n(u)} \lambda_{\alpha}^{OK}(\mathrm{u})\ \mathrm{Z}(u_{\alpha})$$

with

$$\sum_{\alpha=1}^{n(u)} \lambda_{\alpha}^{OK}(u) = 1$$

Goovaerts (2005) finds that OK is usually preferred to SK because it requires neither knowledge nor stationarity of the mean over the entire area

Ordinary Kriging is referred to as BLUE, that is, the "Best Linear Unbiased Estimator" by Isaaks and Srivastava (1989). It is considered linear because its estimates are weighted linear combinations of the available data. It is unbiased because it tries to make the mean residual of errors equal to 0. The qualification best relates to the fact that it tends to minimize the variance of the errors.

Ordinary kriging uses a probability model to fit the distribution by calculating the bias and the error variance. It then assigns weights to the nearby samples that ensure that the average error is 0 and the variance minimized. In order to minimize the error variance with regard to the constraint on the weights, an additional term called the Lagrange parameter, $\mu_{OK}(u)$, is introduced such that:

$$L = \sigma_{E}^{2}(u) + 2\mu_{OK}(u)\left[1 - \sum_{\alpha=1}^{n(u)} \lambda_{\alpha}\,(\mathrm{u})\right]$$

Like with the simple kriging, once the weights are determined, the OK error variance is also determined. Due to the insertion of the Lagrange parameter μ (coefficient matrix), the solving of the ordinary kriging weights requires the augmentation of the variable and solution matrices (with 'ones'). On an estimation of porosity, Bohling (2005b) found and estimate of 12.93% and a standard deviation of 0.490% for ordinary kriging against 12.83% with a standard deviation of 0.488% for simple kriging. The resulting maps looked very similar.

Isaaks and Srivastava (1989) explain that ordinary kriging solves for an equation of the form D = w*C to determine the value of the estimated value D, using a weight w and the known value C. The C and D matrices measure the statistical distance but additionally, the C matrix includes the variability due to the spatial continuity. For example, 2 samples taken on a water table 10m apart are likely to be alike than 2 samples taken 10m apart on a quartz vein. The C matrix records distances between each sample and every other sample, providing the OK system with information on the clustering of the available sample data. The C matrix adjusts the raw inverse statistical distance weights in D to account for possible redundancies between the samples. In other words, all samples of the same neighborhood will not be given the same weight; rather, the weight of part of the sample data will be lessened to reduce the effect of redundancy due to the clustering. As said Isaaks and Srivastava (1989), "… some of the weight is redistributed to other samples that are farther away yet less redundant".

However, they observe that "the ambitions of ordinary kriging are unattainable because the mean error or the residuals as well as the error variance are always unknown".

d) Kriging with a trend

Kriging with a trend is the name attributed to the former "Universal kriging" (Bohling, 2005). It is much like ordinary kriging, except that instead of fitting just a local mean in the neighborhood of the estimation point, a linear or higher-order trend is fitted in the (x,y) coordinates of the data points. Similarly, Goovaerts (1997) asserts that "Kriging with a trend considers that the unknown local mean m(u') smoothly varies within each local neighborhood W(u), hence over the entire study area. The trend component is modeled as a linear combination of functions $f_k(u)$ of the coordinates:

$$m(u') = \sum_{k=0}^{K} a_k(u')\, f_k(u')$$

with $a_k(u') \sim a_k$ constant but unknown $\forall\, u' \in W(u)$". Including such a model in the kriging system involves the augmentation of the coefficient, variable and solution matrices with two more Lagrange parameters as well as two extra columns and rows in the **K** matrix whose (non-zero) elements are the x and y coordinates of the data points.

Bohling, (2005) warns that a higher order trends may be fitted (cubic, quadratic) but in practice, it is rare to use anything higher than a first-order trend. Also, if the variable of interest does exhibit a significant trend, a typical approach would be to attempt to estimate a "de-trended" semivariogram and then feed this into kriging with a first-order trend. Goovaerts (1997) instead recommends performing simple kriging of the residuals from a global trend (with a constant mean of 0) and then adding the kriged residuals back into the global trend.

Chapter 3. RESEARCH METHODS

Prior to assessing the variability between different spatial interpolation methods both qualitatively and quantitatively, the data needed to be prepared.

1. Preprocessing

1. 1 Digitization of the Magmont mine map document

The map of the mine area supplied by USGS was in pdf format. It was a handmade map with both local and UTM coordinates. The map also integrated the main road network and the geographic references of the quadrangle 37091f. These references made it easy to digitize and georeference the basemap for integration into other existing Missouri datasets. Georeferencing was completed using Arcmap 10.4.1, to a residual error (RMSE) of less than 1m. The georeferenced map was projected in state plane NAD83 Missouri East FIPS 2401 (feet), the projection system for the thesis.

1. 2 Data acquisition

a) Subsurface information

Subsurface information consists of the geologic descriptions of the drilling chips and drilling core as well as their associated assay values for lead. Geologic information has been compiled by the USGS from different exploration programs undertaken on the area. It is to be noted that the geologic descriptions, the information available on the study area map, and the assay data were not matching for all holes. For example, the scanned map had 501 holes, whereas the geologic description file had information for 182 holes and the assay file comprised 365 holes. Therefore, only the holes having complete information on assay and geology within the study area were retained for

analysis. Subsequently, a total of 83 drill hole data was obtained from this matching operation.

For the sake of 3D orebody top and bottom surfaces, two files were constituted: a collar file and an assay file. The collar file had to contain at least information on hole name and coordinates, collar elevation, azimuth, dip and depth. Relevant information was extracted and compiled from the excel files received from USGS as well as from GIS. GIS was used to generate and extract the coordinates and elevation values of the drill hole collar, which were missing in the original data sets. Hole dip values were missing from the datasets. A former geologist who worked on the project and still had his notes indicated that all holes within the study area were drilled vertically (-90°). Hole depths were extracted from the geology file. Similarly, top and bottom elevations of the lead orebody were retrieved from the 'assay' file.

b) Surface information

Surface information was constituted by elevation values of the land surface. These values were derived from five LAS tiles covering the study area, namely: 24-12, 24-13, 25-12, 25-13 and 37091f1_NE (source: http://www.msdis.missouri.edu/data/lidar /download /index.html). The tiles had up to 8 returns, the last one corresponding to the ground level. This last return was therefore retrieved and processed to generate elevation point data which served to build the land topography by each of the interpolation methods. Almost 64-million points were generated over the entire study area. To avoid edge effects during processing, all last return points were included in the processing. Subsequently, points extended 3300 feet, 1600 feet band 750 feet from the eastern, southern and western boundaries of the study area respectively.

To alleviate processing time and memory requirements, a random sampling was performed on the dataset to generate the sample data. Each of the 5 tiles was resampled using the minimum sample size (n) formula to make sure they are representative of the study area (source: Campbell, B. J and al, 2011): $n = \left((\sigma * t)/e\right)^2$ where σ is the standard deviation of heights, e the acceptable error of average value, and t is a value of Student's distribution with n-1 degrees of freedom. The bootstrap formula with 1000 iterations was used to calculate the standard deviation because it has the advantage of reducing the effect of outliers, should they exist. Since the sample size was big, the Student distribution was replaced by a normal distribution and t replaced by the z-score. A 95% confidence level (z-score = 1.96) and a margin of error (e) of +/- 5% were considered. from this, a total of 1,437,211 points was generated. It should be noted that the elevation values for the tile 37091f_SE were in feet while the others were in meters. Therefore, 37091f_SE was converted to meters.

2. Map building

All maps of the surface were created in Arcmap 10.4.1, using elevation values extracted from the LiDAR data. From the literature review, Bohling, G. (2005a) warned that significant deviations from normality and stationarity could cause problems in some interpolation methods' performance and suggested therefore that it is always best to begin by looking at a histogram or similar plot to check for normality and a posting of the data values in space to check for significant trends. The random generated sample was then tested for normality of the distribution of elevation values through the study area. The resulting histogram showed a slightly skewed distribution with the mean shifted to the right (figure 10).

Considering the potential effect of the factors discussed in the literature review on the performance of interpolation methods, the choice of the interpolation parameters was made in such a way to optimize the quality of the generated maps. That way, the assessment of the variability of the different methods could be less unbiased.

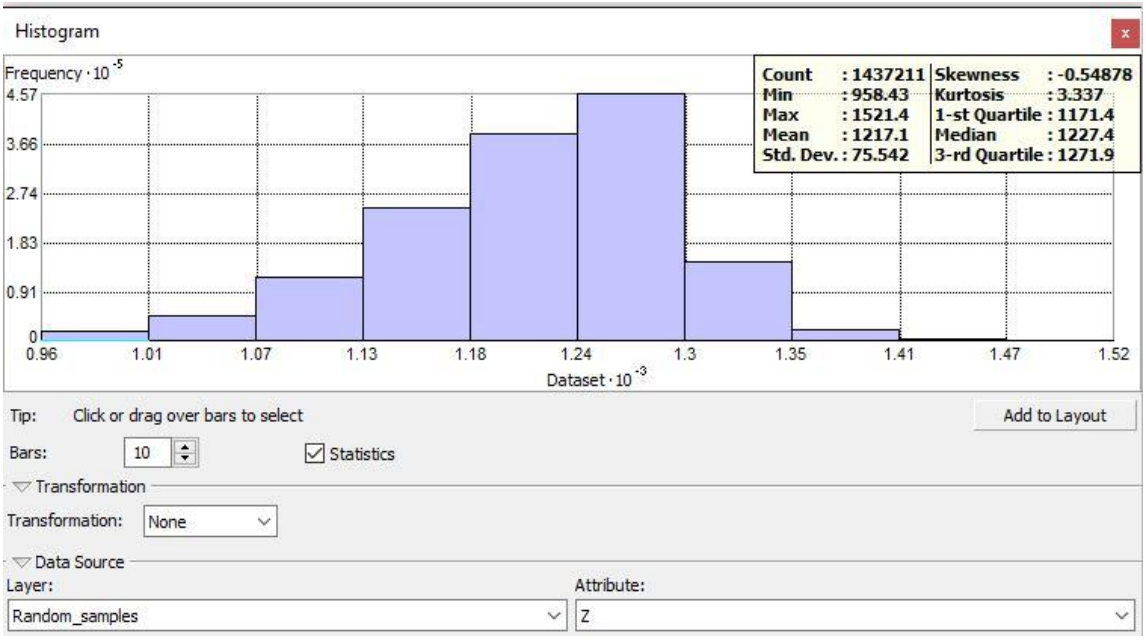

Figure 10: histogram showing the distribution of elevations at the Magmont mine area

As for the subsurface maps, elevation values for the top and the bottom of the mineralization intervals were used to build the top and bottom surface respectively. Those points were used as input for the subsequent interpolation methods. It has to be mentioned that the subsurface maps were completed for only regular spline and natural neighbor because the statistical test showed that their values were not significantly different from the original. The map algebra was also performed on the top and bottom surfaces of the orebody to check for the consistency of the results obtained on the surface data. Prior to any analysis, a distribution test was performed to check for normality.

A test for the sensitivity of interpolation methods to samples size and sample density was performed on about one quarter of the random samples previously generated. The same methodology was applied as previously, that is the estimated values were retrieved for each method and compared to the original's. The same, math algebra was performed on the resulting maps to analyze the distribution of the differences.

Armap gives many options to access the interpolation tools within the toolbox. The configuration of the toolboxes may also differ slightly according to the access path. Table 1 summarizes the location of the interpolation methods used in this thesis.

Table 3: location of interpolation methods within Arcmap 10.4.1 toolbox and its extension geostatistical analyst tool

Toolbox	3D analyst tool	Spatial analyst tool	Geostatistical analyst tool
Interpolation method	• Inverse distance weighting • Kriging • Natural neighbor • Spline • Triangulated irregular network	• Inverse distance weighting • kriging • Natural neighbor • Spline	• Inverse distance weighting • kriging • radial basis function (spline, thin plate spline)

The 'geostatistical analyst tool' has a wizard assisting in the automatic choice of the optimal parameters. Therefore, it was preferentially used to perform the interpolation

whenever possible. For the sake of comparison, all maps were classified using the same number and range of classes.

2. 1 Triangulated irregular network (TIN) method

A TIN map was built using the ‘create TIN’ function under the 3D analyst tool. This map served as a reference map for further comparisons. The following specifications were used based on the descriptions provided by the Arcmap documentation:

- Points were specified as “mass points”, to allow the assignment of values to the nodes used in the triangulation of the surface
- All nodes were used because Arcmap limits to 6 million, the number of nodes below which the computation is efficient
- The elevations’ column was specified for the interpolated surface to be generated within the limits of the study area; otherwise, choosing the “none” keyword would result in the feature’s elevation being interpolated from the surrounding surface.
- In case there would be breaklines, the ‘constrained Delaunay’ option was left unchecked to allow the TIN to densify each segment to produce multiple triangle edges. This way, the estimate should be smoother.

2. 2 Ordinary kriging method

Based on the description of the factors influencing ordinary kriging performance in the literature review, the choice of the parameters was done to meet the most optimal results. The choices involved especially the parameters of the semivariogram (figure 11) namely: the fitting function, the nugget effect, the sill and the range. The geostatistical analyst tool contains an optimization function which helps choose automatically the best

estimation parameters. In the case of the present study, the optimization tool returned the following parameters:

- 12 lags were defined
- Lag size: 4.672039
- Partial sill: 31.75868
- The fitting model was automatically set to “stable”
- Neighbor type: standard
- Maximum neighbors:5
- Minimum neighbors:2
- Sector type: 8 sectors
- mean error: 0.007489 foot
- average standard error: 5.028181%

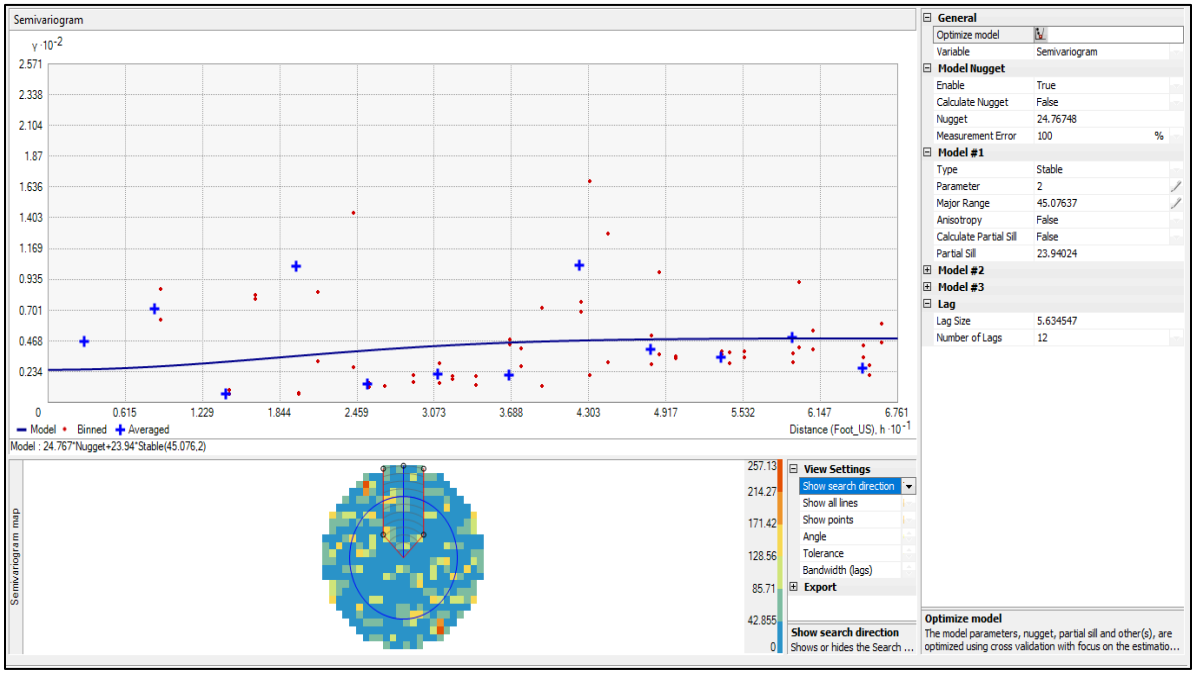

Figure 11: semivariogram of ordinary kriging

A cross validation was completed on the dataset, resulting in a regression function of the prediction errors of approximately: 0.99756 x + 3.33719 (figure 12).

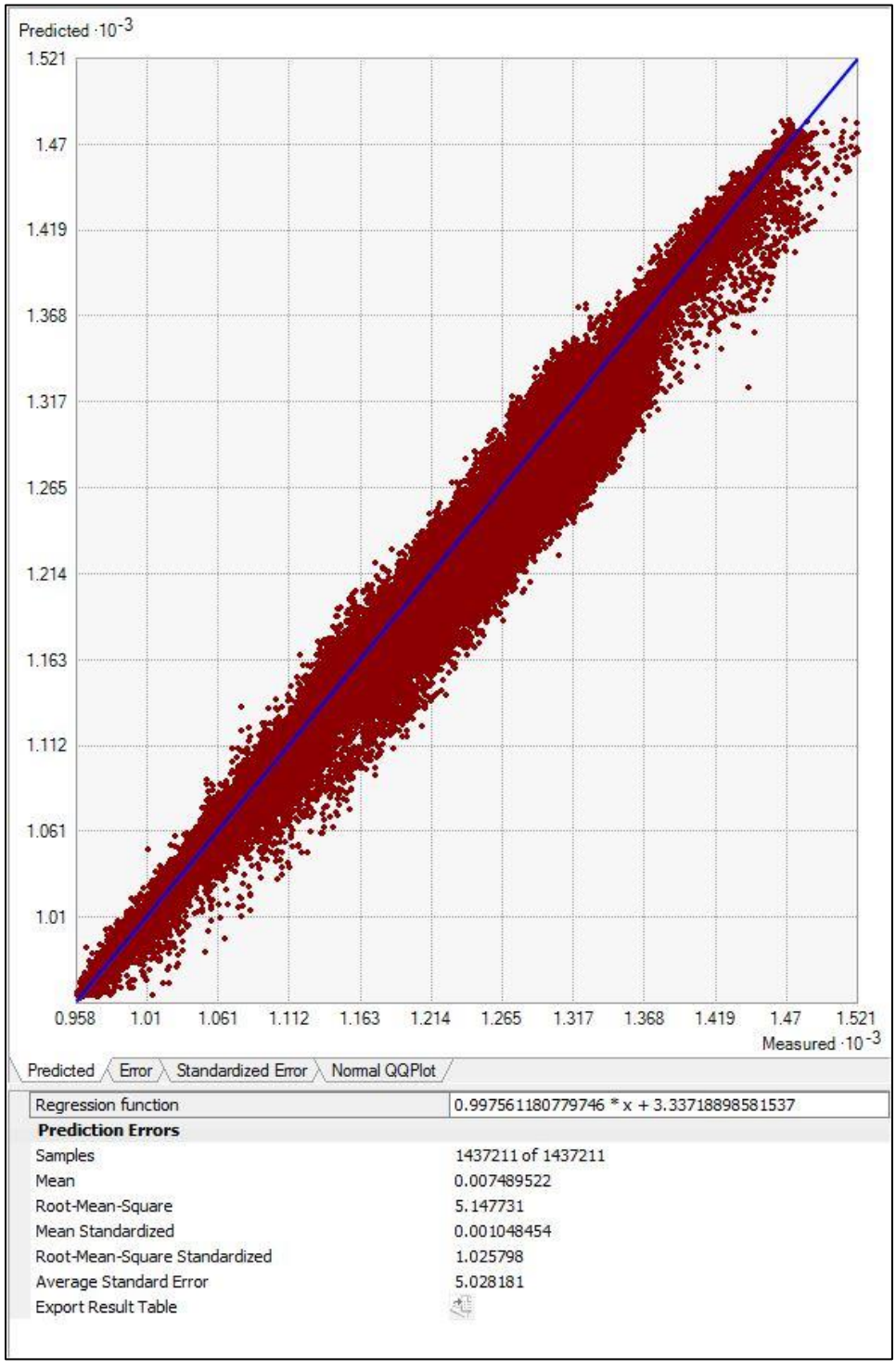

Figure 12: Ordinary kriging prediction errors regression graph

2. 3 Simple Kriging Method

As with the ordinary kriging, simple kriging also used the geostatistical wizard to generate the surface map. Similarly, the optimization tool returned the following parameters for the semivariogram (figure 13):

- fitting function: exponential
- Nugget: 69.9
- Number of lags: 12
- Lag size: 356.5225
- Maximum neighbors:5
- Minimum neighbors:2
- Sector type: 8 sectors
- Mean error: 0.007736%
- Average standard error:4.07784

The cross validation generated a prediction error regression function as: 0.999 x + 1.36748 (figure 14).

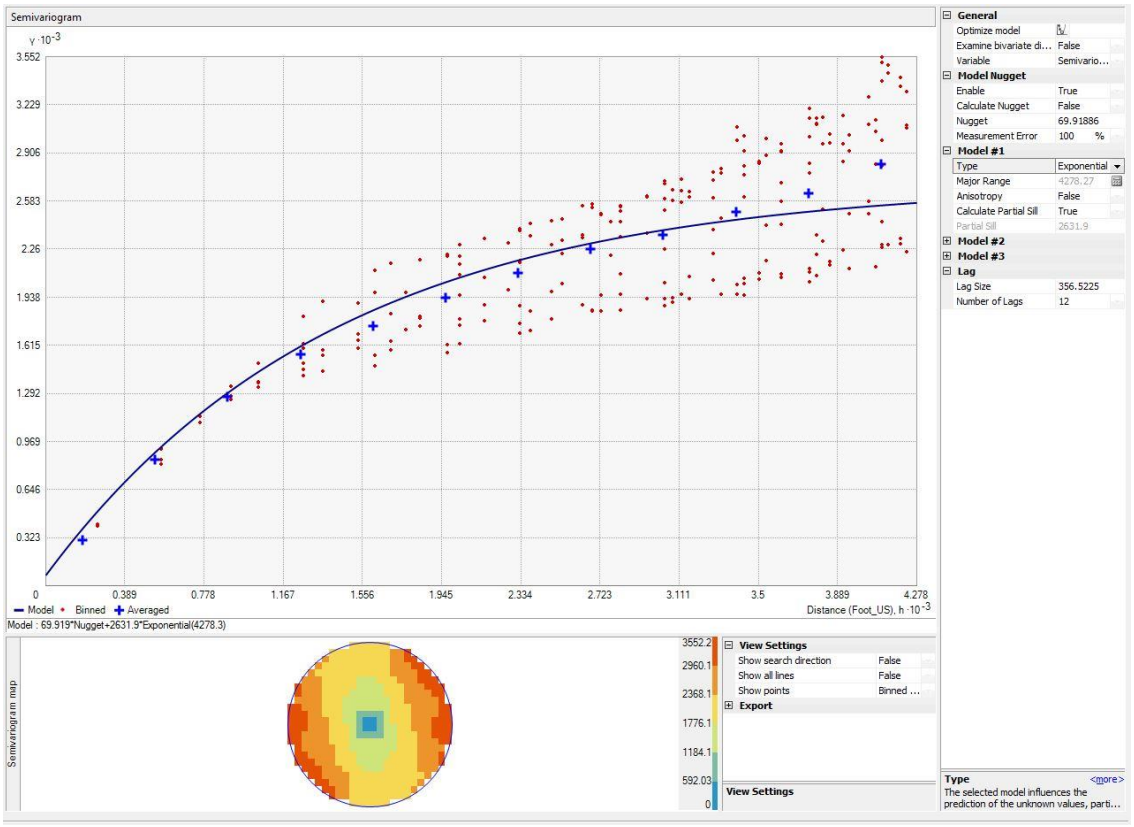

Figure 13: simple kriging semivariogram

2. 4 Universal kriging method

The geostatistical wizard was also used to build the topographic map for universal kriging. Following the recommendations in the literature review, a second order polynomial function was used to remove the trend. Arcmap offers constant, first, second and third order function for the trend removal but the second order appears to be the most used and also higher order can rather bring more inconveniences. Once again, the model optimization function was used to get the best fit parameters (figure 15). Consequently, a value of 40 was generated for the "exploratory trend surface analysis" whose values vary from 0 to 100, 0 constraining the algorithm to behave as a global polynomial function and

any value greater than between 0 and 100 making it to use local polynomial interpolation. A goodness of fit of 4.904272 was obtained. Other parameters include:

- Nugget: 0.001474
- Model type: stable
- Partial sill:1.474772
- Lag size: 0.3979775
- Number of lags:12
- Octant search: 8 sectors
- Mean error: 0.006892
- Average standard error:1.230284

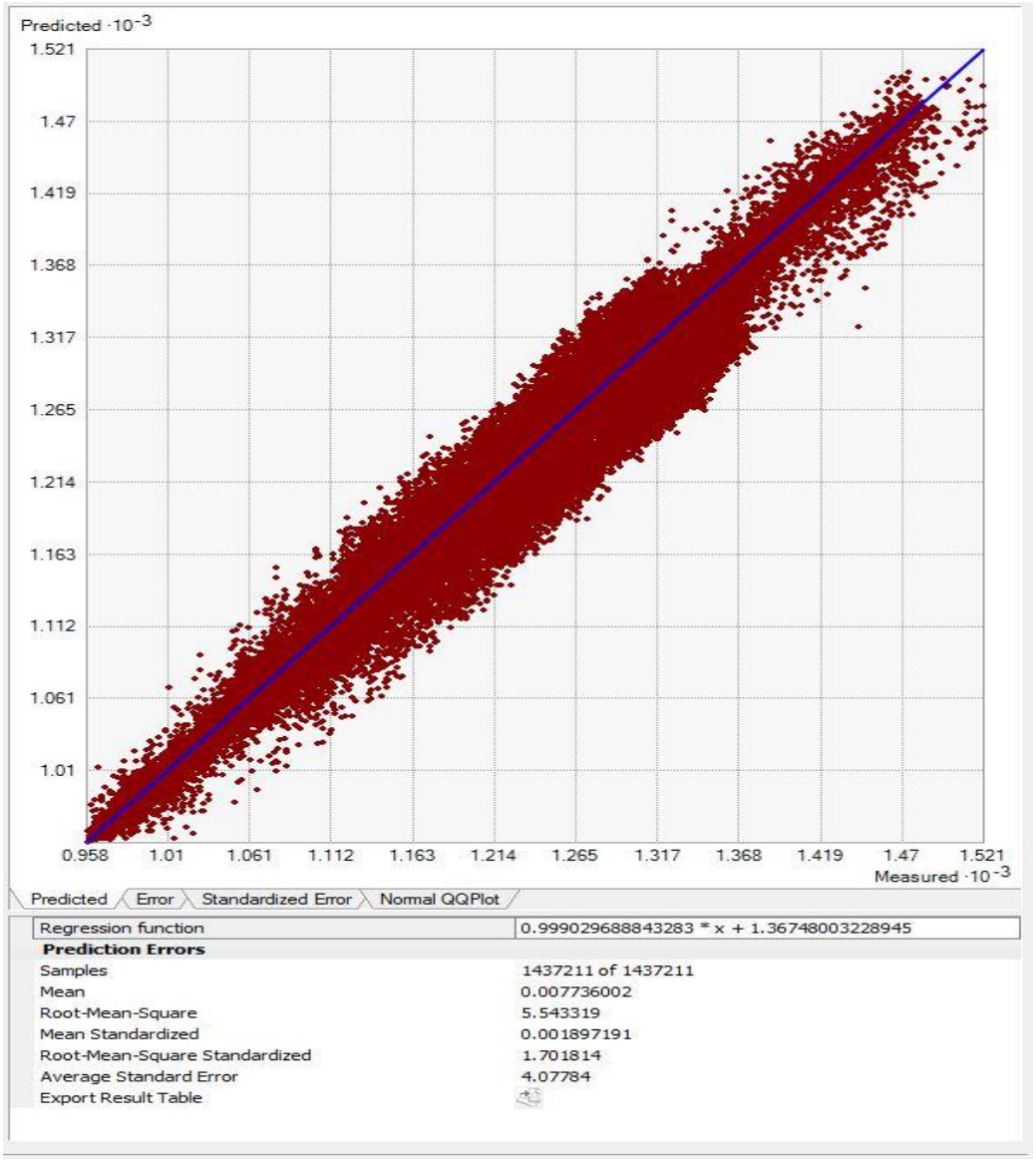

Figure 14: simple kriging prediction errors regression graph

The cross validation returned the prediction errors regression function: 0.9989 x + 1.6241 (figure 16). An advanced mode is available in the wizard to help parameterize the search function in case no data was found in the neighborhood. Given the relative abundance of data in the study area, this function was not used.

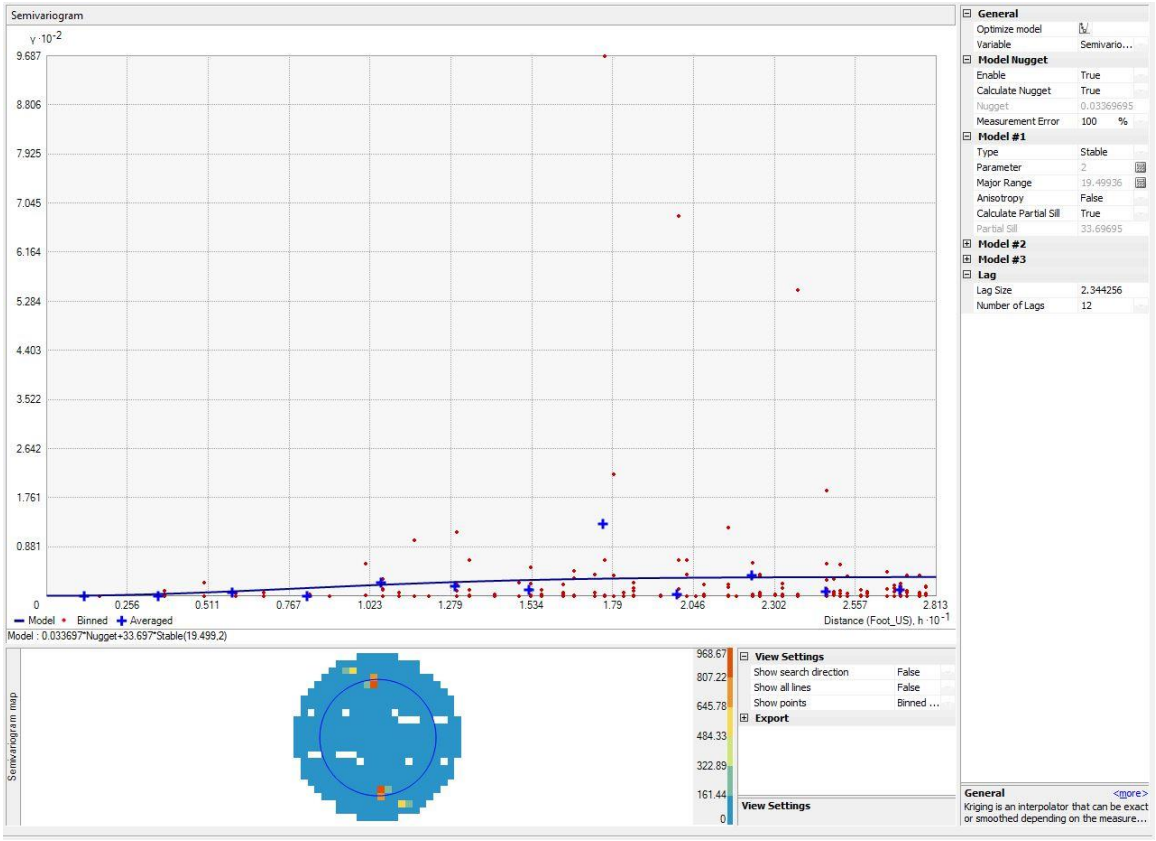

Figure 15: universal kriging semivariogram

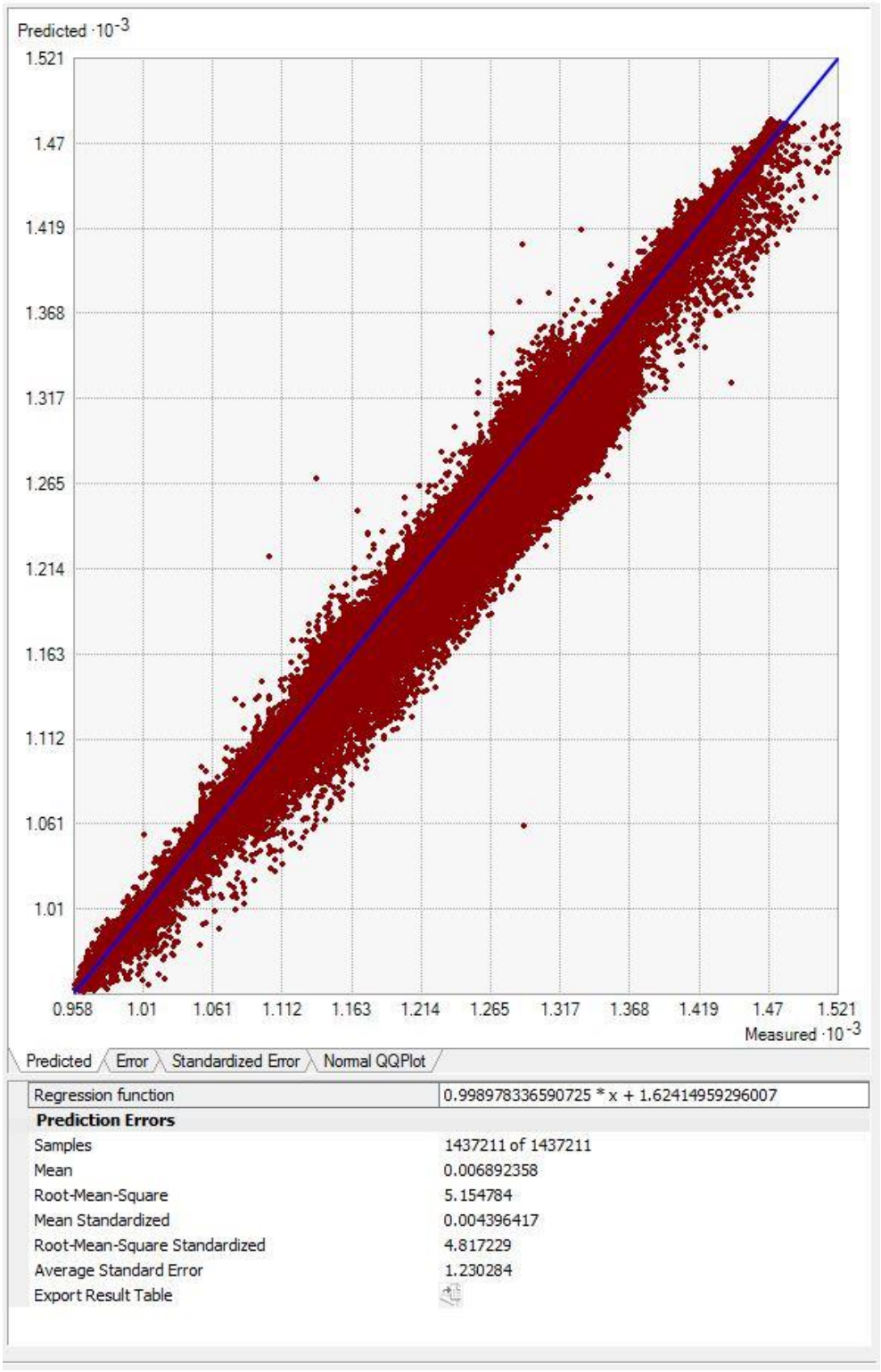

Figure 16: universal kriging prediction errors regression graph

2. 5 Inverse distance weighting method

Inverse distance is also a model available in the geostatistical wizard. From the literature review, the inverse distance method has a power variable whose choice influences the performance of method by controlling the influence of known values on the interpolated values, based on their distance from the predicted point. Like for the kriging interpolation methods, the wizard offers the possibility to automatically set the optimal weights of the reference points through the power component. The resulting parameters were:

- Sector type: 8 sectors
- Minimum neighbors: 10
- Maximum neighbors: 15
- Power: 1.9491
- Root Mean Square Error: 5.35679

The regression function for the error prediction was of the form: 0.9966 x + 1.4941 (figure 17).

2. 6 Nearest neighbor

The nearest neighbor interpolation algorithm was not available as a tool in Arcmap to produce an isopleth map. Instead, QGIS was used to generate the corresponding map. An arbitrary choice of 150 feet was made for the search radius a search angle of 360 degrees considered for the definition of the area within which the nearest neighbors were to be looked for.

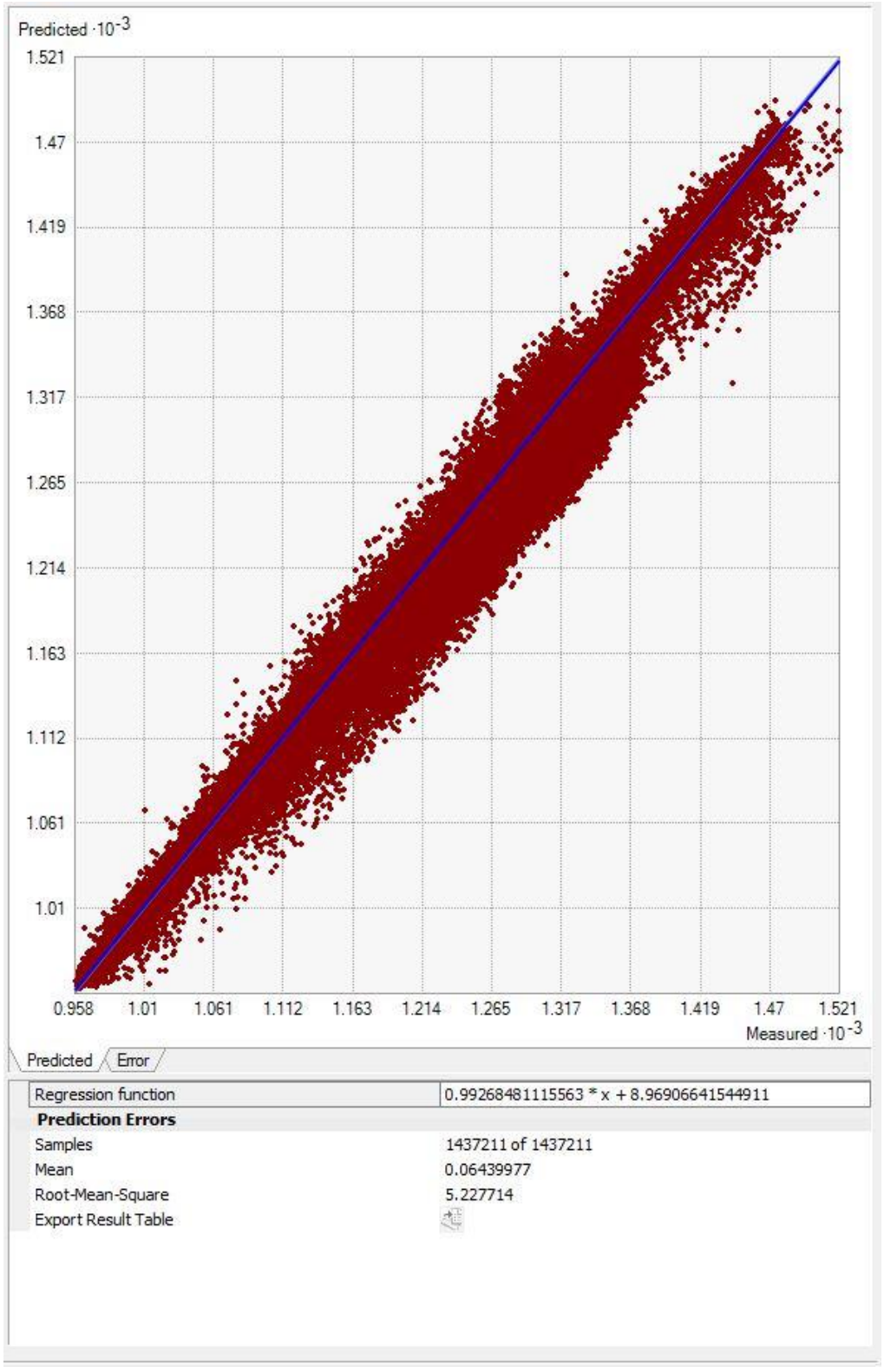

Figure 17: inverse distance weighting prediction errors regression graph

2. 7 Natural neighbor method

The implementation of the natural neighbor method is straight forward in the 3D analyst tool or the spatial analyst tool. It only requires the definition of the output cell size, at which the output will be created. The default value of 82.4065 ft generated by the algorithm was considered. By default, Arcmap generates that value by taking the shorter of the height of the study area and dividing it by 250.

2. 8 Spline method

According to Arcmap documentation, there are two options for the spline interpolation method: the regularized option and the tension option. With the regularized option, higher values used for the weight parameter produce smoother surface; typical values being 0, 0.001, 0.01, 0.1 and 0.5. Another determinant factor is the number of points per region used for local approximation; the higher the number, the smoother the surface of the output raster.

Due to the complexity of the spline algorithm as mentioned in the literature review, the spline function was accessed through “radial basis functions” under the geostatistical analyst tool rather than the spatial analyst because it has more options for the choice of the neighbors and therefore control the output better. The wizard allowed the choice of the optimal parameters as follow:

- Kernel function: completely regularized spline
- Kernel parameter: 1.6
- Radius: 7852.2446 feet,
- Minimum neighbors: 8

- Maximum neighbors: 8
- Search sectors: 8
- Spline type: regularized
- Weight: 0.5
- Root Mean Square error: 6.9290
- Number of points per region used for local approximation: 12 (default value)

The cross-validation process allowed the estimation of the error function as: 0.9988 x + 1.70744. It must be noted that spline does not have a prediction error.

2. 9 Thin plate spline method

Thin plate spline used the following parameters:

- Kernel function: thin plate spline
- Kernel parameter: 1e20
- Radius: 7852.2446 feet,
- Minimum neighbors:8
- Maximum neighbors: 8

The subsequent mean error was 0.00644 and the regression function: 0.9988 x + 1.493669 (figure 18).

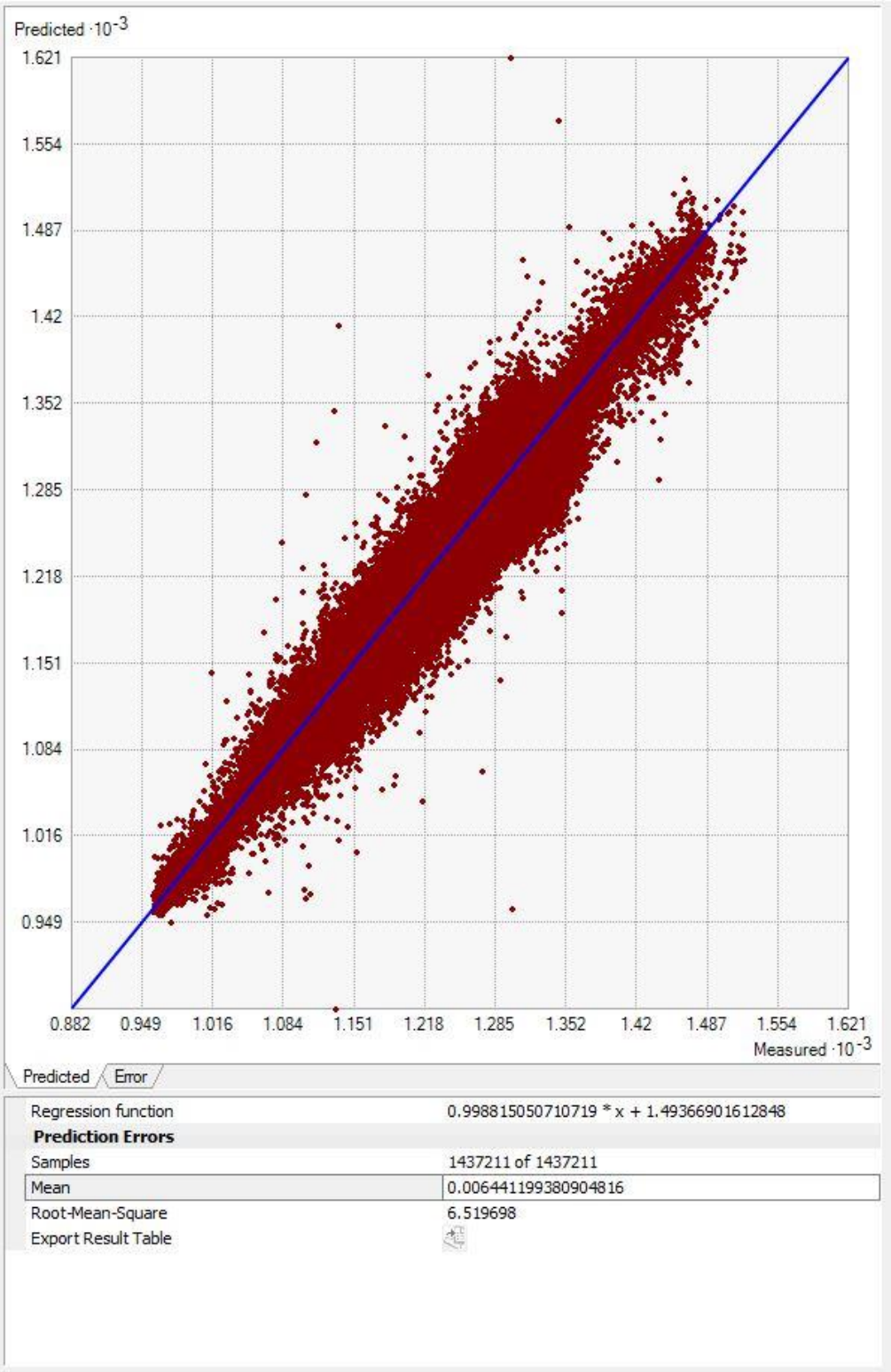

Figure 18: thin plate prediction errors regression graph

3. Assessment of the variability among interpolation methods

3. 1 The quantitative assessment

a) The statistical method

Each interpolation method generated a ‘new’ dataset based on the original point values. The interpolated values were retrieved and then compared to the ‘original values’. The geostatistical analyst tool allowed the retrieval of those values as a separate table for OK, SK, IDW and thin plate spline. It is to be noted that the computation of the interpolated points goes along with that of the errors. For the TIN, spline, natural and nearest neighbors however, the interpolated values were not automatically computed as a separate output. Therefore, a conversion operation from raster to points was necessary to retrieve them. All generated points were then compared to the original values through a statistical paired t-test, using ‘R’. The null hypothesis was the assumption that: ‘the interpolated values are the same as the original ones’ with a confidence of 95%: if the p-value returned less than 0.05, then the interpolated values could be considered different from the reference one, otherwise the null hypothesis could be rejected.

b) The math algebra method

To assess the ‘variability among the different interpolation methods, the difference operation was used within the map algebra tool. Based on the results of the statistical test, the natural neighbor map was used as a reference and the other maps compared to it. The resulting differences were then grouped in nine classes to highlight the losses and gains of each method about the reference elevations. Those classes were: <-100, [-100, -30], [-30, -3], [-3, -1], [-1,1], [1,3], [3,30], [30,100] an >100. Also, a

pattern analysis of the differences was conducted to check for the eventuality of the clustering of the data, since sample density can influence the precision of the measurements at a given location.

3. 2 The qualitative assessment

The qualitative assessment was purely descriptive and consisted in the comparison of the mathematical functions used by each method to make estimations. The comparison relied on the guidelines proposed by Li and Heap (2014) and Bohling (2005) as well as some observations made during the processing.

Chapter 4. RESULTS

4. The interpolation maps

4. 1 The surficial maps

The reference elevation values range from 959 feet to 1501 feet with a mean value of 1212 feet; the elevations generated by the eight SIMs however ranged from 984 feet to 1491 feet. These values were grouped into eleven equal interval classes of 50 feet width, from 950 feet to 1500 feet, to build surficial maps that are comparable (figure 19 to 26).

a) Triangulated irregular network

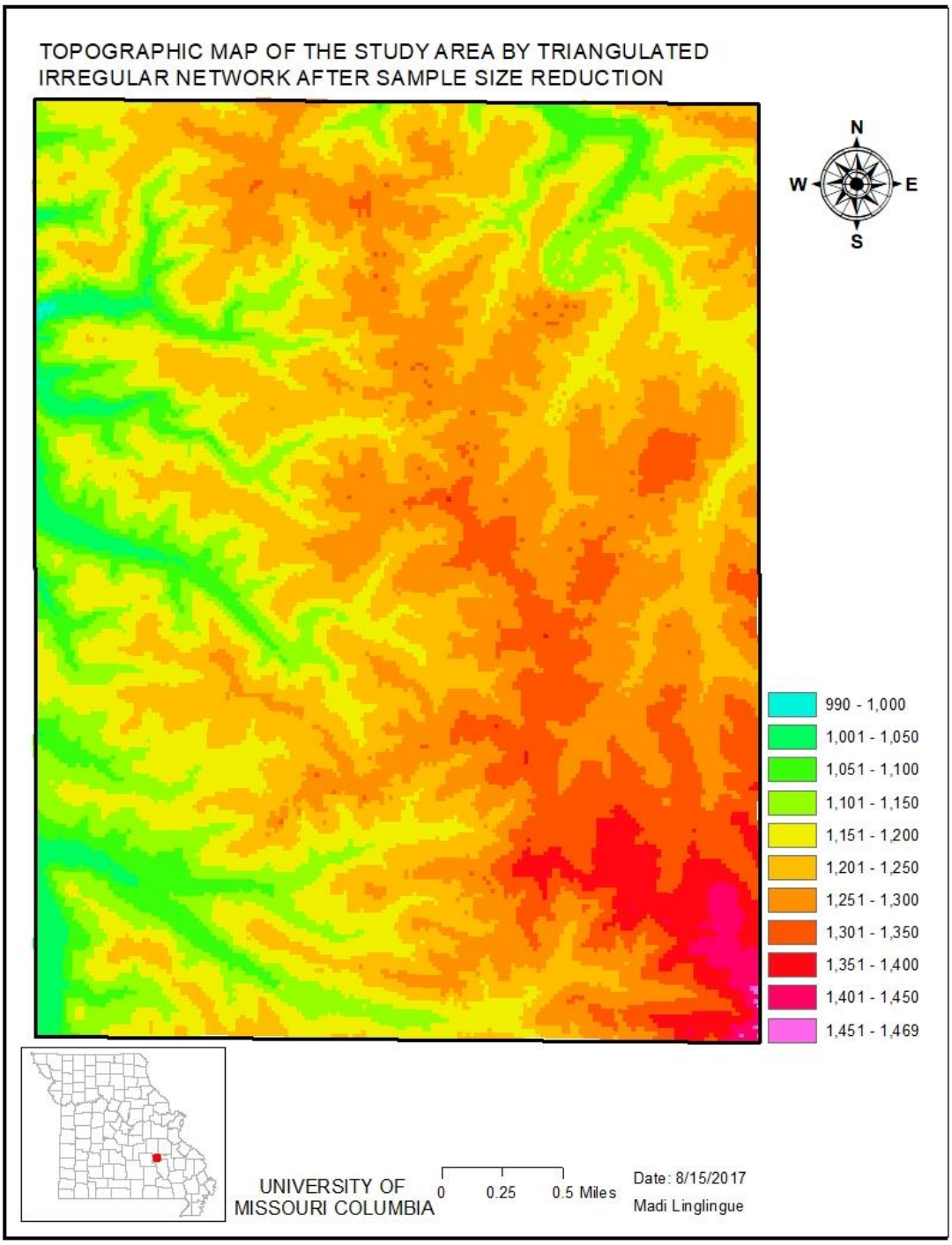

Figure 19: topographic map generated by triangulated irregular network method

b) Ordinary kriging

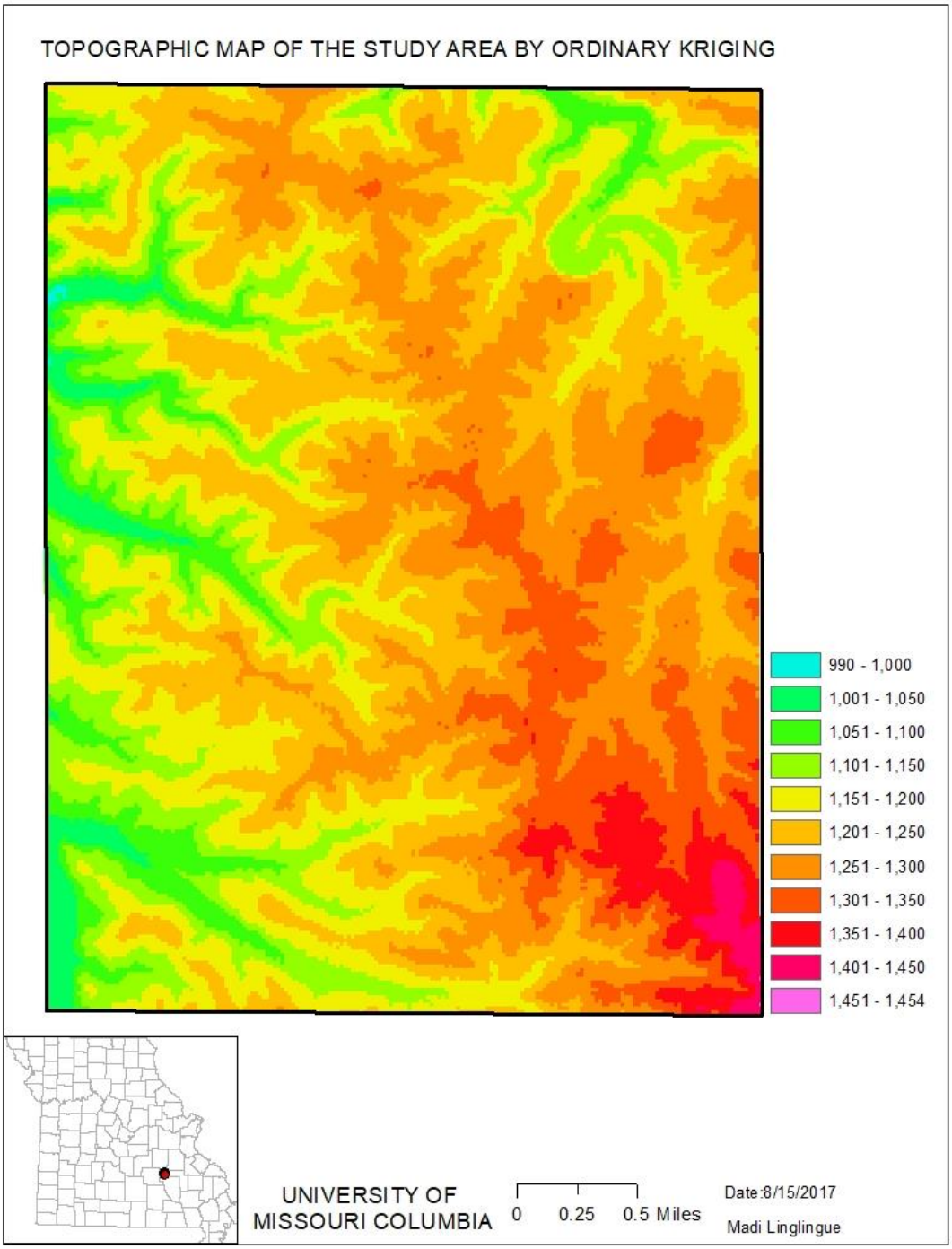

Figure 20: topographic map generated by ordinary kriging

c) Simple kriging

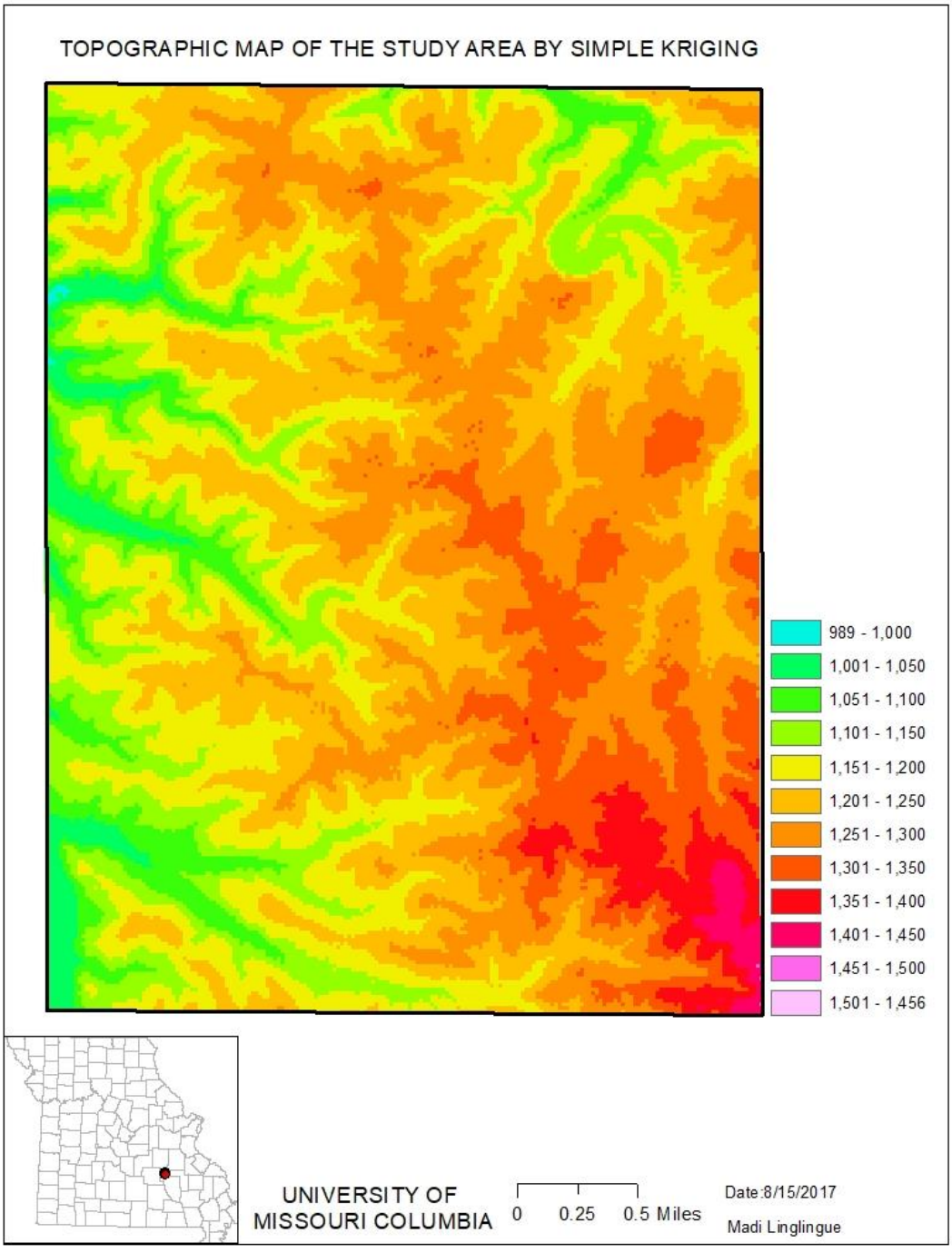

Figure 21: topographic map generated by simple kriging

d) Inverse distance weighting method

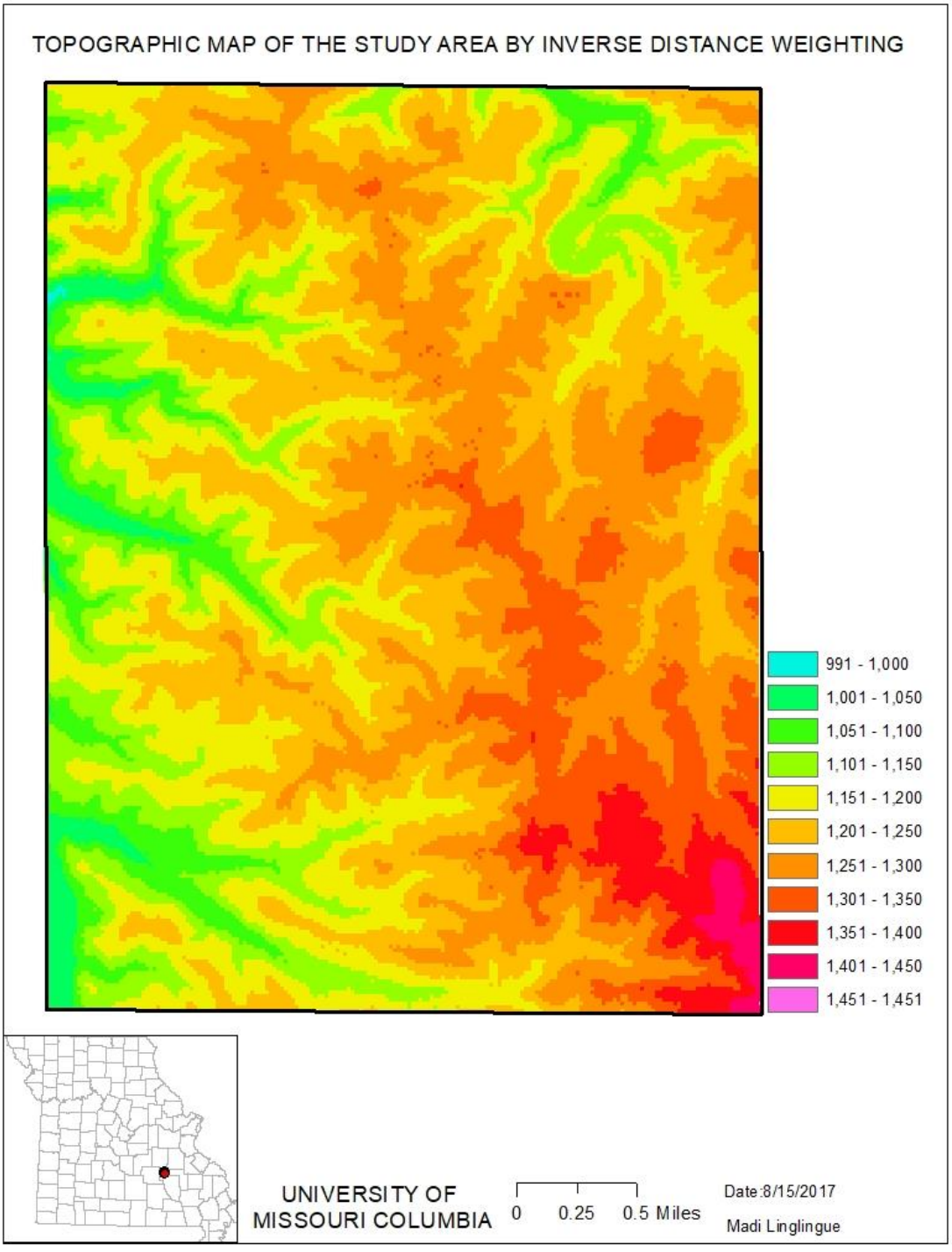

Figure 22: topographic map generated by inverse distance weighting

e) Spline

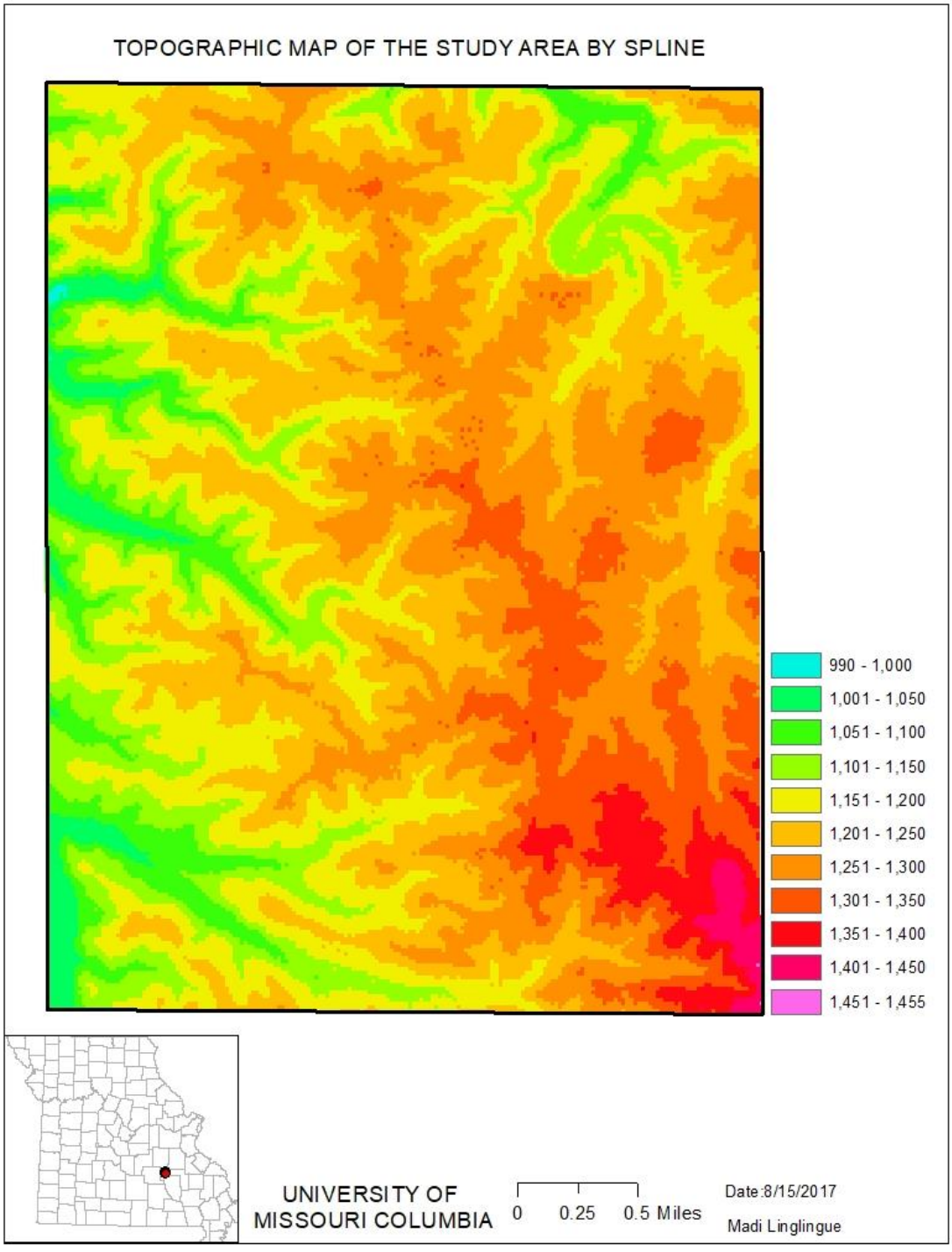

Figure 23: topographic map generated by the spline method

f) Thin plate spline

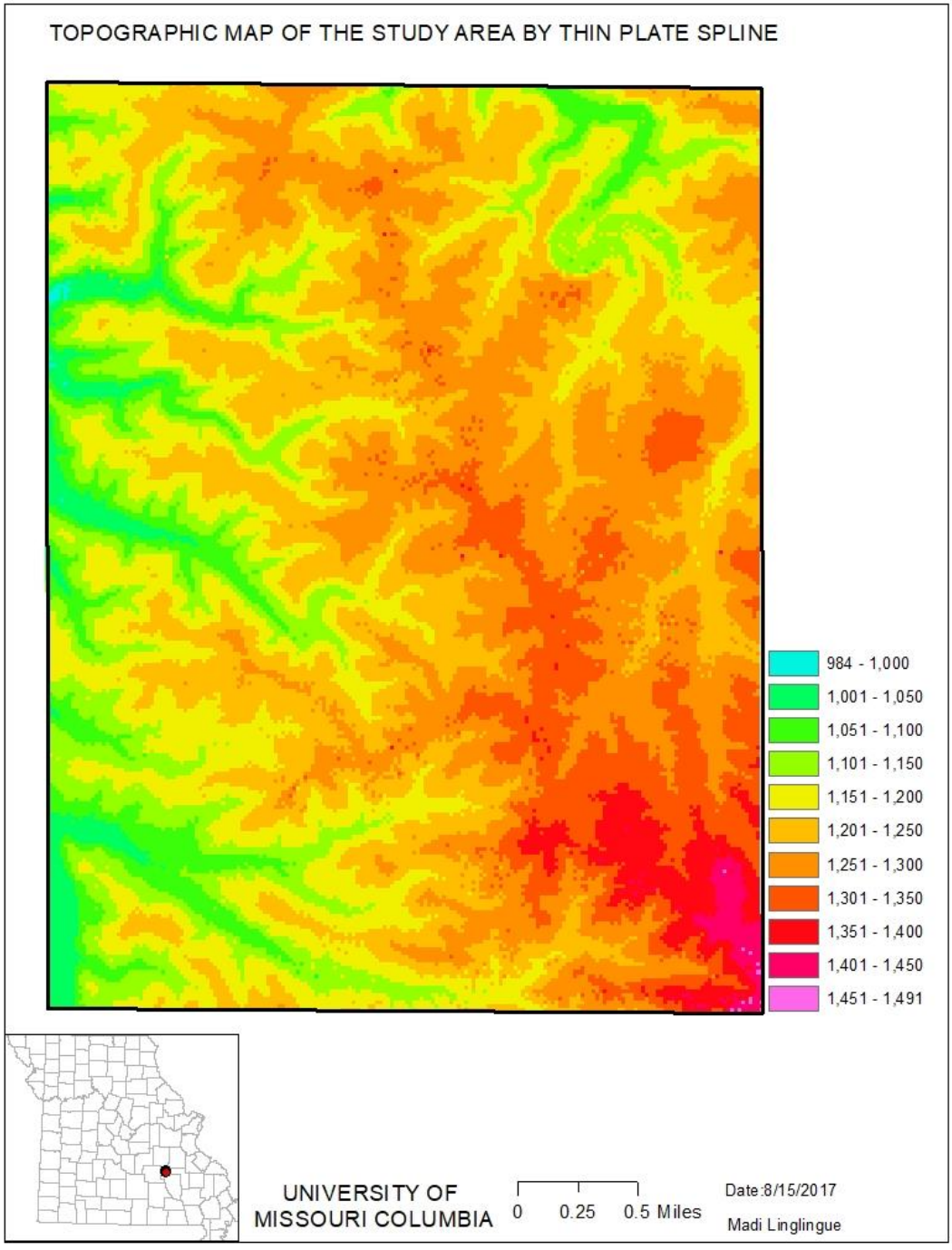

Figure 24: topographic map generated by thin plate spline method

g) Natural neighbor

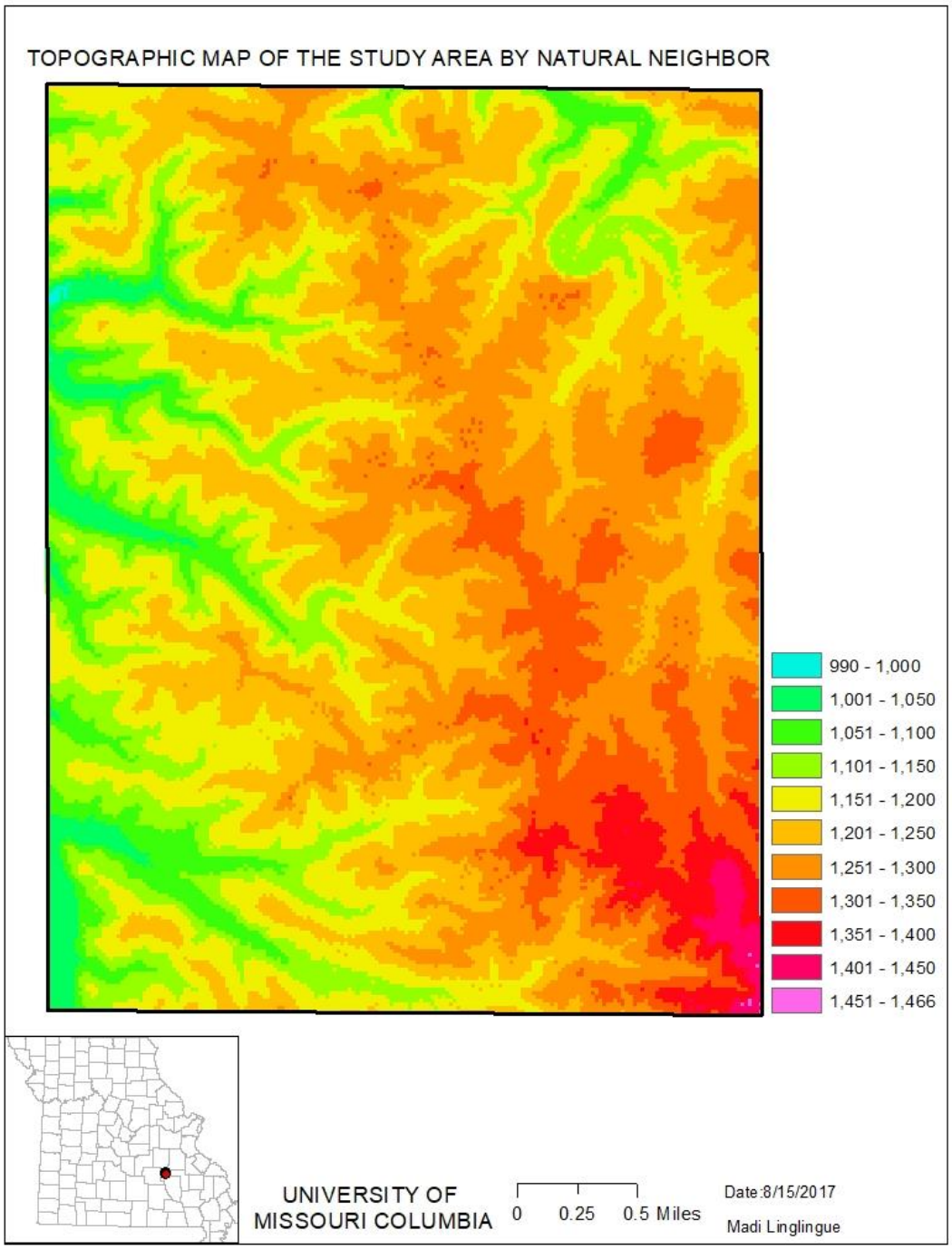

Figure 25: topographic map generated by the natural neighbor method

h) Nearest neighbor

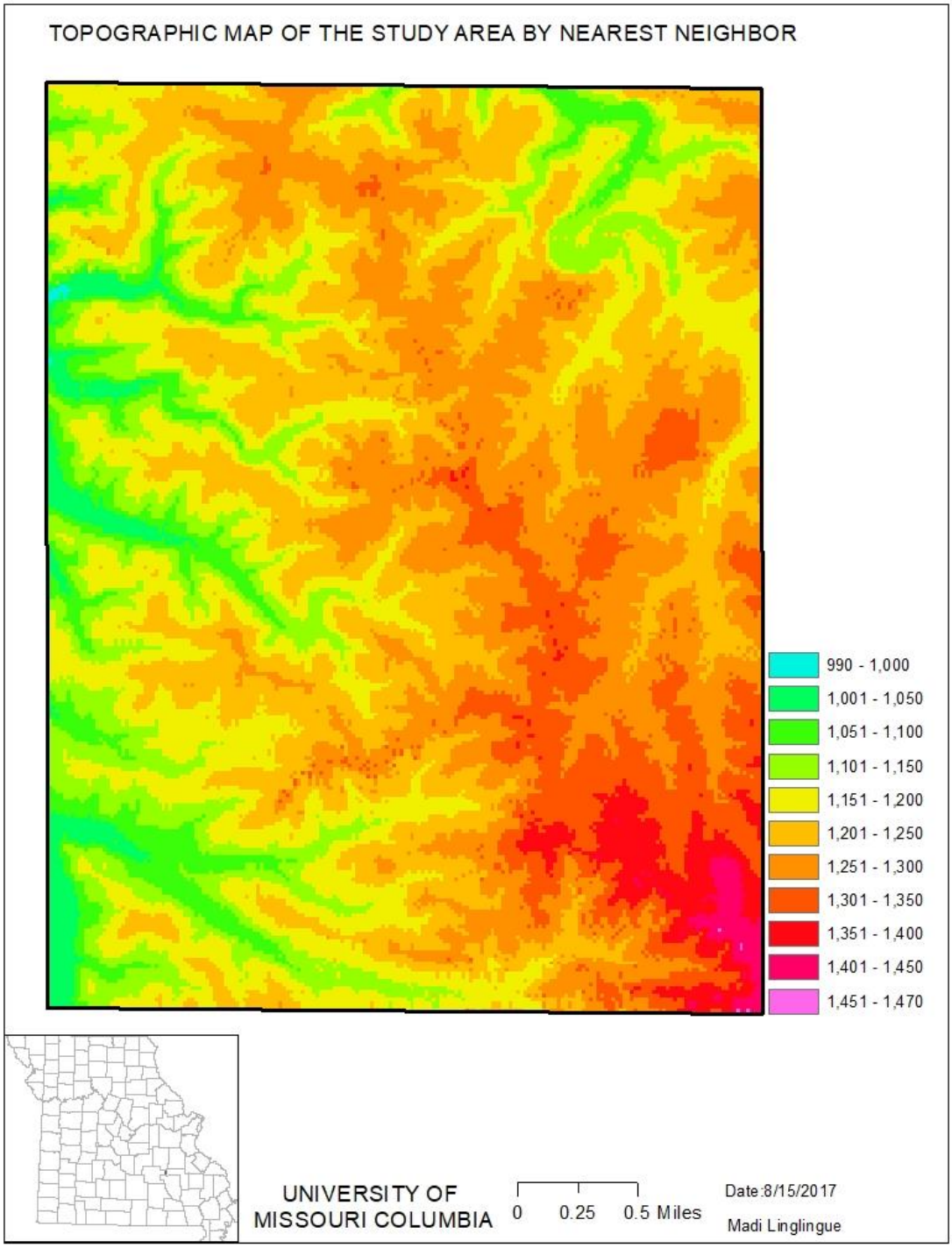

Figure 26: topographic map generated by the nearest neighbor method

All maps showed an elevation feature to the southeast of the study area prolonged by a divide trending northwest. Topographic highs are also observed along the eastern edge of the study area and at a smaller extent along the southern border. This topographic configuration is responsible for the two main drains located east and west of the divide respectively. This configuration was supported by the trend analysis performed under the geostatistical tool in Arcmap 10.4.1 (figure 27). The tool gives two cross sectional representations of the topography along a west-east profile (plane XZ, in green) and north-south (plane YZ, in blue).

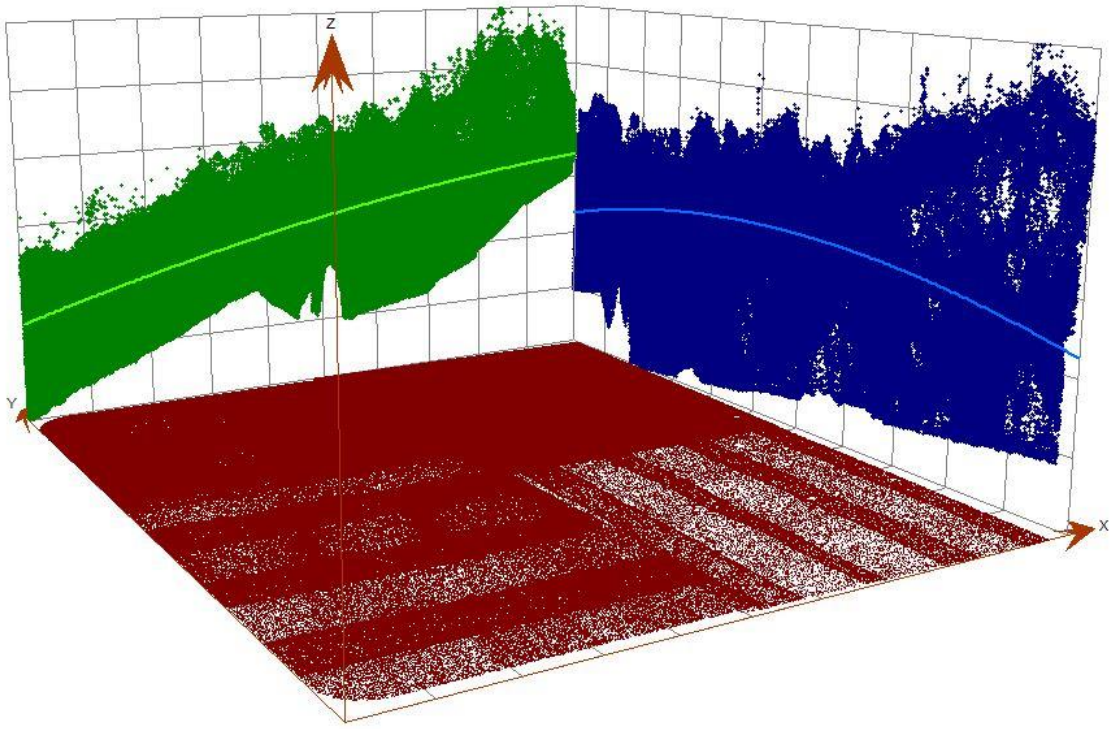

Figure 27: elevations at Magmont mine area raise from north to south then from west to east

Visually, all maps look similar. To test the sensitivity of interpolation to sample size, about 25% of the previous sample size were taken and processed (figure 28 to 34).

4. 2 The maps resulting from resampling of the random samples

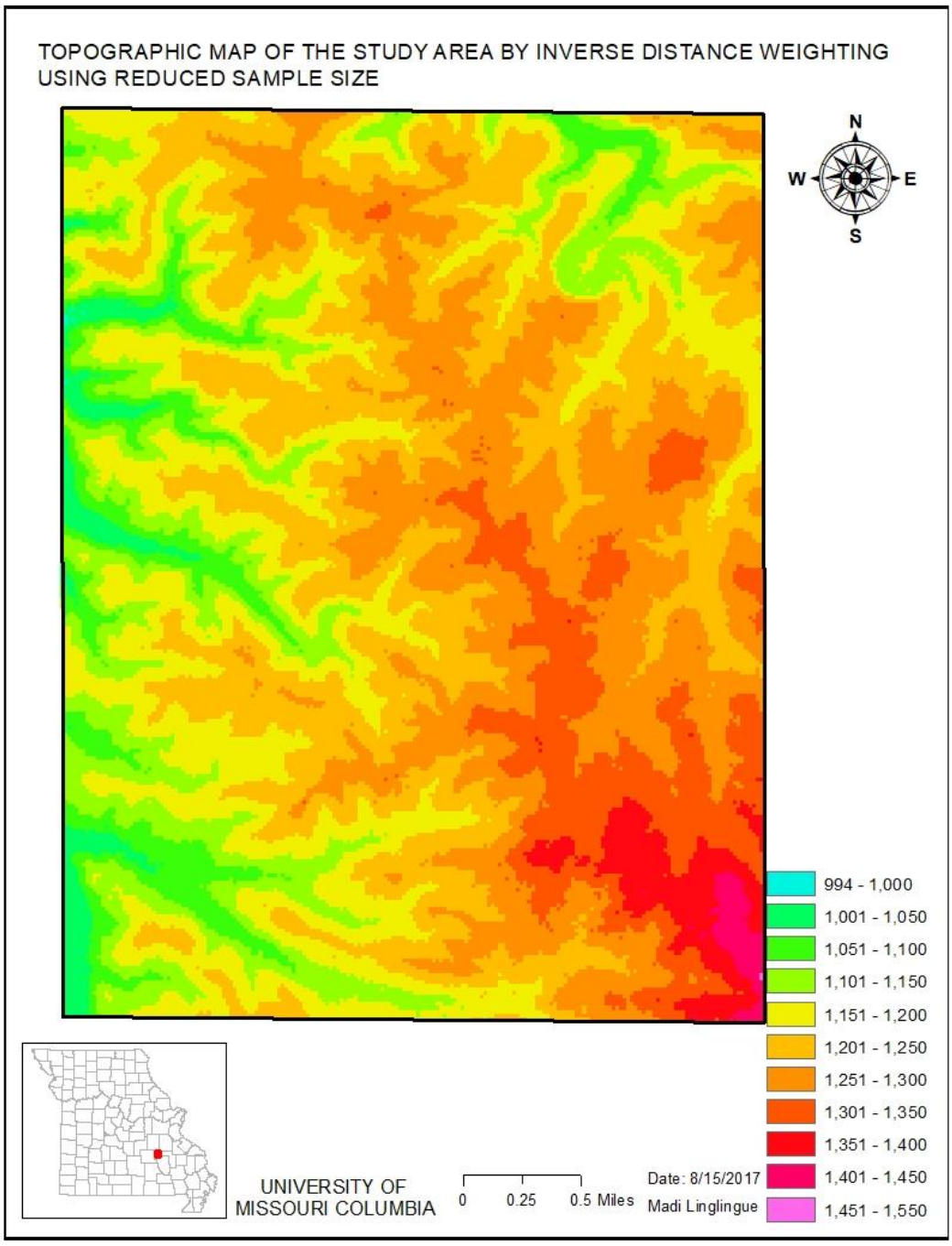

Figure 28: inverse distance topographic map after sample size reduction

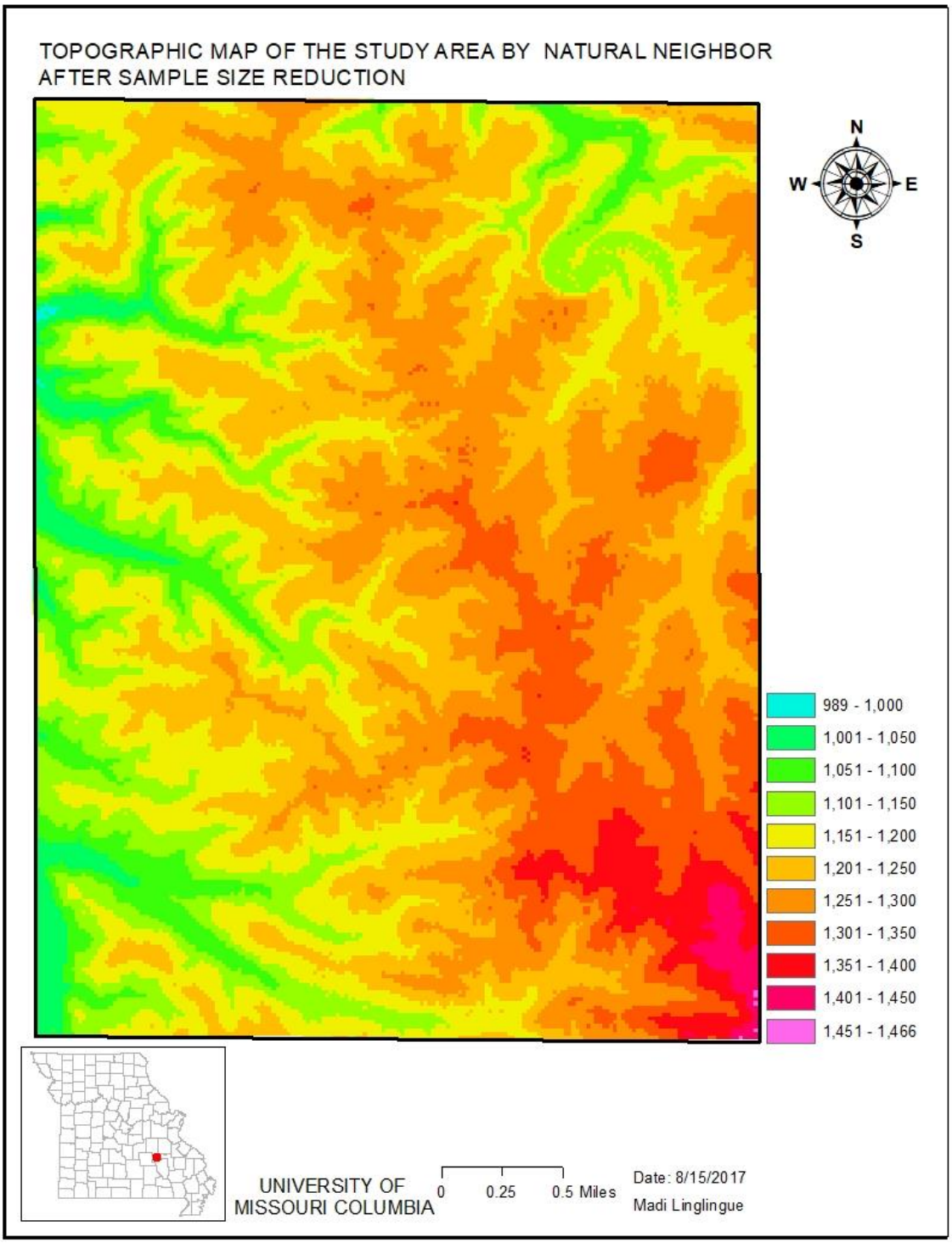

Figure 29: natural neighbor topographic map after sample size reduction

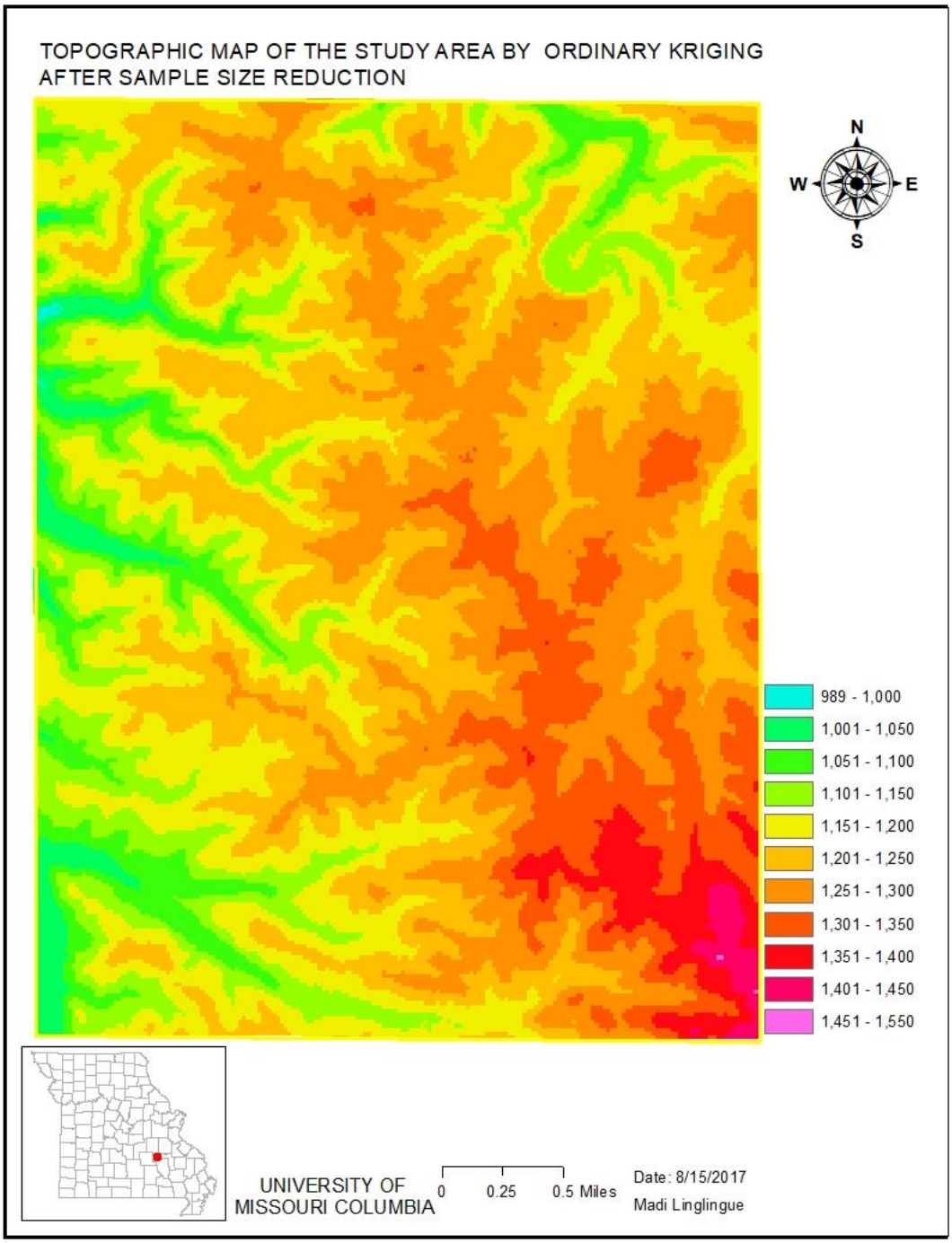

Figure 30: ordinary kriging topographic map after sample size reduction

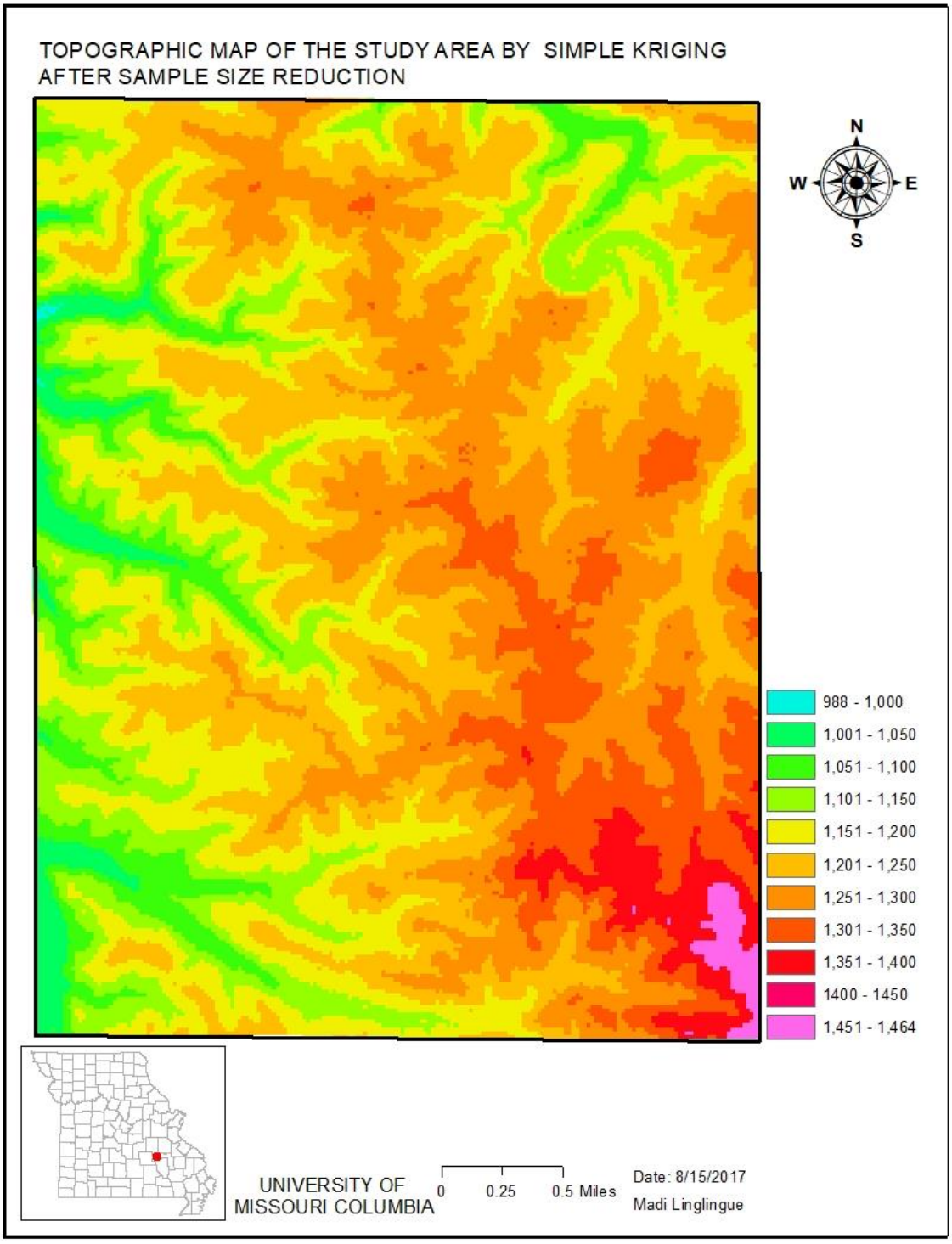

Figure 31: simple kriging topographic map after sample size reduction

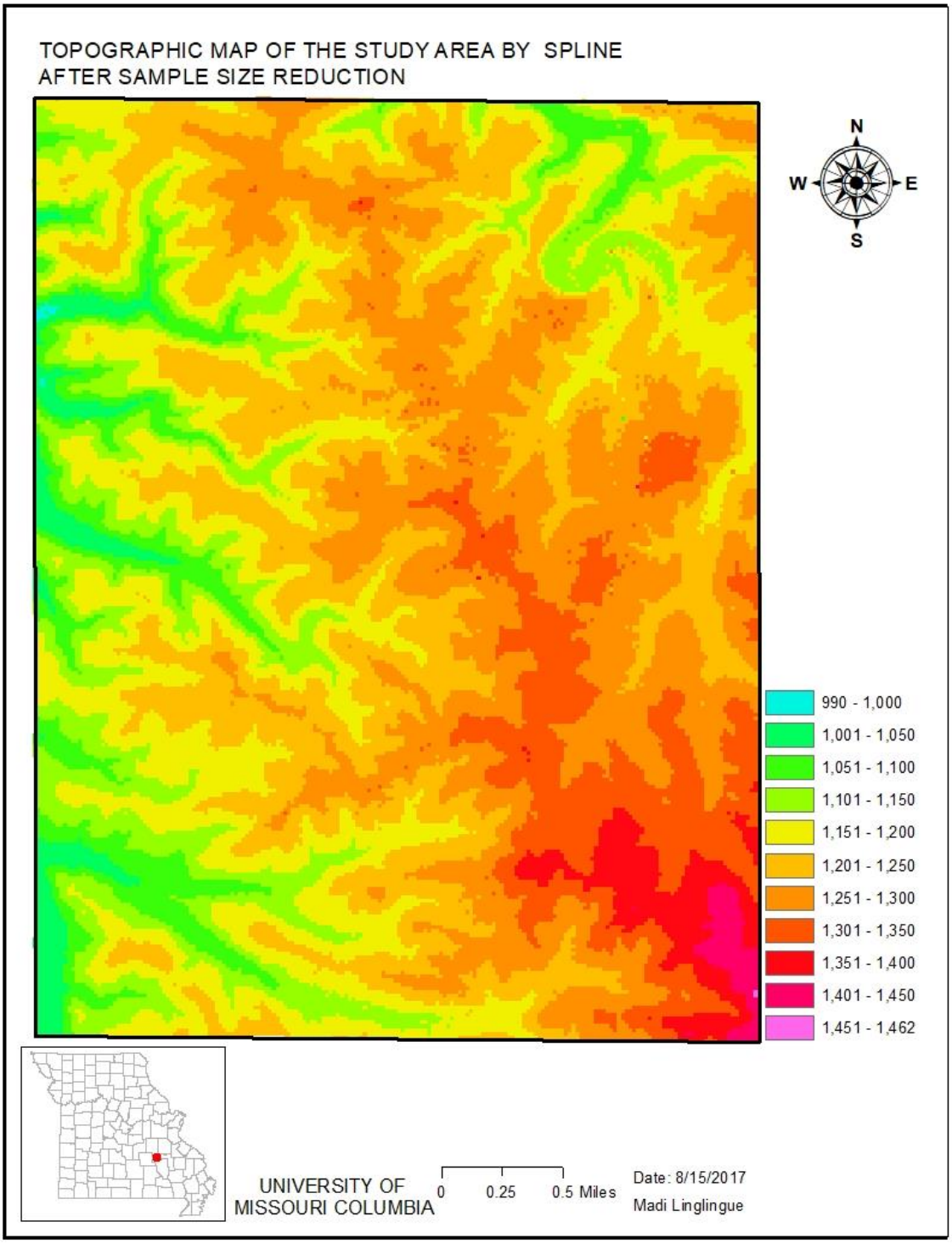

Figure 32: spline topographic map after sample size reduction

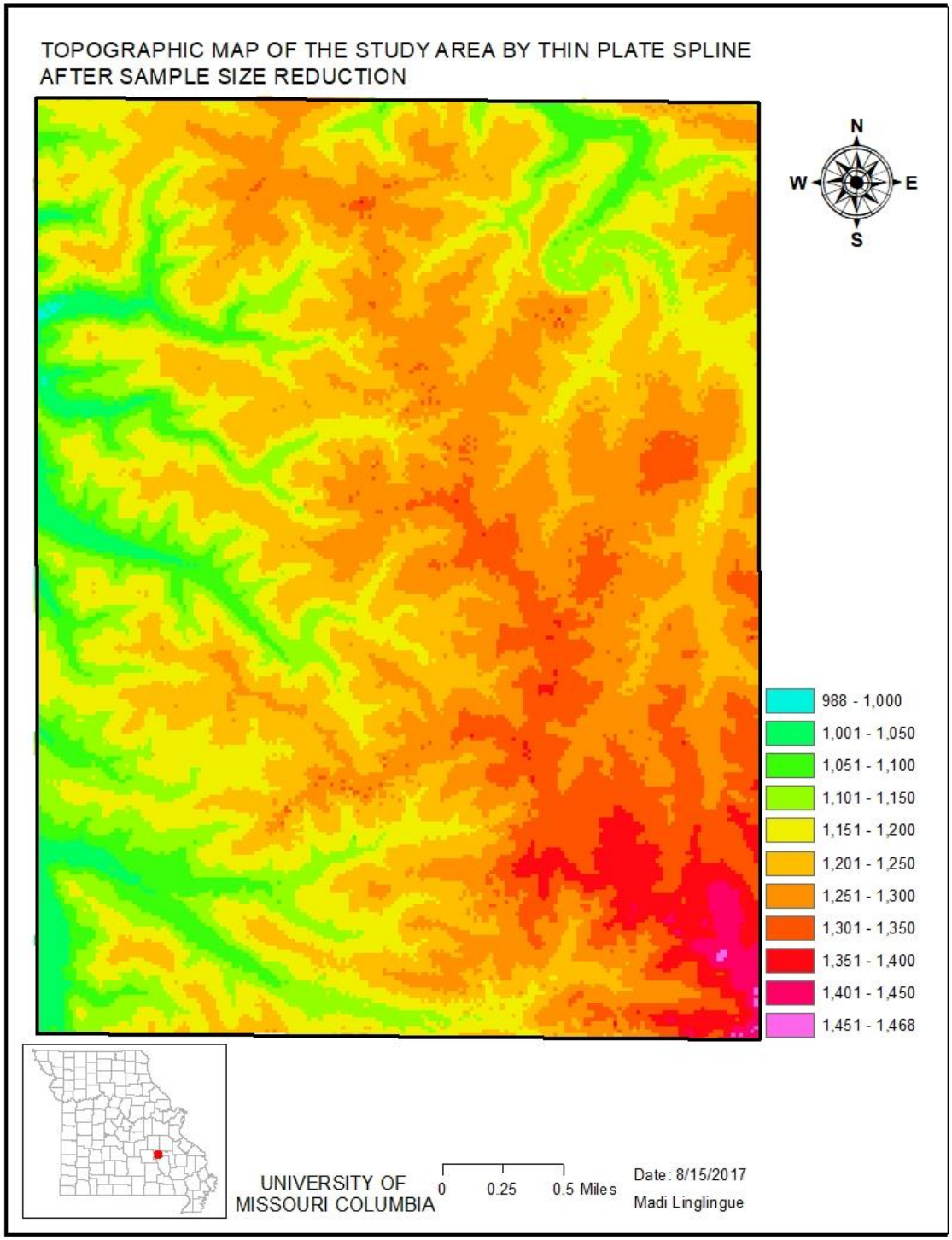

Figure 33: thin plate spline topographic map after sample size reduction

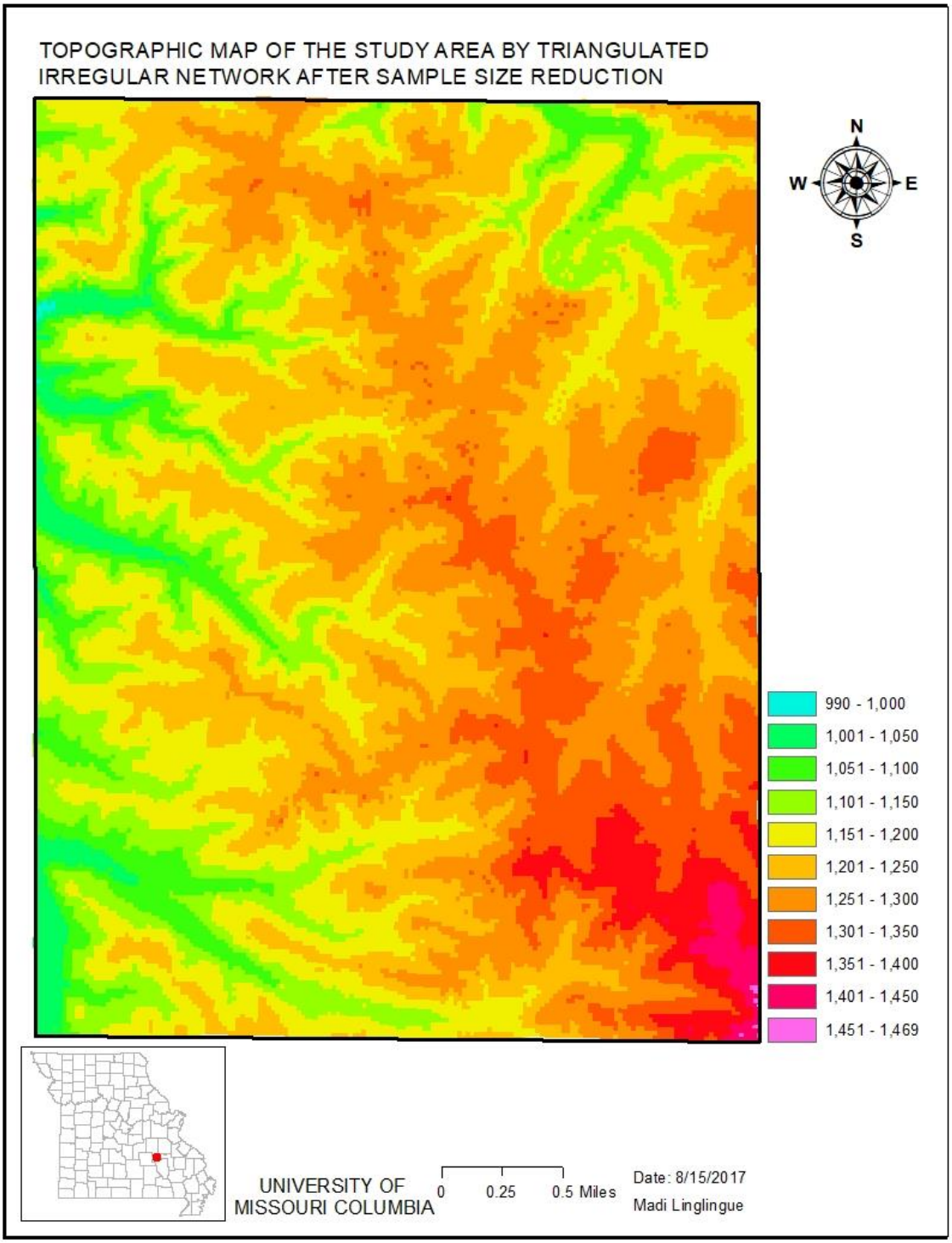

Figure 34: triangulated irregular network topographic map after sample size reduction

After sample size reduction, elevations ranged from 968 feet to 1469 with a mean of 1217m feet for the maps generated by the different SIMs. Elevations ranged from 959 feet to 1520 feet for the reference values.

5. The 3D maps

The 3D subsurface models for the drill holes generated by natural neighbor and spline are presented in figure 35 and figure 36. Each model shows the drill holes from the surface through the ore body.

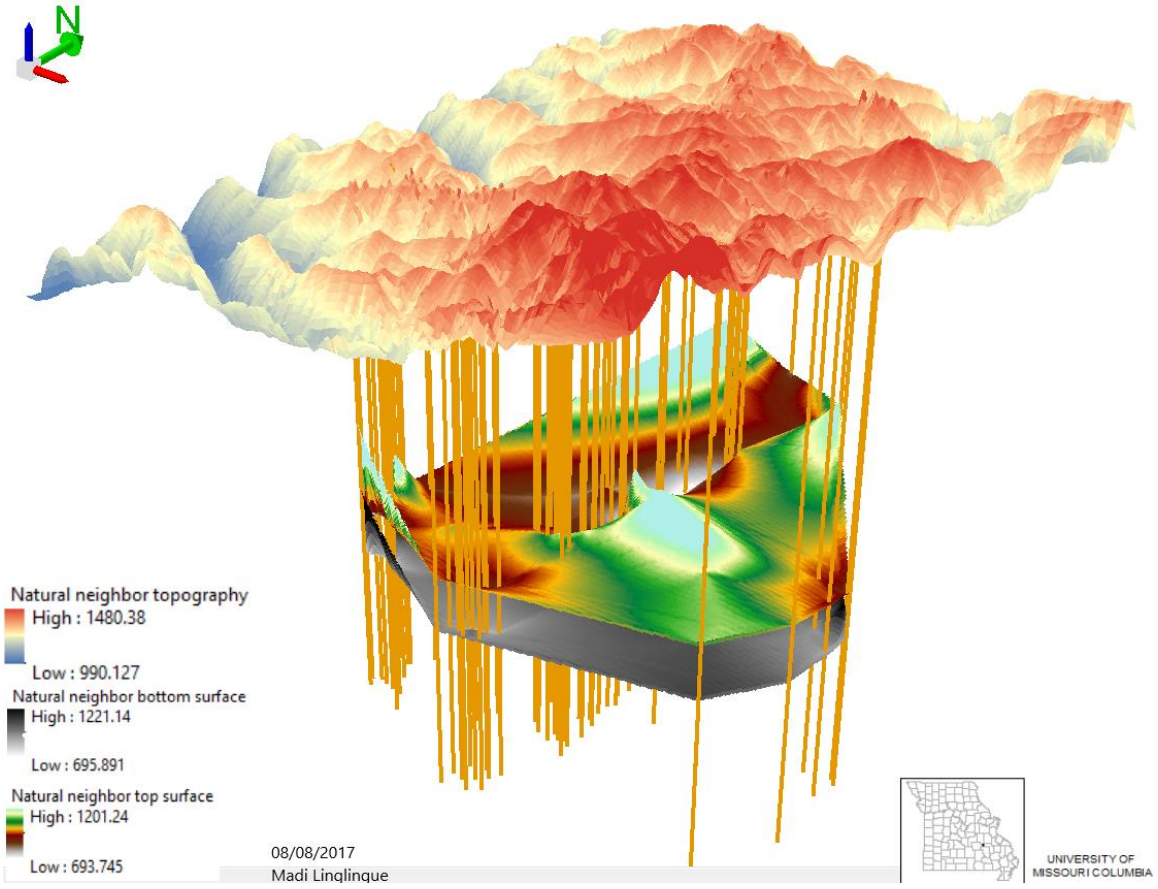

Figure 35: Subsurface representation of the Magmont mine orebody top and bottom surfaces by natural neighbor interpolation

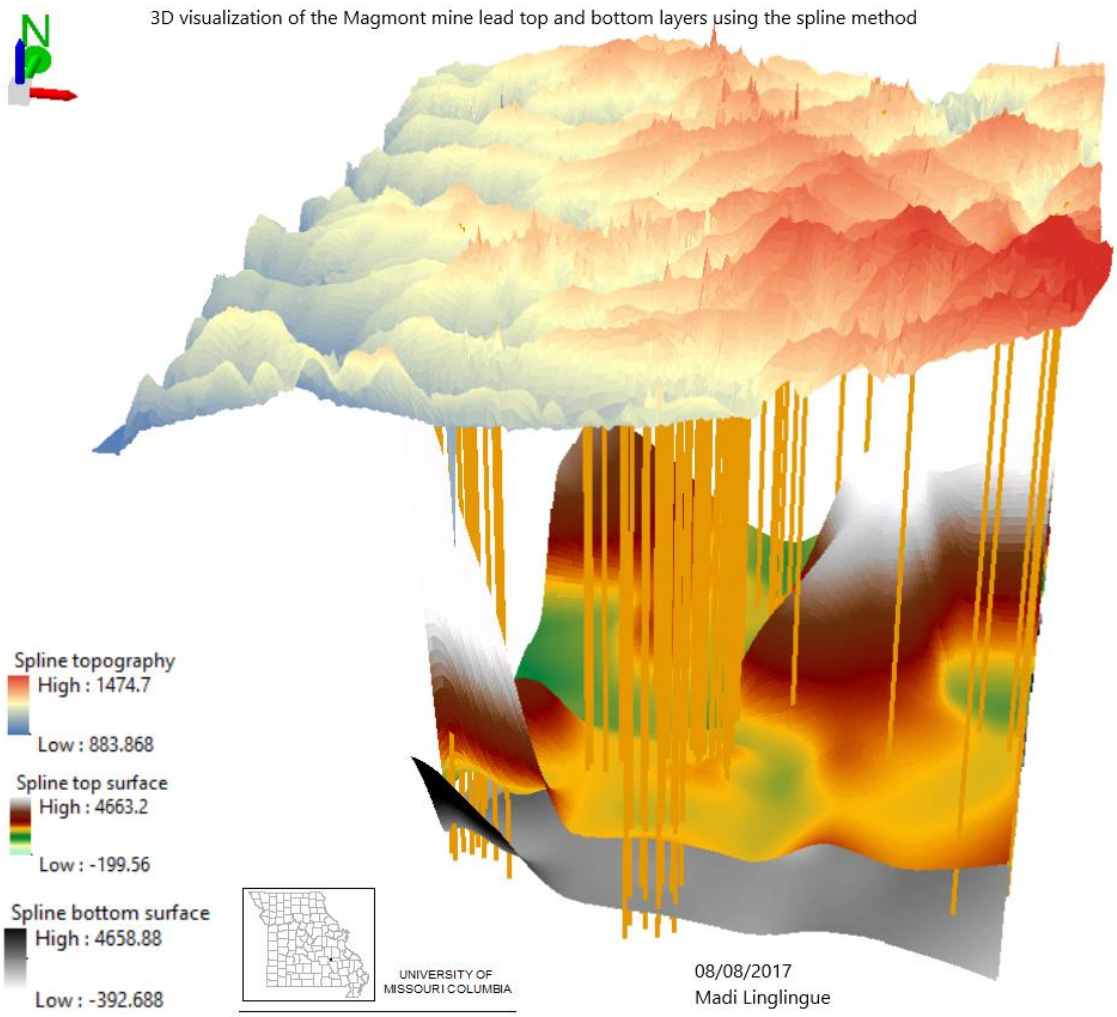

Figure 36: Subsurface representation of the Magmont mine orebody top and bottom surfaces by spline interpolation

Individual maps of the top and bottom surfaces of the orebody generated by each of the two methods above are shown from figure 37 to figure 40.

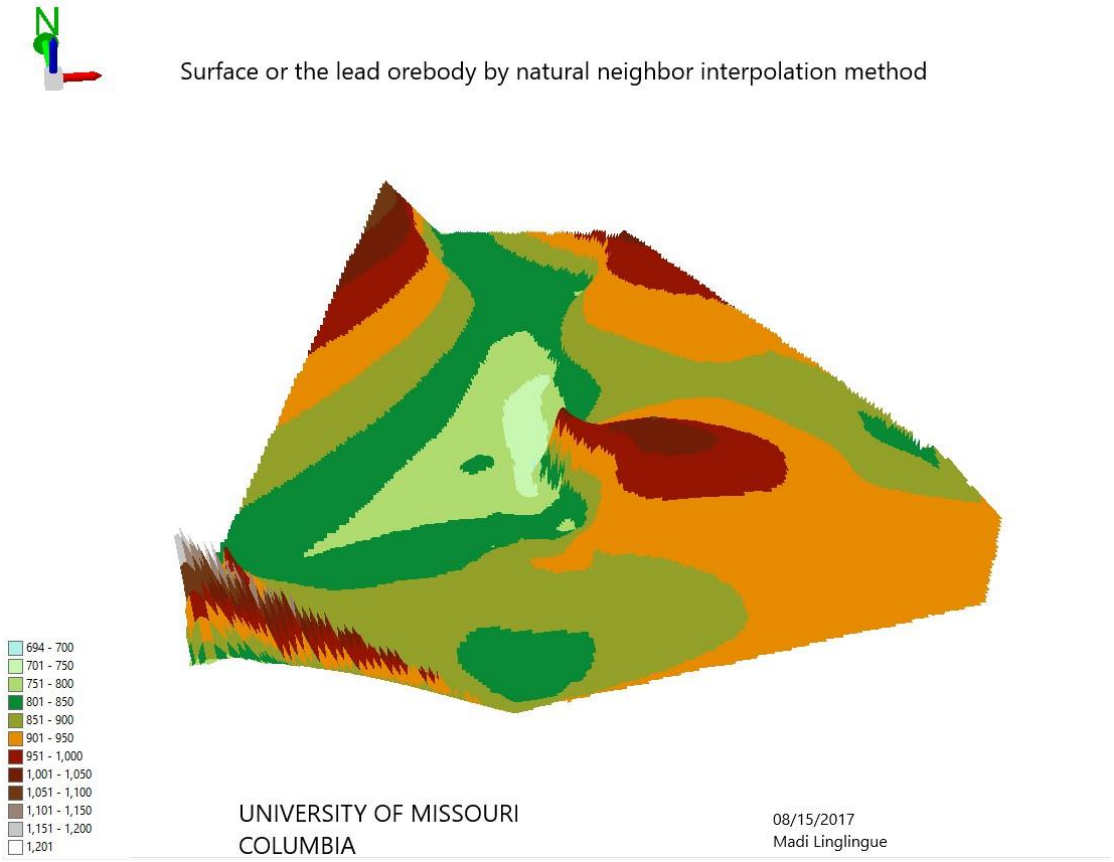

Figure 37: top surface of the lead orebody by natural neighbor

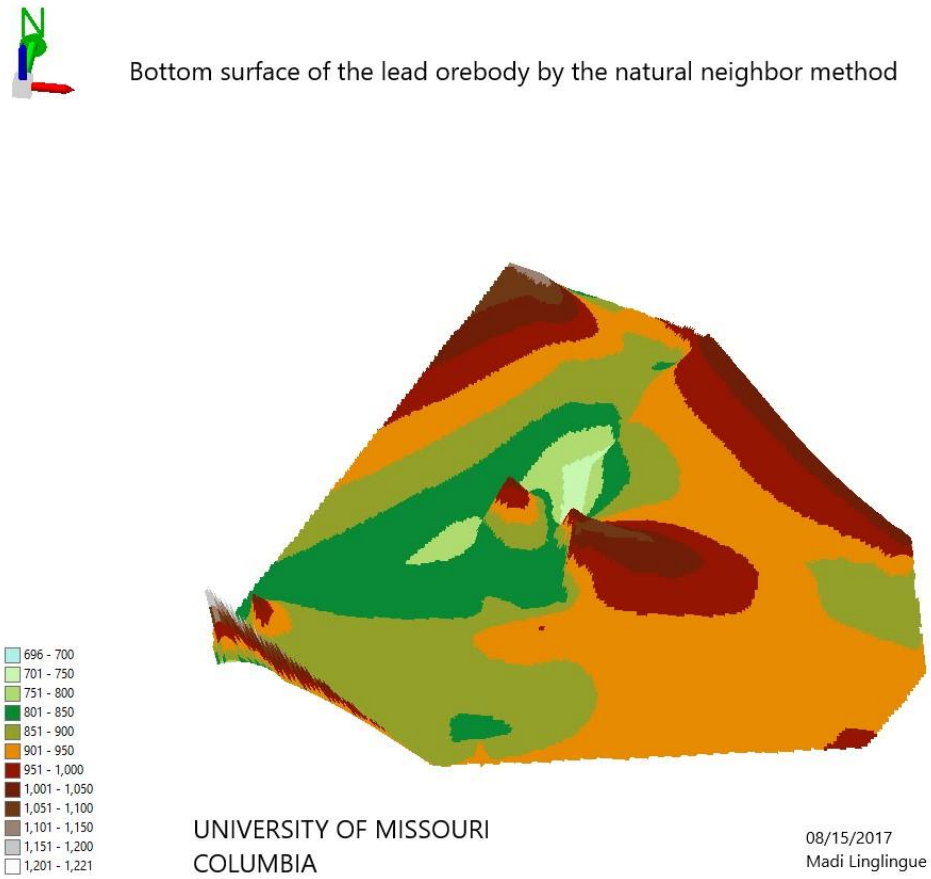

Figure 38: bottom surface of the lead orebody by natural neighbor

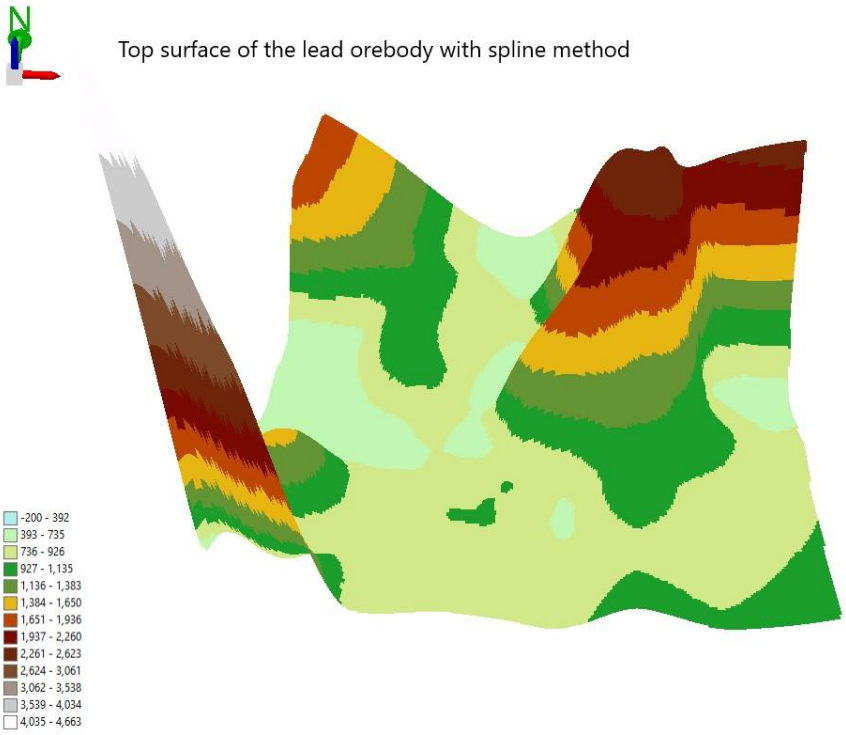

Figure 39: top surface of the lead orebody by spline

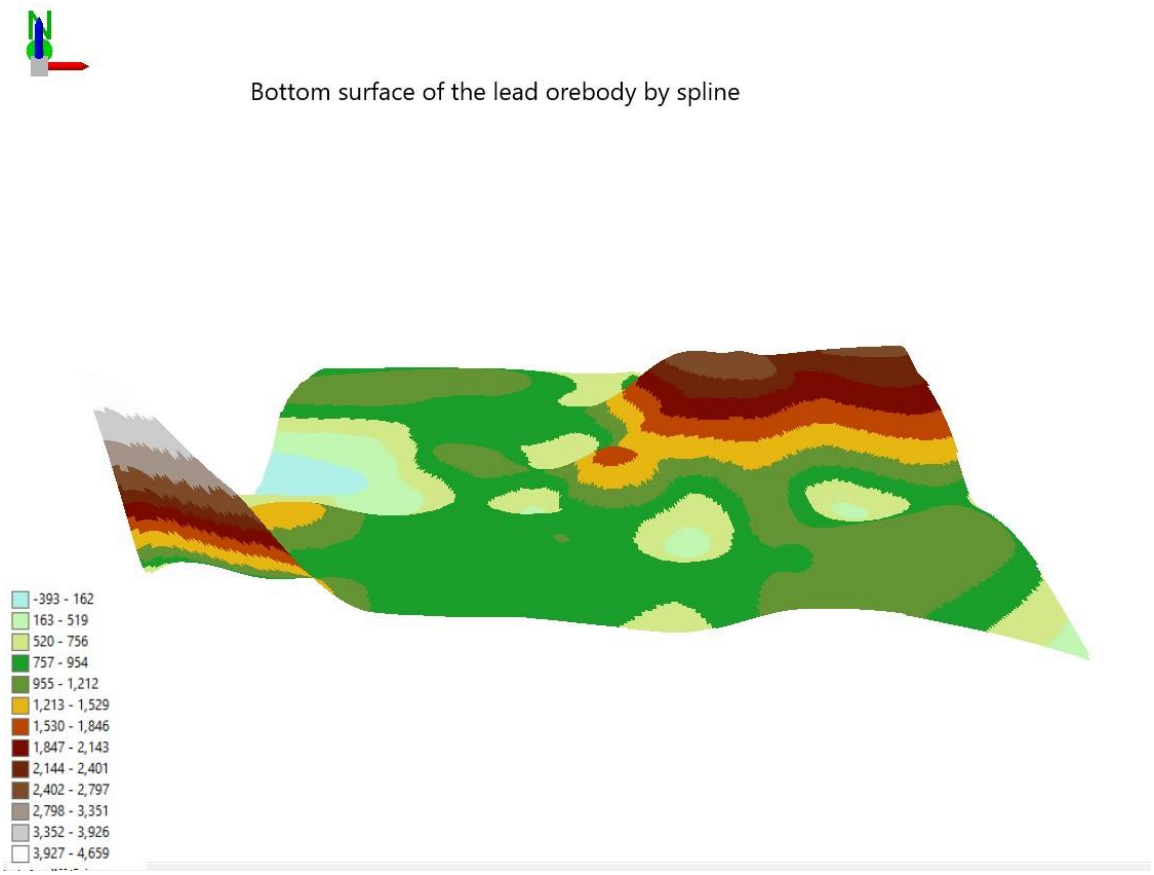

Figure 40: bottom surface of the lead orebody by spline

6. The statistical comparisons

A paired t-test of the eight methods against the original data extracted from the LAS tiles returned six p-values less than 0.05: ordinary kriging, simple kriging, thin plate spline, nearest neighbor, triangulated irregular network and inverse distance weighting. On the other hand, spline and natural neighbor returned p-values greater than 0.05 (table 4). Therefore, it could be concluded that the six methods' estimates are significantly different from the original values and that the last two are not. In the case of graphical comparisons, this means that the elevation values generated by these methods are different from the reference method's (natural neighbor). Seen globally, the distribution of the elevations returned by these methods are different from that of the original ones. While at some points, their estimates might be better or at least the same as those of natural neighbor or the original values, at the scale of the entire study area, they are globally different. Based on the p-values, it could be said that spline and natural neighbor are the methods that most agree with the original values. Furthermore, natural neighbor agreed the most with the original values because of its highest p-value. Subsequently, natural neighbor was considered as the reference method for graphical comparisons with the other methods.

Table 4: results of the statistical paired t-test of each method against the original values; p-values >0.05 (spline and natural neighbor) mean that methods are not significantly different

Method	P_value	Comment
Ordinary Kriging	0.011	Significantly Different
Simple Kriging	0.0105	Significantly Different
Thin Plate Spline	0.0012	Significantly Different
Spline	0.6233	Not significantly Different
Inverse Distance Weighting	0.000	Significantly Different
Triangulated Irregular Network	0.000	Significantly Different
Natural Neighbor	0.7217	Not significantly Different
Nearest Neighbor	0.000	Significantly Different

Table 5 shows that the original elevations (generated directly from the LAS tile) ranged from 989.23 to 1501.29 feet. The interpolated values from the same dataset however returned different ranges for both the minimum and maximum values. The minimum ranged from 983.78 feet (thin plate spline method) to 992 feet for inverse distance weighting. As for the maxima, they all underestimated the original values with values ranging from 1450 feet for inverse distance weighted to 1504.30 for the nearest neighbor method. However, all methods returned a mean height around 1217 feet, comparable to that of the original value.

Table 5: statistics of the interpolated elevations against the original values

Interpolation method	Minimum	Maximum	Range	Mean	Standard Deviation
Inverse distance weighting	991.71	1450.37	458.66	1217.11	65.64
Ordinary kriging	989.97	1453.52	463.55	1217.06	65.78
Simple kriging	989.89	1455.70	465.81	1217.05	65.87
Thin plate spline	983.78	1490.33	506.55	1217.06	66.08
Spline	990.47	1454.62	464.15	1217.06	65.84
Natural neighbor	990.12	1465.71	475.59	1217.06	65.89
TIN	989.28	1478.41	489.13	1217.02	65.89
Nearest neighbor	990.03	1504.30	514.27	1217.01	66.04
Reference elevations	989.23	1501.29	512.06	1217.06	66.00

The similarity of means however did not imply a similarity of the resulting topographic surfaces. For example, the difference between the highest and the lowest topographic elevations ranged from 463.55 feet for ordinary kriging to 634.23 feet for thin plate spline whereas the amplitude of the elevations for the natural neighbor was 517.36 feet and that of nearest neighbor was 514.27 feet. At some locations, then, different methods could return similar values but at others, they might not.

7. Math algebra comparison

The computation of differences based on spatial location with the math algebra tool returned a map for each method compared to natural neighbor. The associated statistics are shown in table 6 and table 7.

Table 6: statistics of the distribution of the differences of each interpolation method against natural neighbor

	Simple Kriging	**Inverse Distance Weighting**	**Spline**	**Thin Plate Spline**	**Triangulated Irregular Network**	**Ordinary Kriging**	**Nearest neighbor**
Minimum difference	-16.62	-22.51	-125.46	-78.61	-59.37	-166.76	-81.96
Maximum difference	42.07	38.05	219.94	247.52	55.15	249.35	72.77
Range	58.7	60.56	345.4	326.12	114.51	416.11	154.73
Mean difference	0.01	-0.05	0	0.02	0.44	0.02	-0.01
Standard Deviation	2.5	2.27	3.35	2.67	5.92	6.24	8.96

From table 6, it could be seen that the amplitude of the difference between natural neighbor values and the interpolates' ranged from 58.70 feet for simple kriging to 416.11 feet for ordinary kriging. The largest variabilities were returned by ordinary kriging with a minimum difference of -166.76 feet and a maximum value of 239.35 feet (table). Apart from nearest neighbor and triangulated irregular network, all other methods agreed with

the original values for 52.36% up to 82.45% of the estimates, within a 1 foot margin (table 7). Triangulated irregular network agreed with natural neighbor for 22.04% of the data whereas nearest neighbor agreed with natural neighbor for 16.13% of the values.

An analysis of the differences showed that most differences are clustered a few feet to tens of feet away from zero, of which the majority range between -1 and 1 foot. Consequently, the extreme variabilities are not the ones characterizing each method with regard to natural neighbors but could be considered as outliers (table 4). Maximum differences did not exceed an absolute value of 7m for simple kriging, inverse distance, spline and thin plate spline. For ordinary kriging, nearest neighbor and triangulated irregular network however, the most common differences could reach 20 to 30 feet in absolute value.

Table 7: statistics of the distribution of the most frequent differences

	SK	IDW	Spline	TPS	TIN	OK	Nn
Frequent differences	902172	906743	906182	905470	910614	908589	913188
Minimum difference	-4.87	-7.37	-7.98	-6.85	-16.95	-16.95	-30.73
Maximum difference	6.84	6.56	5.77	6.15	19.56	16.32	29.13
Range	11.71	13.92	13.74	13	36.54	33.26	59.86
Mean difference	-0.13	-0.16	-0.04	0.03	0.47	0	0.13
Standard Deviation	1.55	1.69	1.1	1.37	5	3.21	7.68
Percent frequent differences	97.59%	98.09%	98.02%	97.95%	98.50%	98.29%	98.78%
Frequency number between -1 and 1	574430	550126	762211	662117	203740	484041	149118
Percent frequency between -1 and 1	62.14%	59.51%	82.45%	71.62%	22.04%	52.36%	16.13%

The visual maps returned by the math algebra were shown below

7. 1 Comparison between natural neighbor and spline methods

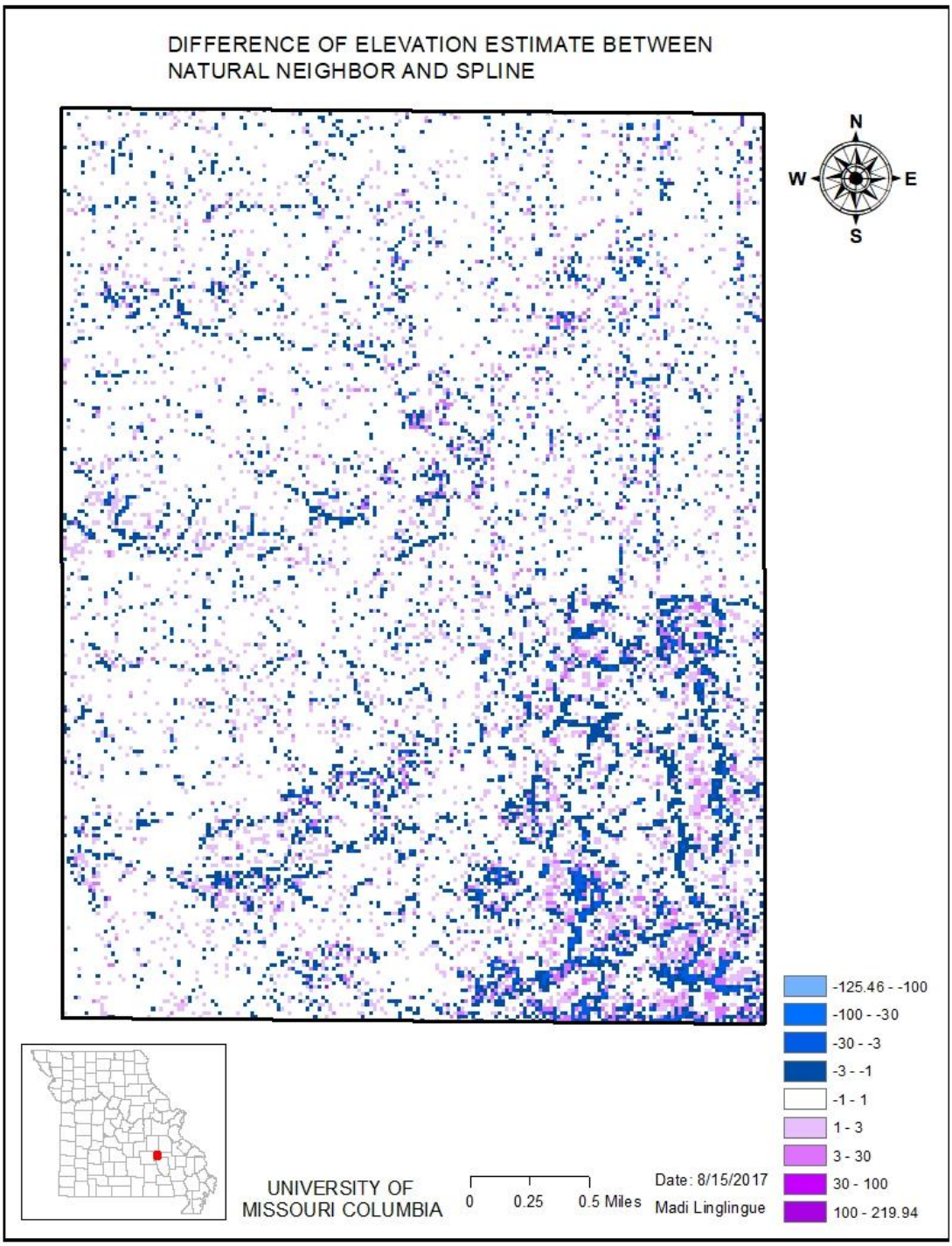

Figure 41: difference map between ordinary kriging against and spline using math algebra

Visually, figure 41 shows that almost all differences lie within 3 feet away from the reference value. Such ‘clustering’ is confirmed by table exhibiting that most differences range from -7.98 feet to 5.77 feet around zero. More importantly, table 6 shows more than 80% of the most frequent differences belong to the interval -1 to 1 foot (table 2 and figure x). The map shows a clustering of values in the south-eastern corner at the location corresponding to a high topography (figure). Similarly, but with a least emphasis, some linear patterns were observed in the northern half of the study area: the patterns to the western border correspond slightly to the rivers.

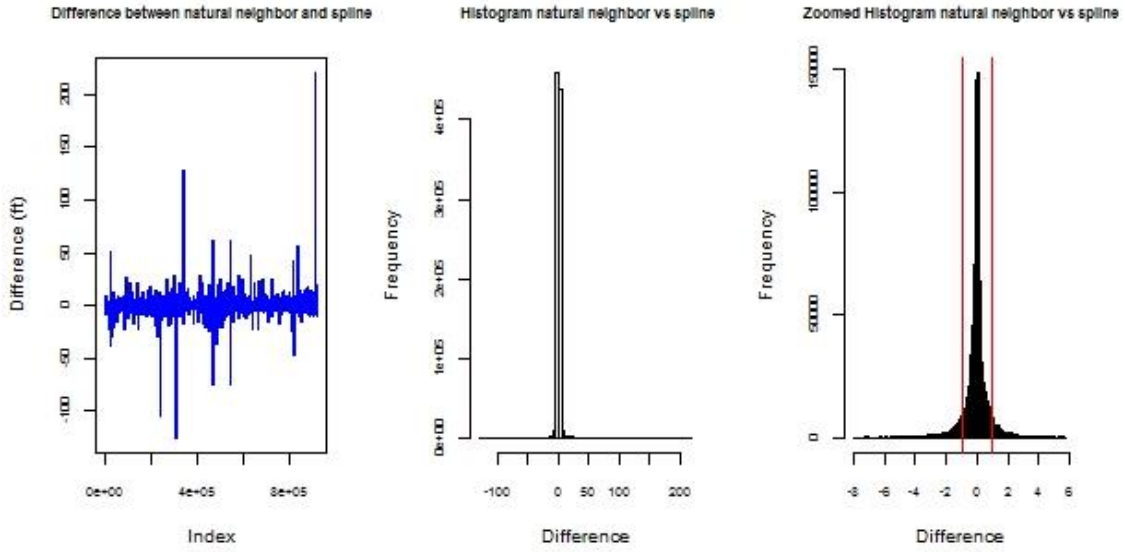

Figure 42: distribution of the differences between natural neighbor and thin plate spline

7. 2 Comparison between natural neighbor and thin plate spline methods

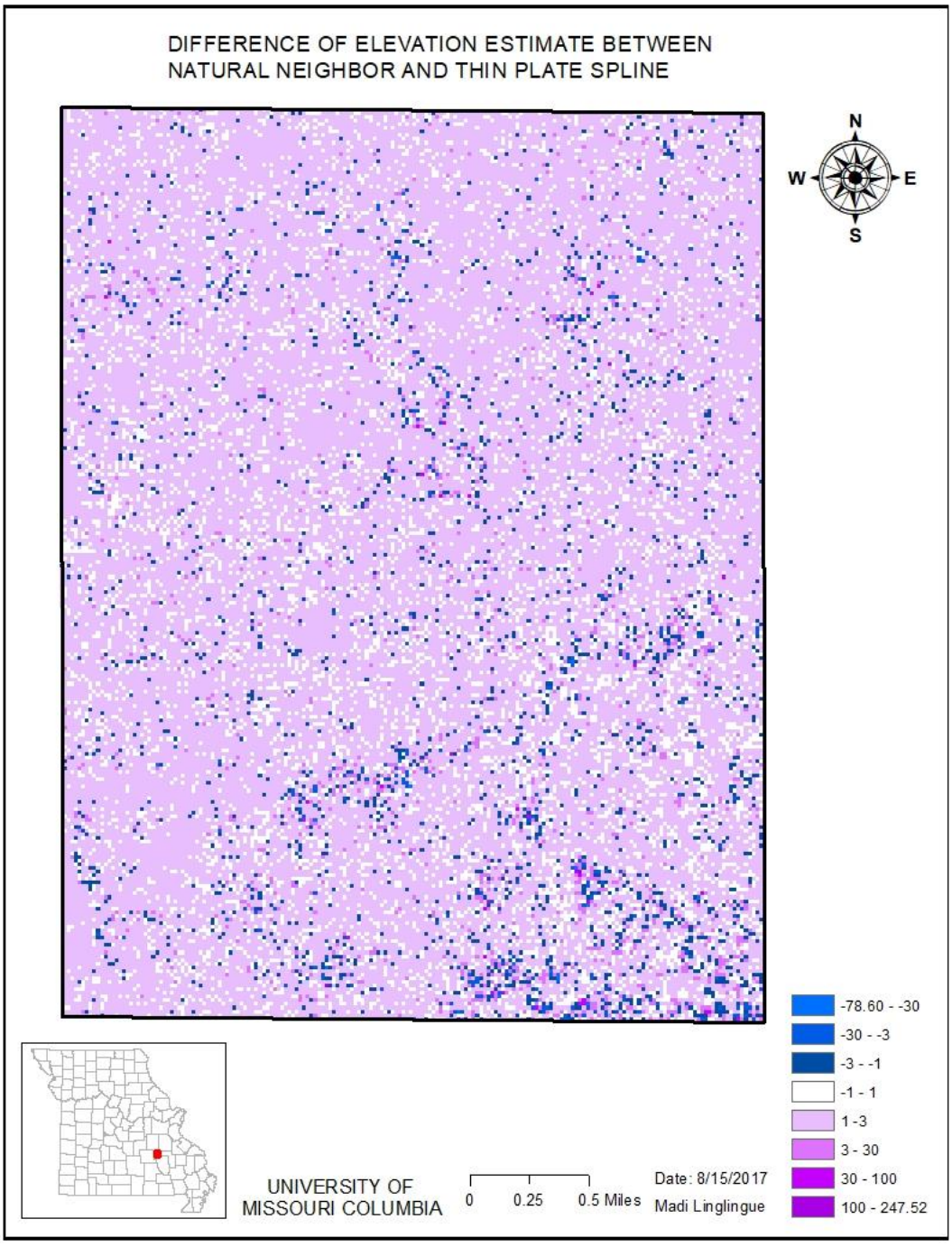

Figure 43: comparison between natural neighbor and thin plate spline interpolation methods using math algebra

Table 2 shows that thin plate spline interpolates differ from those of natural neighbor by values ranging from – 78 to 248 feet. Most frequent differences lie between -6 and 6 feet (98% of differences), of which almost 72% are within -1 and 1 foot (figure l). Some clustering of values <-3 or >3 feet were seen to the south.

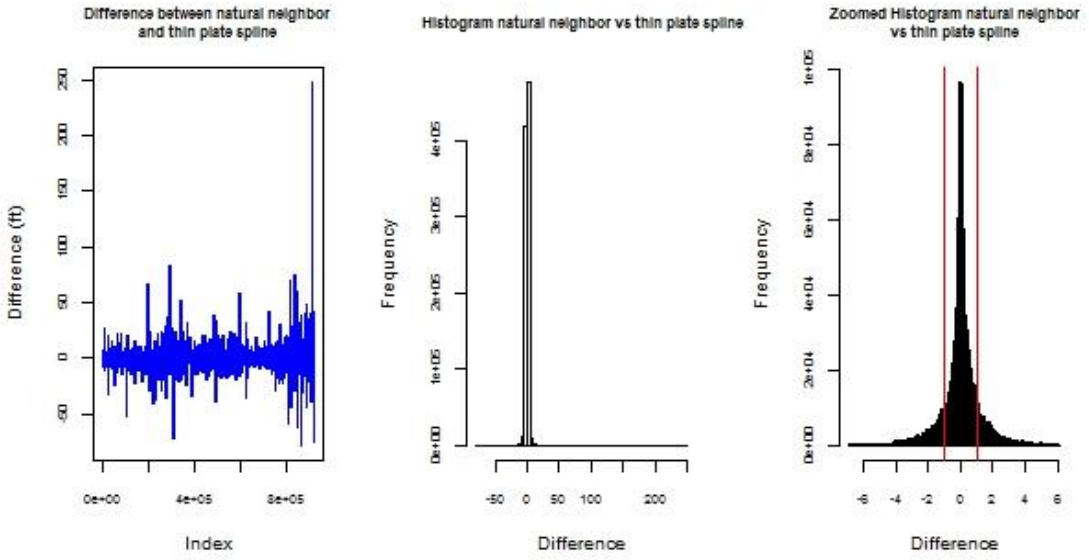

Figure 44: distribution of the differences between natural neighbor and thin plate spline

7. 3 Comparison between natural neighbor and ordinary kriging methods

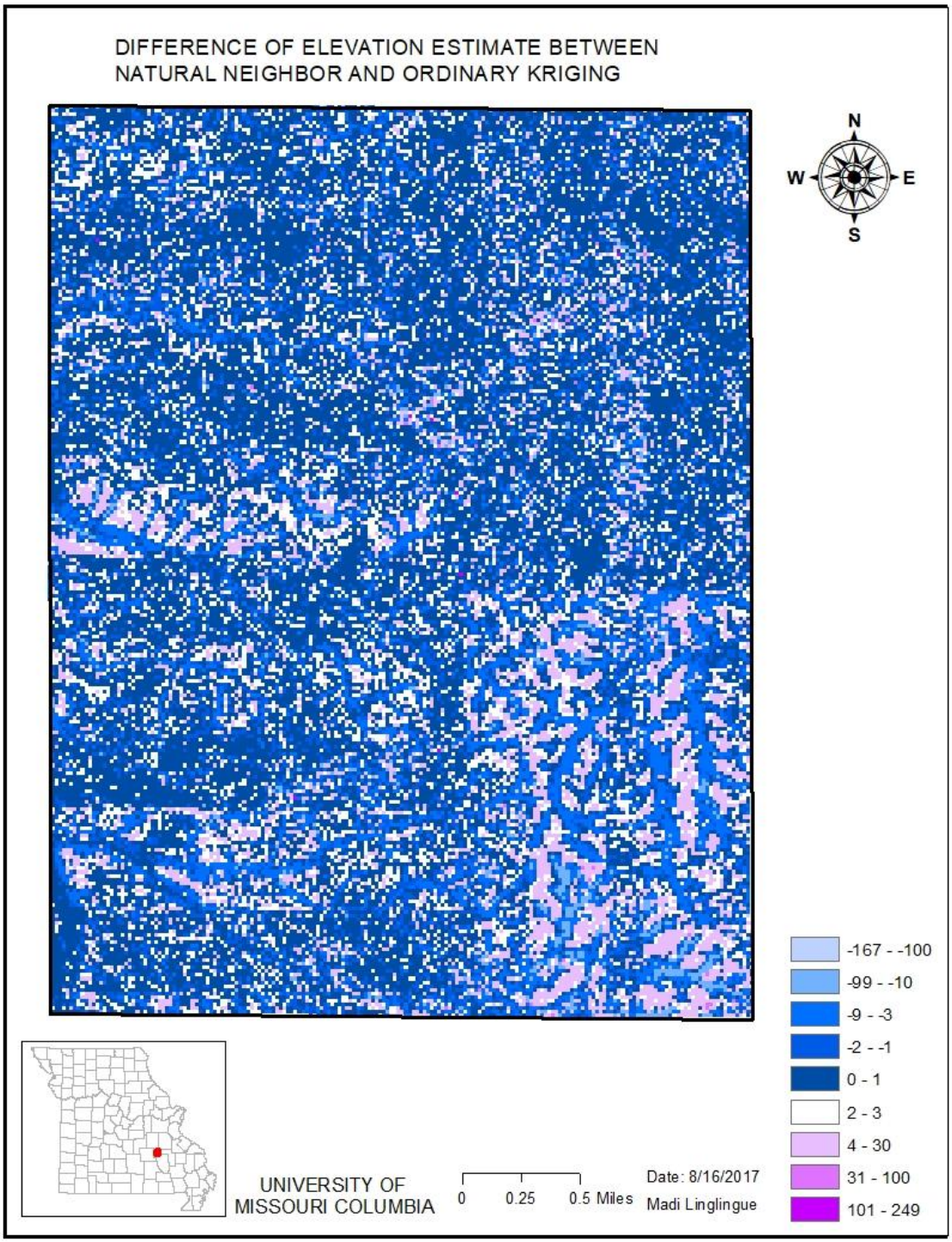

Figure 45: comparison between natural neighbor and ordinary kriging methods using math algebra

Visually, the difference between natural neighbor and ordinary kriging are dominated by the class -30 to 30 feet. Ordinary kriging had the largest dispersion with the amplitude of the differences reaching 416 feet (table and figure 46). Table however indicates that the most frequent differences range from -16 feet to 16 feet within which 52% of the frequencies is in the interval -1 to 1 foot.

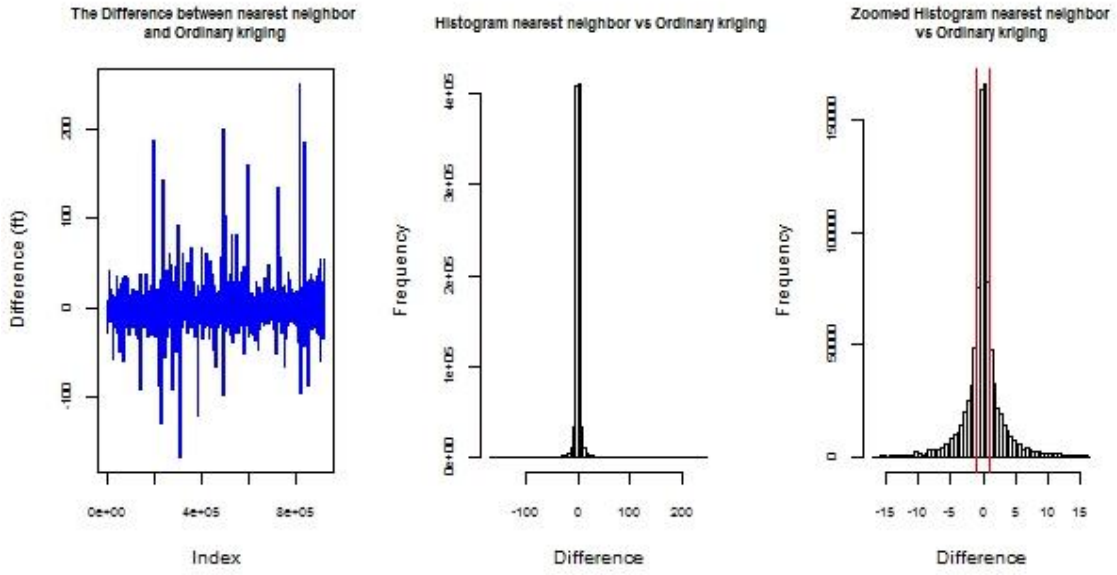

Figure 46: distribution of the differences between natural neighbor and ordinary kriging

Clustering was observed in the south-east and on the western half at locations corresponding to topography highs and lows.

7. 4 Comparison between natural neighbor and nearest neighbor methods

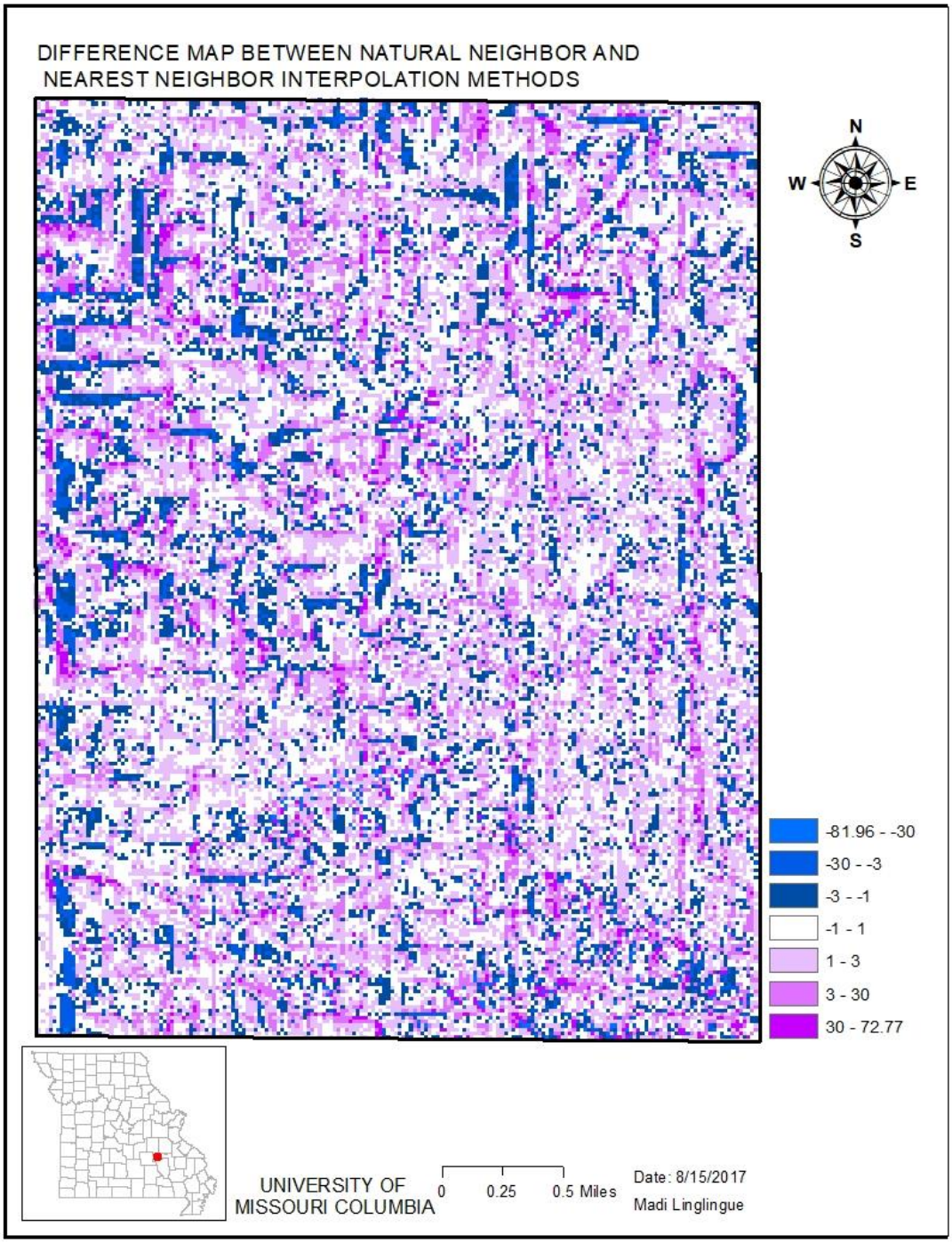

Figure 47: comparison between natural neighbor and nearest neighbor interpolation methods using math algebra

Figure 14 shows that differences between natural neighbor and nearest neighbor are dominated by elevations differences pertaining to the class -30 to 72 feet and secondarily by the class -30 to -81.96 feet. According to table, 16% of these dominating class differ by +/- 1 foot. Spots of elevations differences ranging from both 30 to 100 feet and -30 to -100 feet were observed for around 2-3% of the data (red and cyan dots). However, they did not define a clear pattern. The differences between natural and nearest neighbor displayed systematic rectilinear east-west and north-south patterns, without defining a clear geometric feature.

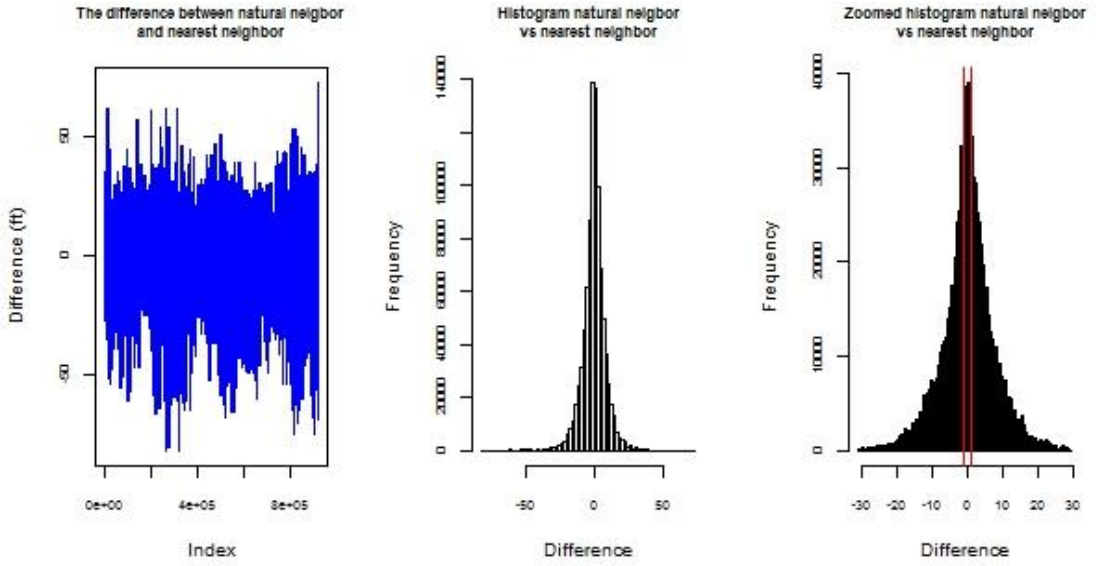

Figure 48: distribution of the differences between natural neighbor and nearest neighbor

7. 5 Comparison between natural neighbor and inverse distance weighting

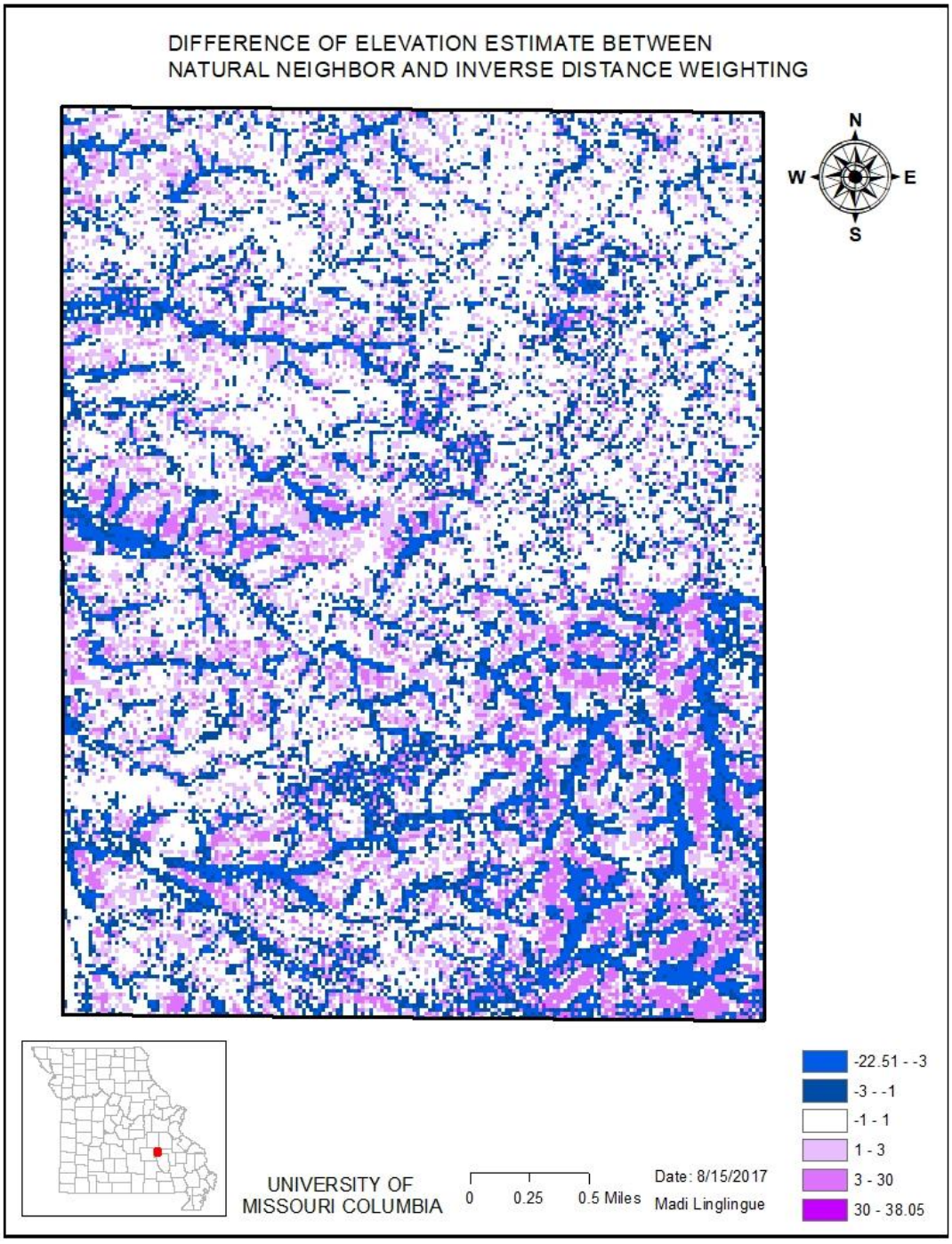

Figure 49: comparison between natural neighbor and inverse distance weighting using math algebra

The amplitude of the differences between natural neighbor and inverse distance weighting range from -22 to 36 feet, meaning the absence of outliers(table). Table indicates that 98% of the differences against natural neighbor are within 7 feet. Visually, the high negative contrast (-22.5 to -3 feet) coincide with drainage patterns and are surrounded by positive contrasts of the same magnitude. Such configuration suggests an overestimate of the low topography levels and an underestimate of the topography high features. The two methods agree for about 60% of the most frequent differences (table).

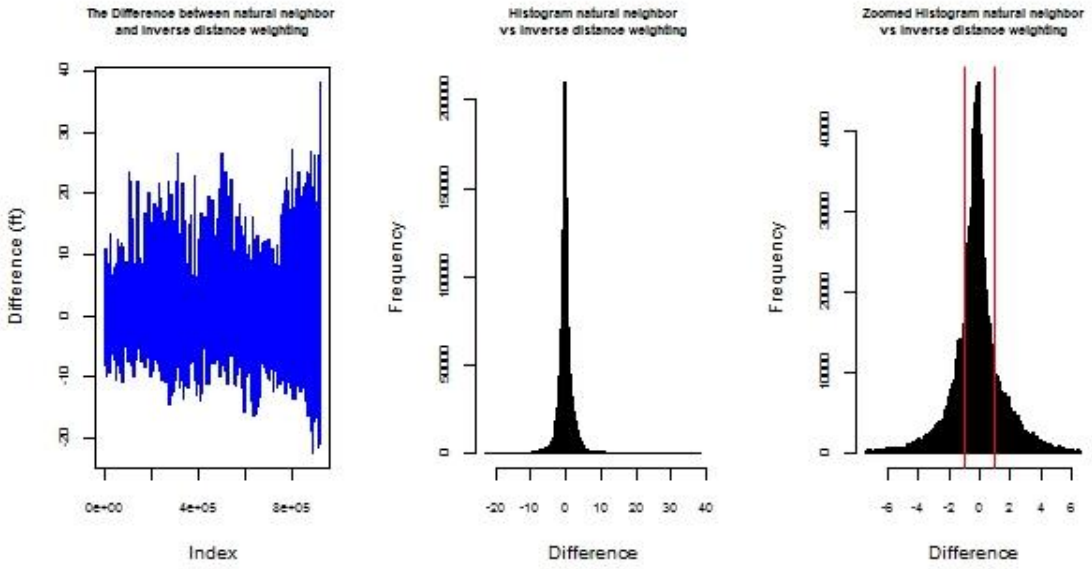

Figure 50: distribution of the differences between natural neighbor and inverse distance weighting

7. 6 Comparison between natural neighbor and simple kriging methods

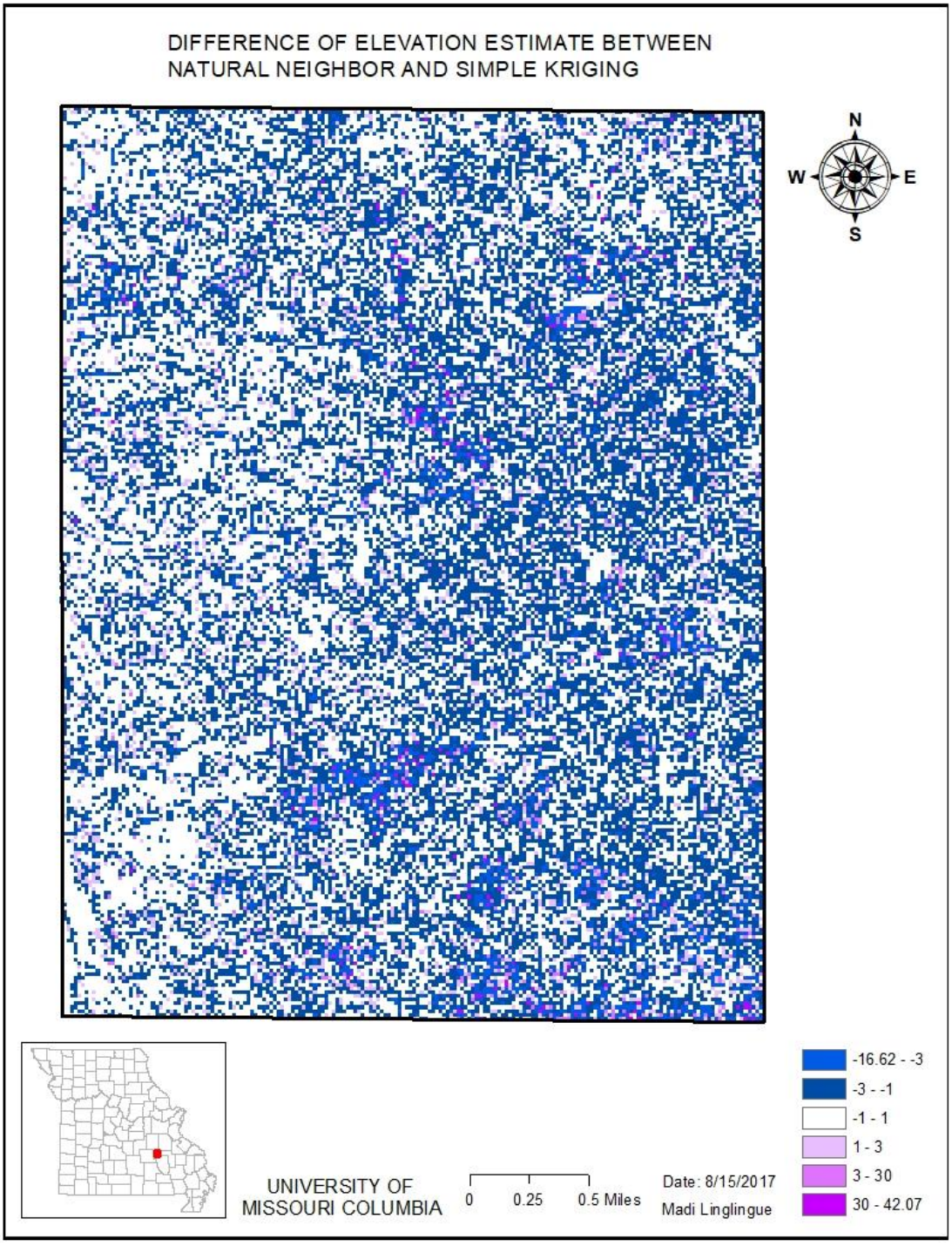

Figure 51: comparison between natural neighbor and simple kriging interpolation methods using math algebra

Visually, the differences between natural neighbor and simple kriging are dominated by the classes -3 to 3 feet and secondly by the classes 3 to 30 feet and -16.62 to -3 feet. According to table, the differences of the estimates between natural neighbor and simple kriging range from – 16 to 42 feet; 97% of those values are included in the interval -4 to 7 feet of which more than 62% agree at less than 1 foot difference. Some rectilinear and cluster-like patterns were noted but they were not systematic.

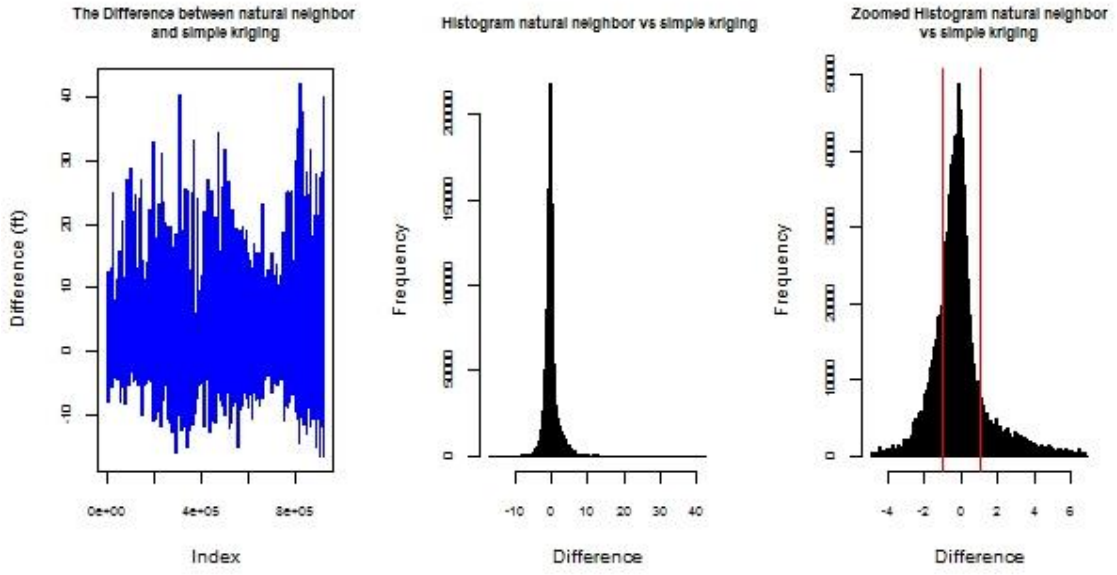

Figure 52: distribution of the differences between natural neighbor and simple kriging.

7. 7 Comparison between natural neighbor and triangulated irregular network interpolation methods

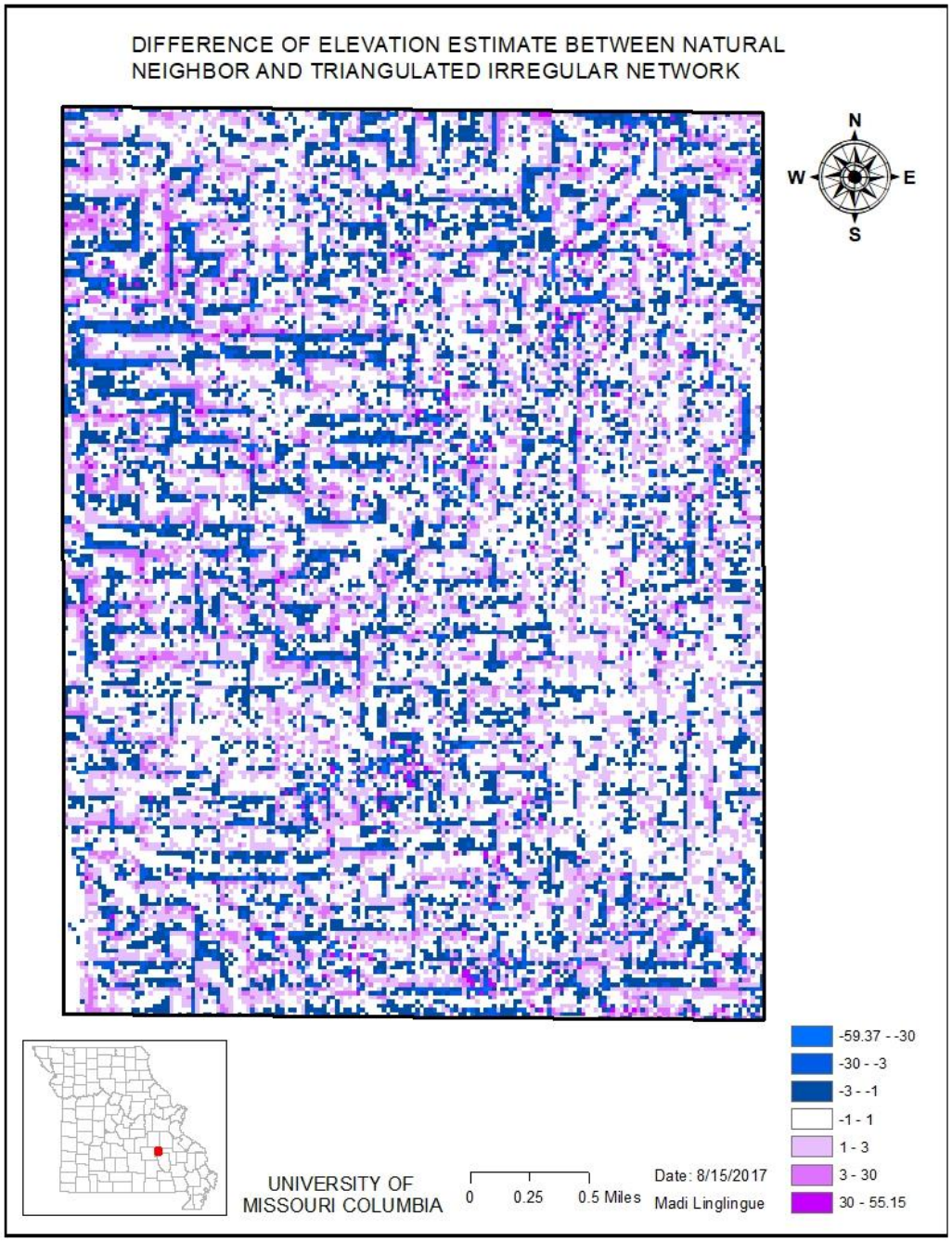

Figure 53: comparison between natural neighbor and triangulated irregular network interpolation methods using math algebra

Table shows that the differences between natural neighbor and triangulated irregular network range between -59 feet and feet and that more than 98% of the differences are observed for differences lying between -16 and 16 feet. In particular, 52% of the values are 1 foot different from the reference value. Visually, the variability of natural neighbor compared to triangulated irregular network is dominated by the classes of differences ranging from -30 to 3 feet. The resulting map exhibits rectilinear north south and east west patterns over the entire study region, without delineating a clear geometric feature.

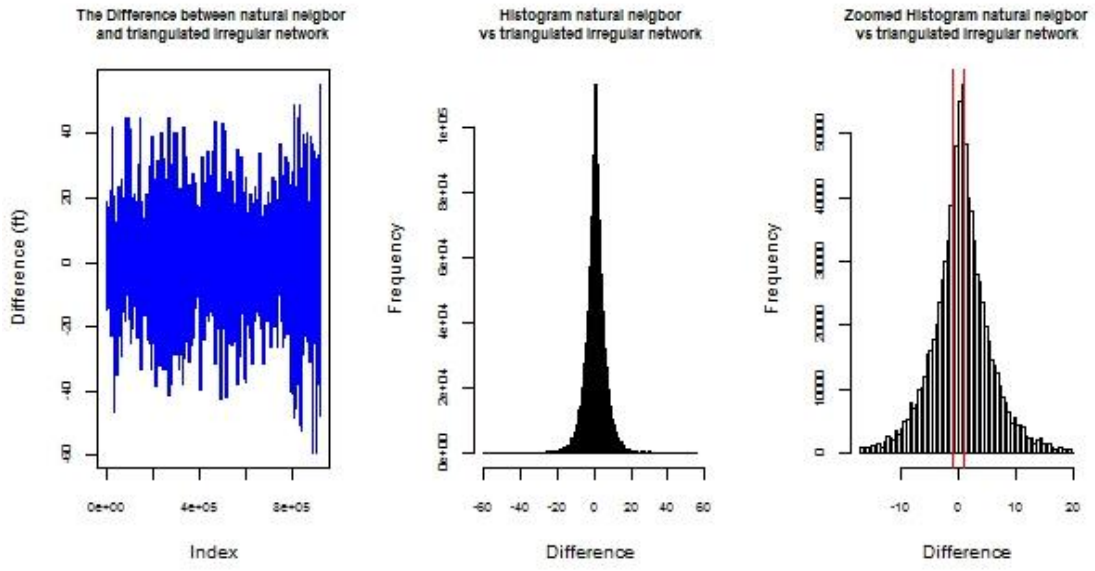

Figure 54: distribution of the differences between natural neighbor and triangulated irregular network

The difference maps resulting from the reduction of the sample size are shown in figures 54 to 60:

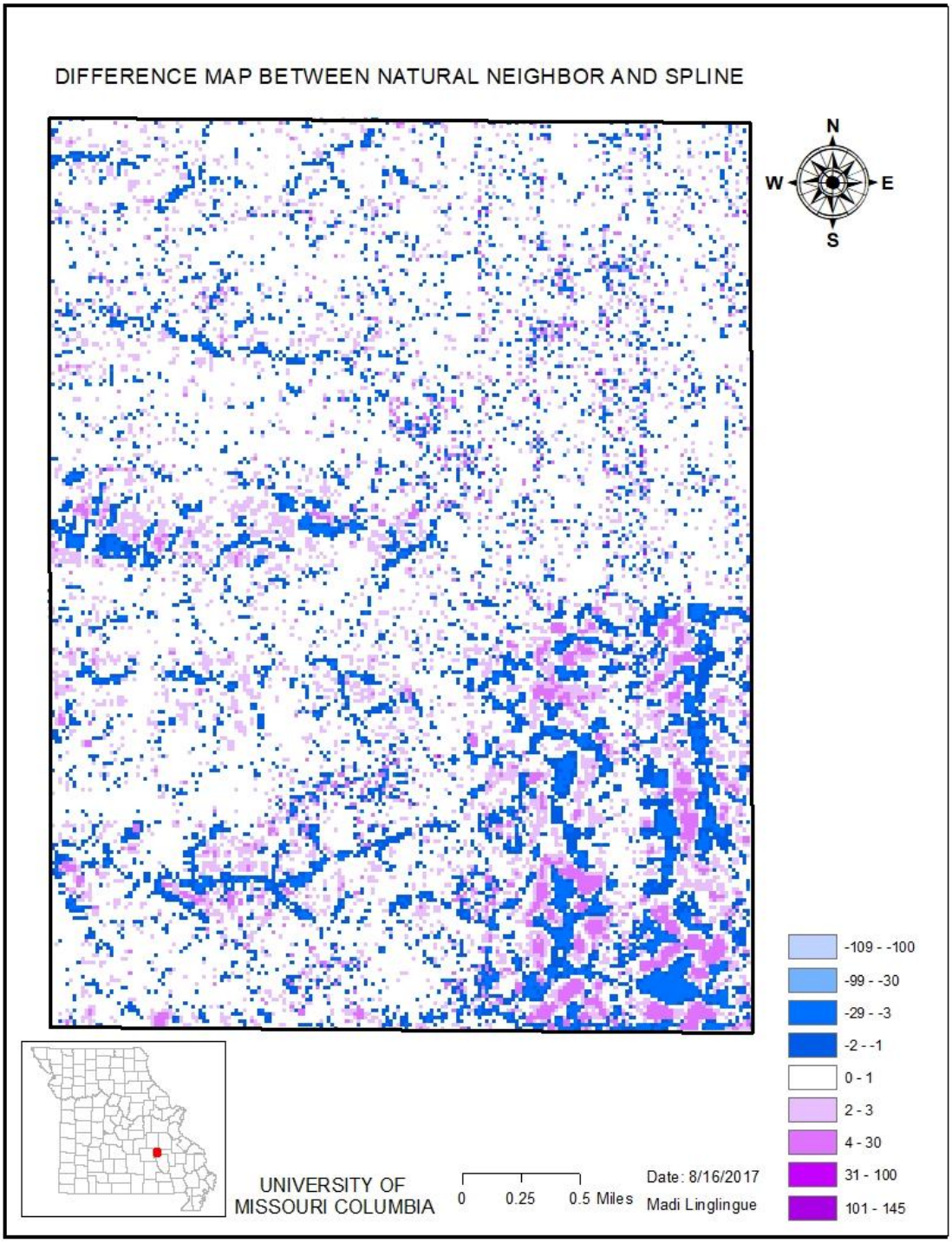

Figure 55: distribution of the differences between natural neighbor and spline after reduction of the sample size

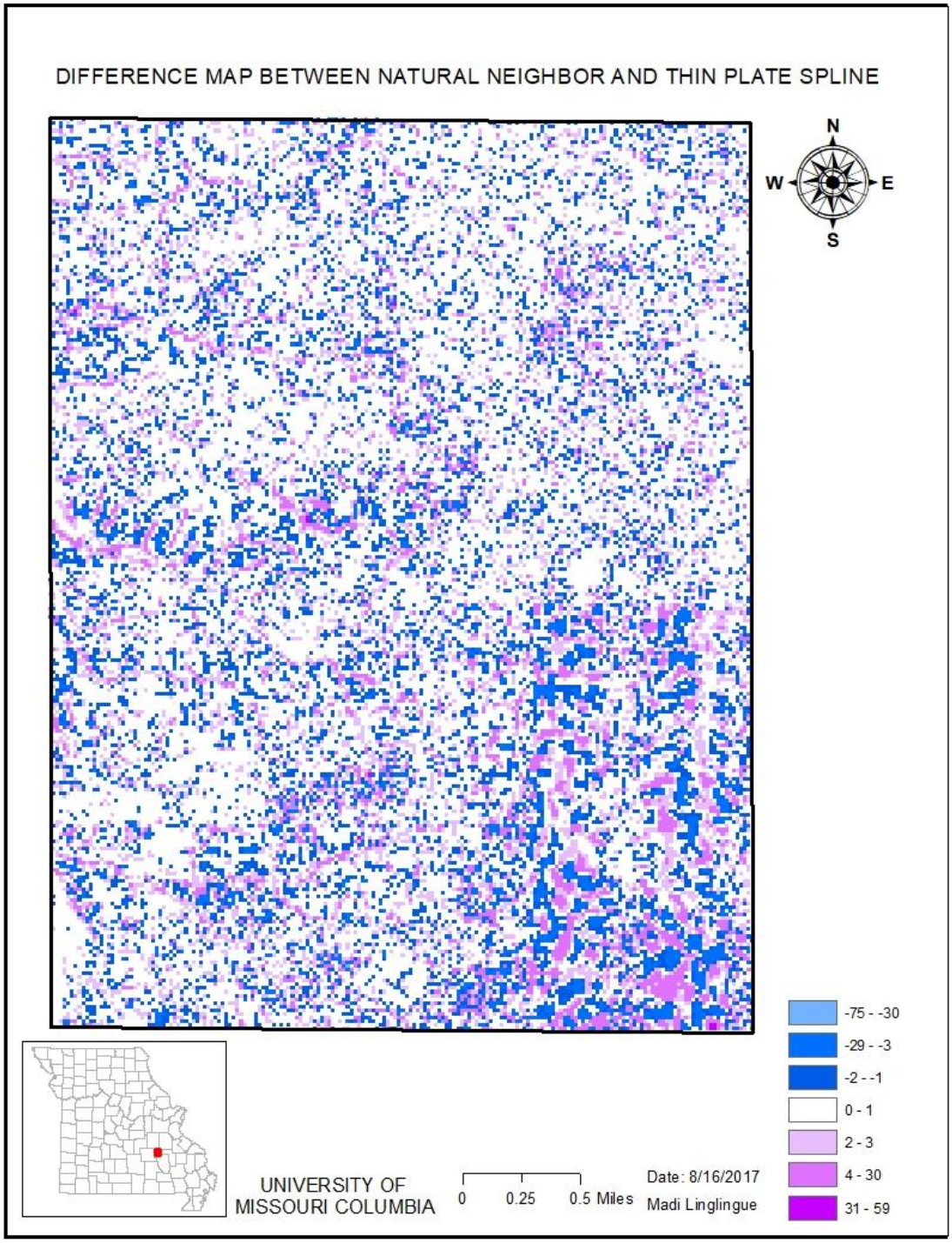

Figure 56: distribution of the differences between natural neighbor and thin plate spline after reduction of the sample size

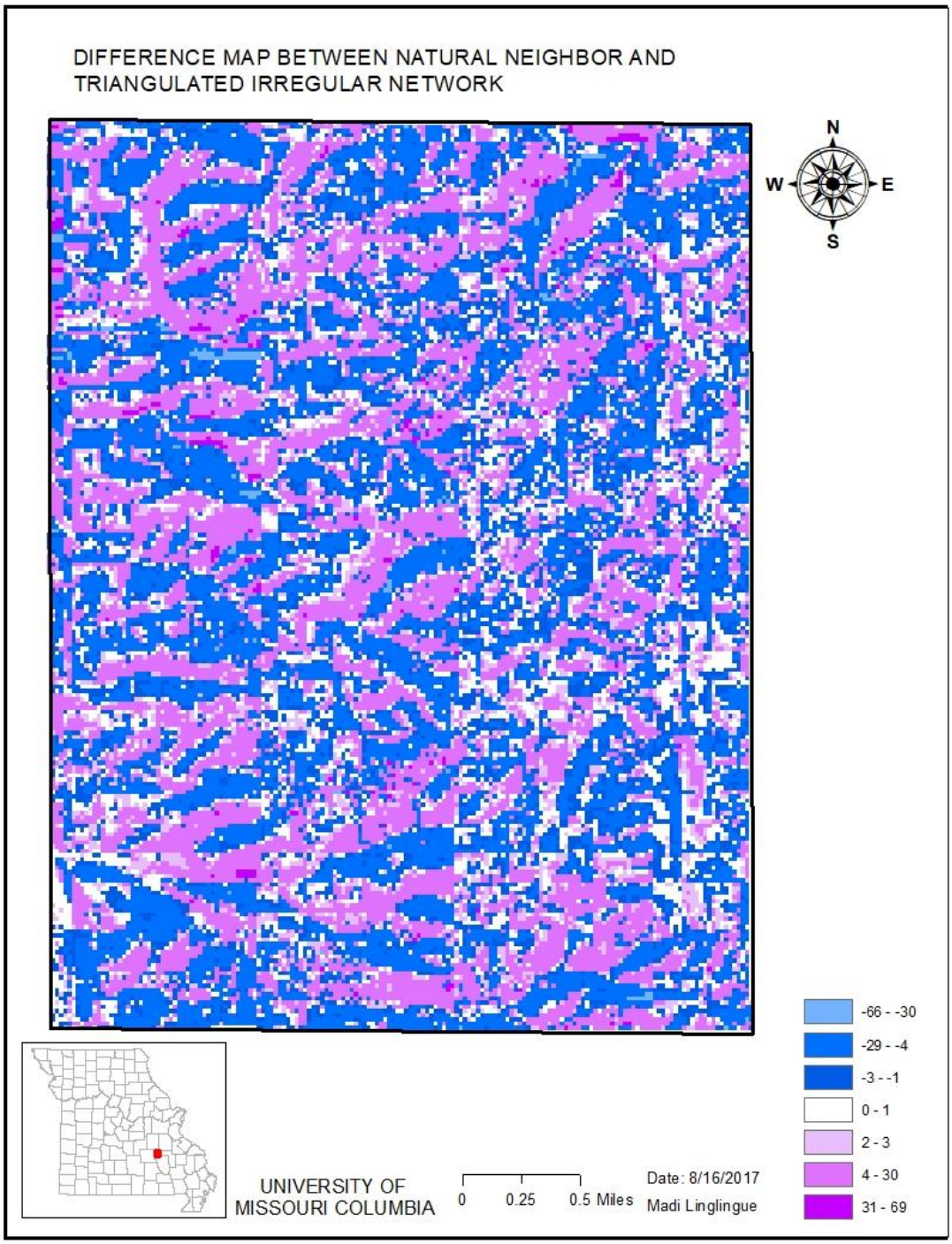

Figure 57: distribution of the differences between natural neighbor and triangulated irregulated network after reduction of the sample size

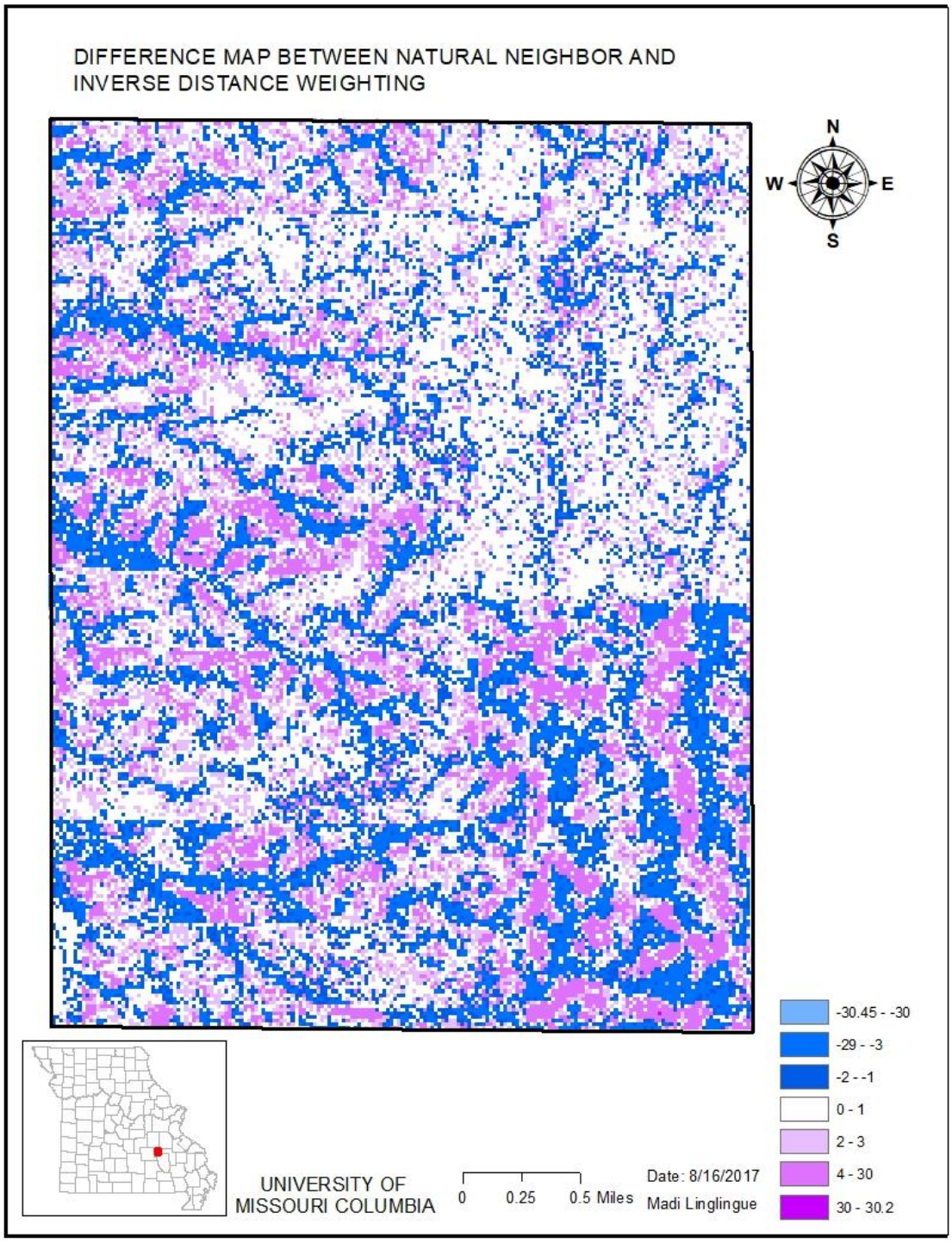

Figure 58: distribution of the differences between natural neighbor and inverse distance weighting after reduction of the sample size

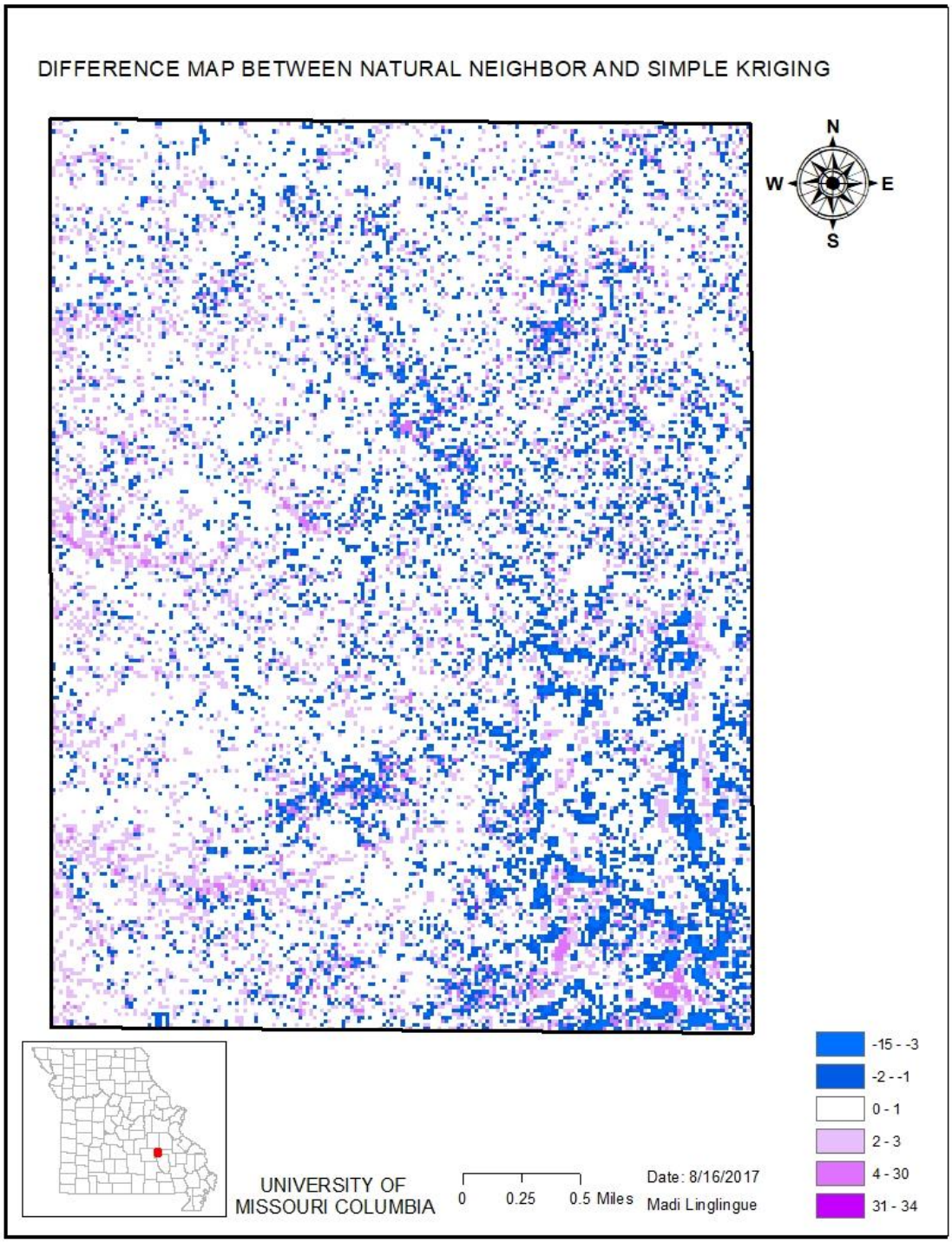

Figure 59: distribution of the differences between natural neighbor and simple kriging after reduction of the sample size

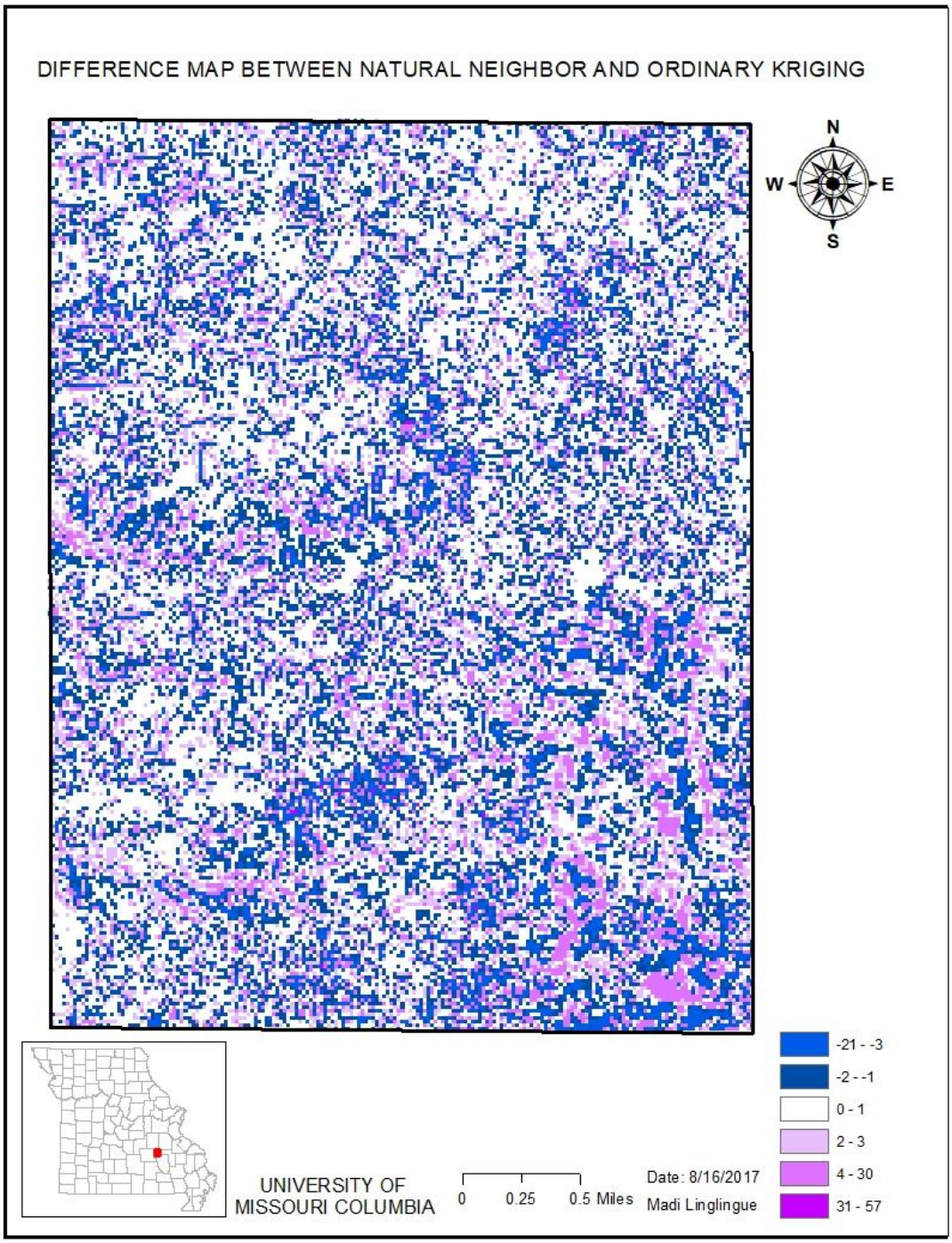

Figure 60: distribution of the differences between natural neighbor and ordinary kriging after reduction of the sample size

The distribution of the differences between the top and bottom surfaces of the lead orebody returned the following maps (figure 61 and 62).

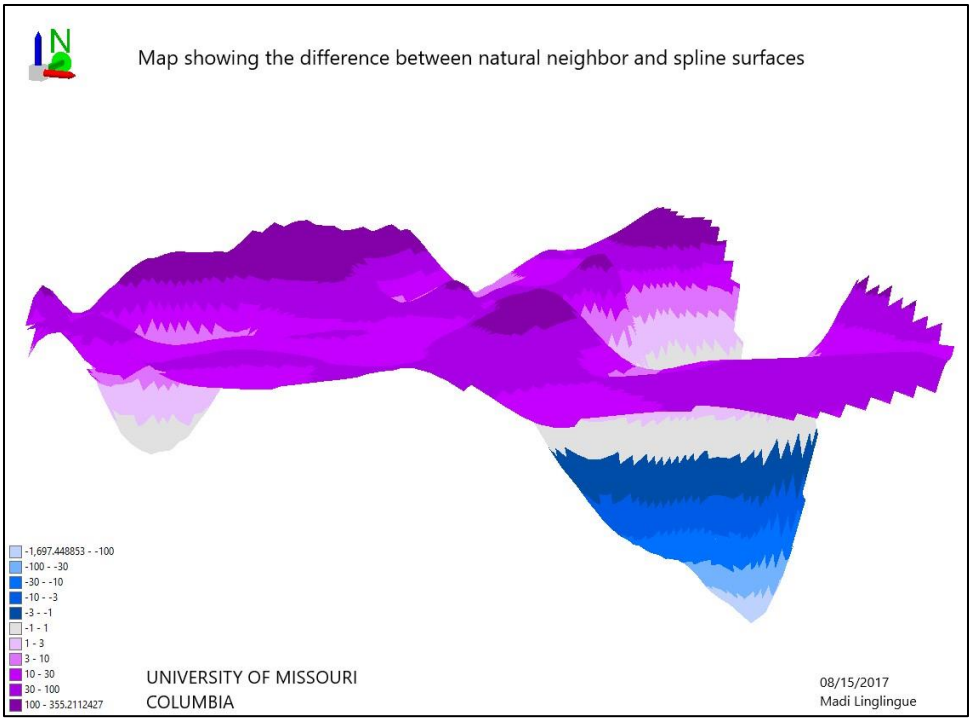

Figure 61: distribution of the differences of estimate between natural neighbor and spline for the top surface of the ore body

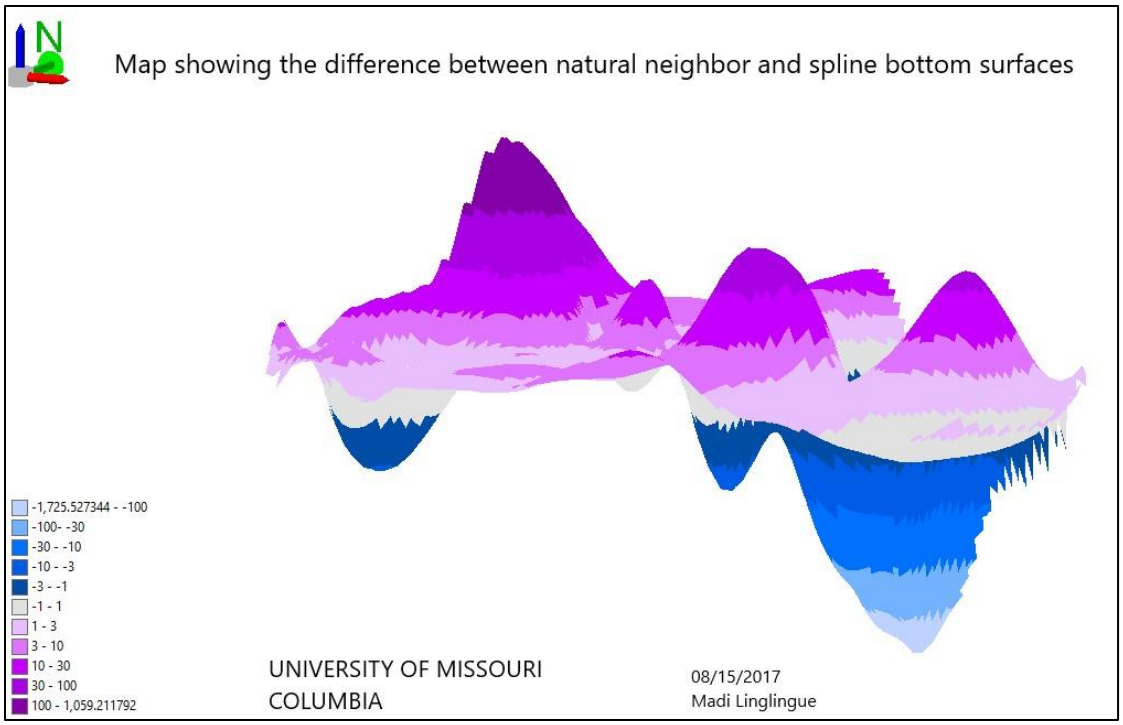

Figure 62: distribution of the differences of estimate between natural neighbor and spline for the bottom surface of the ore body

Chapter 5. DISCUSSION

8. About Qualitative comparison

After reduction of the sample size, the mean value increased from 1212 feet to 1217 feet. This result makes sense statistically: as the sample size increases, the actual topographic patterns are more captured and the mean is more representative. However, due to randomness of the sampling, the variation may have been ‘amplified’.

Given that thin plate spline is a global method (Li and Heap, 2014), it is understandable that with such ‘dense’ samples, the method did not ‘perform well’. In the same line, both minimum and maximum values returned by thin plate spline extended over the range of the reference values. Such a result agrees with the fact that the method is not convex (Li and Heap, 2011), in contrast of natural neighbor for example which is a convex method. It is to be reminded that as a general rule, all methods overestimate the highs and underestimate the lows because of averaging effect (Bohling, 2005). Therefore, the performance of thin plate spline is not necessarily wrong.

Interpolated elevations were generally different from the reference values, meaning that each model builds estimates based on the overall distribution. This agrees with Bohling’s (2005) observation according to which most algorithms do not worry about the measured values but rather the estimated values at unsampled locations. Furthermore, all methods perform well with dense and uniformly distributed data, regardless of interpolation algorithm. That should be why all SIMs returned the same

mean elevation (1212 feet for the big sample) despite the differences at individual locations.

According to the statistical test, natural neighbor performed well and this result agrees with many features of the method described in the literature review. First, the method is exact, meaning that it returns values similar to the reference value. Second, it is local, meaning that the high sample size was favorable for its optimal performance. In addition, in a relatively low complex topography (with few height variabilities, see figure 27) natural neighbor performs better because it is a gradual method, meaning that its estimates are smooth (Li and Heap, 2014).

9. About data processing

During data analysis, data format and processing issues were encountered. Initial interpolations could not return coherent results for the tile 37091f_SE tile when merged with the other tiles' data. Interpolation was well done for the western tiles whereas a black band was returned for this eastern tile. A close look at the elevations of his tile showed they were about three times less than those of the other tiles, despite the units read in feet. These variations translated into a bimodal distribution when we analyzed the elevations distribution. We assumed therefore that they were in meters rather than feet and made the subsequent conversion. This correction fixed the issue.

Due to the size of this tile 37091f_SE, it was subdivided into two portions, using two overlapping polygon masks. Subsequently, the overlapping area was oversampled. In addition, a computation mistake resulted in an under-sampling of the southern portion.

This might have influenced the rectilinearity of the patterns observed for inverse distance weighting and TIN difference maps.

10. About results

The conclusions we obtained in the statistical tests are subject to criticism because the test for independence of the measurements was not made, which is a sine qua non condition for the t-test to be valid. The current section discusses ways to make the test more valid. For the t-test to be valid, we must make sure that an observation does not influence another one in the neighborhood. In other words, we must make sure that there is no autocorrelation among the observations. One way to achieve that is by considering the value of the range computed during the processing of the semi-variogram for ordinary kriging. From the methodology section, the range value obtained from the kriging interpolation was 4.67 feet (figure x). This means that all sample more than 5 feet away from an estimated location do not 'influence' the estimate. The actual average distance between measurements computed with the 'average nearest neighbor' tool in Arcmap returned a value of 8.07feet (figure 63). The same result could be obtained by calculation with the formula $\frac{1}{2\sqrt{n/A}}$. This distance being greater than the range, it would be good to round it up for example to 10m for use as the convenient lag distance. Figure 63 also shows that with 99% confidence, the distribution of the elevations is different from that of a random process. Rather, it is characterized by clustering as showed figures 64 and 66.

It should also be noticed that the semivariogram denotes the existence of a nugget effect, suggesting that there are uncertainties associated with the data collection (see figure 11 for example).

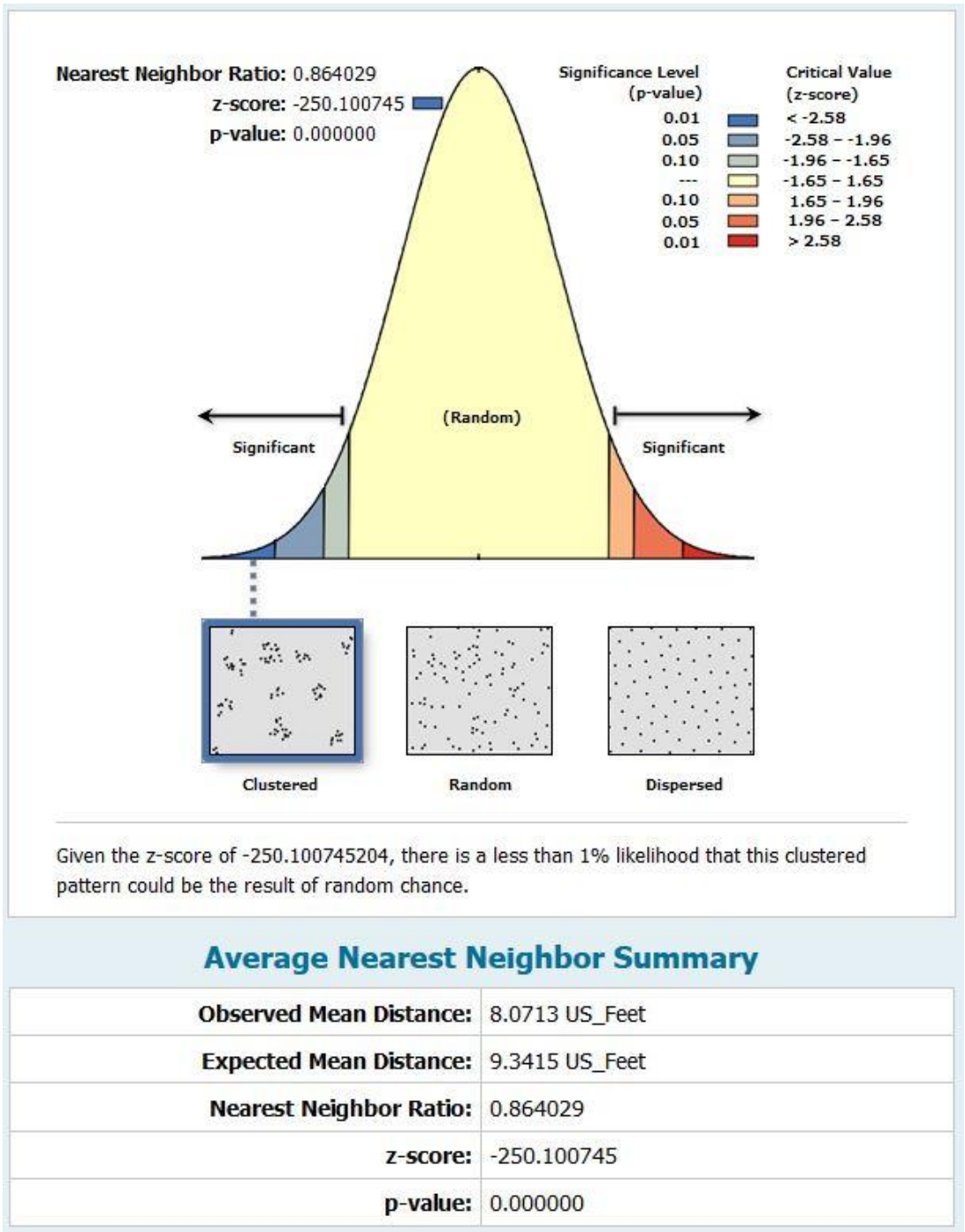

Average Nearest Neighbor Summary

Observed Mean Distance:	8.0713 US_Feet
Expected Mean Distance:	9.3415 US_Feet
Nearest Neighbor Ratio:	0.864029
z-score:	-250.100745
p-value:	0.000000

Figure 63: average nearest neighbor analysis

Given the elevated sample size, even subtle differences become statistically significant, especially for the t-test. If the values compared are not exactly the same, the t-test concludes that the results are significantly different. For a large dataset like the one we used, it makes sense that some slight differences occur. It should be mentioned that the expression ‘significantly different’ does not mean practically different. It translates a global disagreement between each method and natural neighbor. The paired t-test algorithm estimates the frequency of the absolute differences between each estimate and the reference value based on the confidence level to determine if these differences are ‘significant’ or not. With the large sample size that we used, even small differences in estimate become important for the quality of the whole assessment. At the mineral exploration stage, three feet error is acceptable for both horizontal and vertical planes because at the scale activities are performed at this stage, three feet are represented by a few millimeters.

The difference with the other methods returned relatively less precision. But globally, all methods performed well because they all returned a mean elevation of 1212 feet over the entire study area. However, behind the scenes, they are doing very different things, resulting in differences in the value of the interpolated values that sometimes could be very high. Considering the case of thin plate spline interpolation method which was classified as significantly different, it could be observed that 98% of the differences were not in excess of 6 feet, of which 72% ranged within a 1-foot difference. As mentioned above, such a difference may be acceptable in practice, considering the level of precision acceptable at the given state of activities.

Another way to compare the performance of the different interpolation methods would be the computation of the root mean squared error (RMSE) for each method. The RMSE quantifies the margin of error associated with an estimate. The smaller the RMSE, the better the estimate. Formulas exist for the computation of RMSE. The geostatistical tool in Arcmap automatically generates the RMSE associated with each estimate. The SIMs not included in the geostatistical tool however do not allow such a direct computation. But there is a formula to calculate the RMSE:

$$RMSE_{f_0} = [\sum_{i=1}^{N} (Zf_i - Zo_i)^2 \ /N]^{1/2}$$

where N = sample size, Z_f = expected value, Z_o = observed value and i = location. The following results were obtained (table 8). In a similar study, Shahbeik et al (2013) used errors estimation to compare ordinary kriging and inverse distance weighted.

Table 8: RMSE results for the studied interpolation methods

SK	IDW	NAN	TIN	SPL	TPS	NN	OK
6.53	6.69	7.14	7.59	7.94	8.07	8.44	9.83

In light of table 8, some differences are observed with the RMSE values returned by the geostatistical tool, which should not be the case. For example, ordinary kriging returned a RMSE=5.1 (figure 12) while direct calculation returned 9.83 (table 8). It is therefore advisable to integrate RMSE calculation when interpolating to have more control on the validity of the results. In the current thesis, all parameters of the SIMs available in the geostatistical tool should checked to get comparable RMSE with the calculated values.

No method is systematically superior to another because the methods are all data sensitive or area sensitive (Li and Heap, 2014) and their performances are sensitive to model parameters whose choice are sometimes arbitrary. Due to the sensibility of model performance to various factors, we advise that different methods be tested on one's data set before choosing an interpolation method. The desired level of precision, the knowledge of the math behind the algorithm and most importantly the knowledge of the field should be taken into account to help choose the optimal parameters. In mineral exploration, most companies are routinely using kriging interpolation, but we should not assume that it is the most relevant to mineralization assessment. In the case of the present thesis for example, both ordinary kriging and simple kriging returned estimates significantly different from the reference values. More specifically, they were likely "feeling the streams" because their estimates at river beds were higher that of the reference values.

The reduction of the sample size allowed the following remarks: the triangulated irregular network returned anastomosed north-east and east-west rectilinear patterns, similar to the situation before the sample size reduction. However, the patterns were coarser compared to the situation prior to the reduction, suggesting that high sample size 'refines' the differences and contributes to more precision as stated previously in the literature review. To help understand that pattern, a cluster analysis was performed on the values of the difference between natural neighbor and TIN with the "cluster and Outlier analysis (Anselin Local Morans I)" tool under the spatial statistics tool. This test returns a thematic map informing on (1) the areas where no significant variation of the elevation values was observed, (2) areas where low values are clustered, (3) areas where high

values are clustered, (4) the location of high outliers and (5) the distribution of low outliers (figure 63). Figure 63 revealed that the anastomosed patterns were related to clustering of low and high values. Most importantly, it exhibited high and low outliers throughout the entire study area, most often on or near the anastomosed patterns. The outliers appear either isolated or clustered (figure 64).

To support the interpretation, a similar test was performed on the elevation values themselves to check for the eventual existence of an initial clustering which could impact the distribution of the differences (figure 65). The resulting map reflected the topography and additionally displayed spots of outliers on the North-east, north-west and to the south-west of the study area. Given that those outliers were discrete compared to the ones associated with the differences, these initial outliers were unlikely to control the distribution of the formers. Accordingly, no investigation was done to check to which feature they represent physically. Since the area of study was an active mine up to 1972, it is possible that old infrastructures still exist on the ground. Such infrastructures would explain the abrupt contrast in elevation values within short distances since the last return of the LiDAR in one case will hit the top of the infrastructure and the next one will hit the ground surface. So, depending on the height of the infrastructure, big discrepancies could be noted. For future work, it would be worth to check on the ground to what physical feature these outliers correspond because their values affect the normality of the whole dataset.

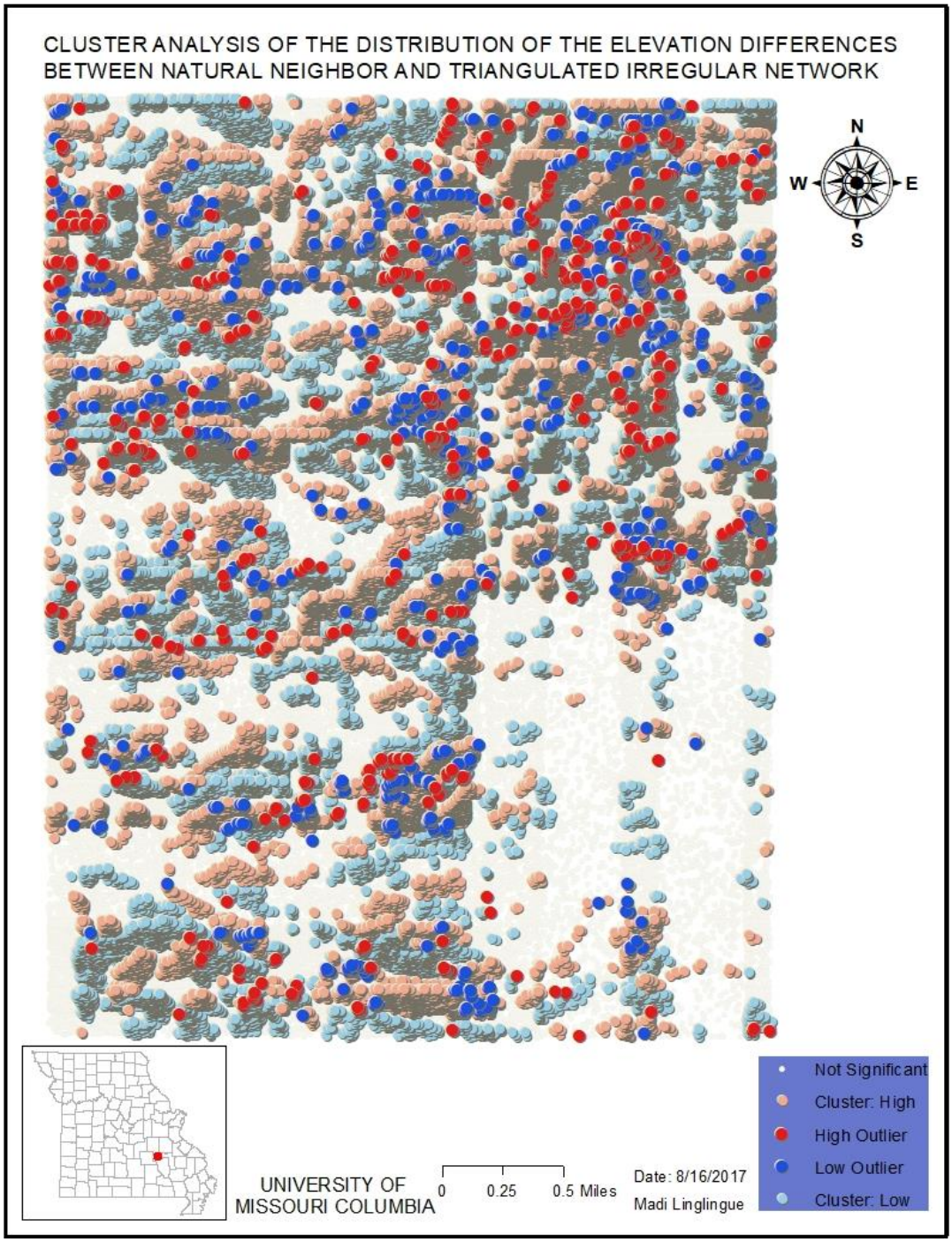

Figure 64: cluster analysis for the difference of the elevation values between natural neighbor and spline

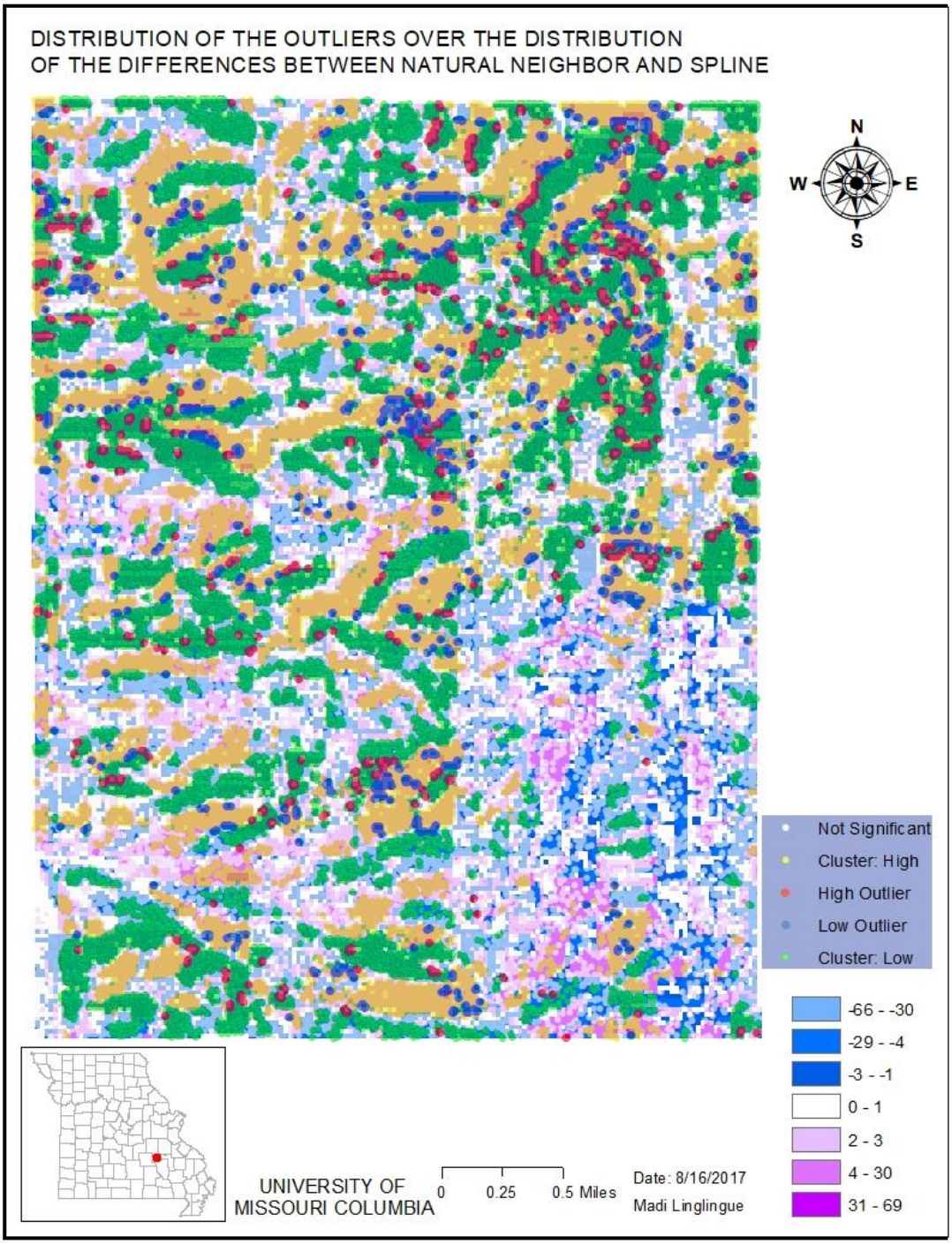

Figure 65: superimposition of the cluster analysis map over the difference of elevations between natural neighbor and spline

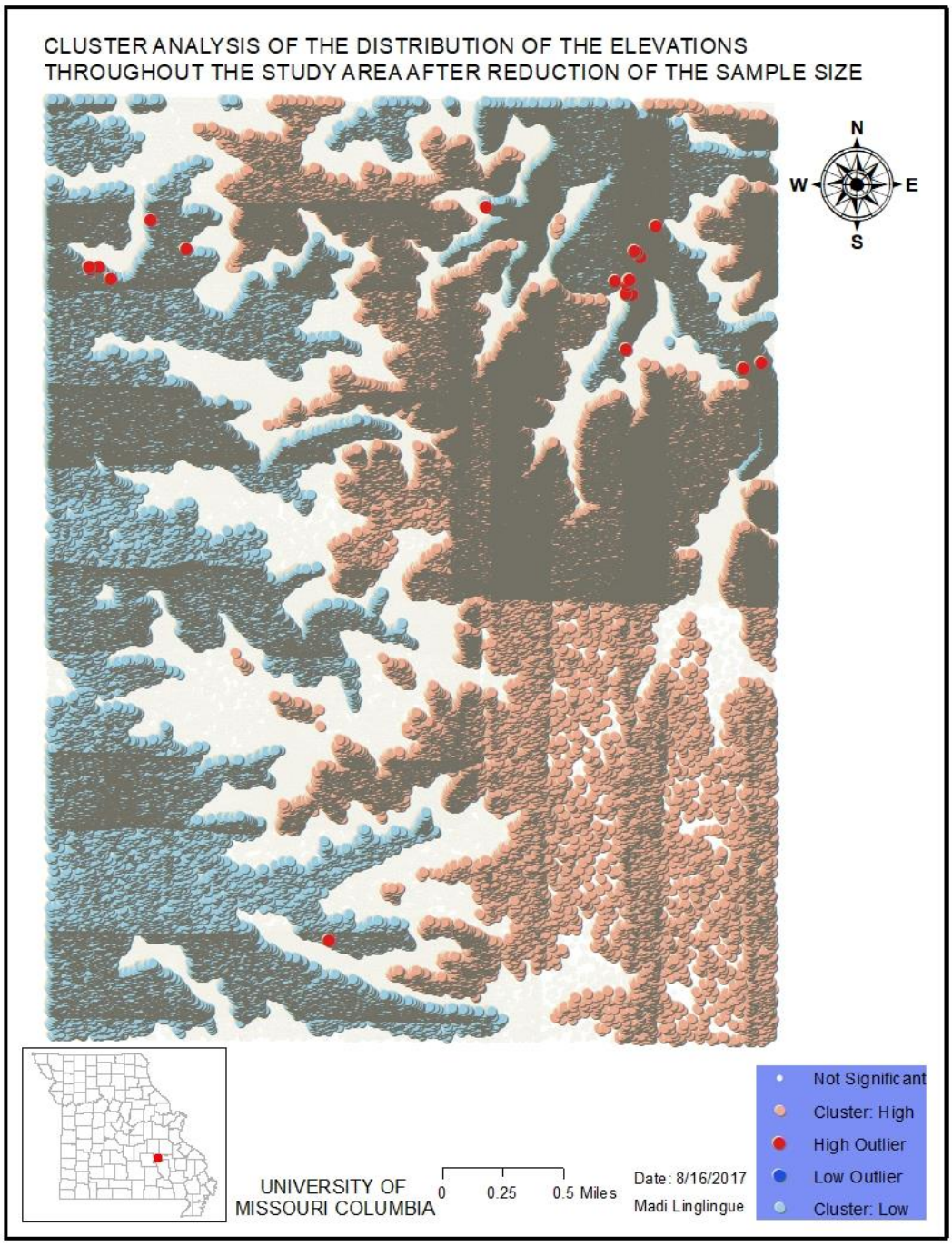

Figure 66: cluster analysis of the elevation values across the study area

Taking advantage of the fact that interpolation methods use the neighboring values in their estimation, a larger dataset than the study area was considered for the processing of the data, from which values for the data of interest were extracted using the clip or extract by polygon tools. Otherwise, interpolation would be affected by edge effect near the borders because the algorithm uses the data inside the study area only.

11. Difficulties

The 3D models did not allow the retrieval of the elevation values for the top and bottom layers derived from the math algebra operation. Subsequently, a statistical t-test was not performed for the 3D analysis. Also, we could not find out how to build the drill sections at scale. The ore body thickness is small before hole depth. So, the orebody might not display well, distinctively from the whole drill profile. We then normalized depths of the drill holes by a factor of 50 and then overlaid the top and bottom surfaces of the lead ore. These surfaces are actually not at the right depth with regard to the drill sections. Another difficulty with the 3D sections is that we did not find a layout to configure outputs as it is in 2D. Consequently, the outputs were exported as pictures and edited in drawing programs.

Chapter 6. CONCLUSION

On a conceptual point of view, the eight interpolation methods studied vary in many ways considering the varied features characterizing and influencing their performances. Quantitative assessments both by the paired t-test and math algebra also showed some differences. The paired t-test concluded that spline and natural neighbor's results were not significantly different from the values generated from the LiDAR scenes. This conclusion was confirmed by the geometric analysis using math algebra which returned that 92% of the respective values did not differ by more than 6 feet from each other, of which more than 82% ranged within 3 feet.

Given the variability of the factors influencing the performance of the interpolation methods, the judicious choice of parameters to meet the optimal performance of a given method is more the realm of art than science. Different outcomes are possible from the same author or among authors. An efficient decision of the method to choose involves a sound knowledge of the math behind the algorithm as well as a knowledge of the region to find the best fit among the many functions available. For example, it makes sense to assume that in such a topographic setting as the Magmont lead mine area, some topographic features follow trends, at least locally. Taking that trend into consideration in the estimation of the elevations must have improved the models' performance. In such situation, universal kriging would have been a good choice with the caution to detrend the data set. Literature review suggests that the trend not be used unless its mathematical expression is known. To generalize, finding the best fit for a region appears complex. It is advisable to consider mixed methods which combine

properties of both simple and complex or univariate and multivariate functions. Today, many machine learning algorithms do well in such combinations (Li and Heap, 2014).

Works cited:

Abzalov, M. 2011. Sampling errors and control of assay data quality in exploration and mining geology, in *Applications and Experiences of Quality Control*. Ed. O. Ivanov. Rijeka, Croatia: InTech. pp 611-644.

Anderson, M. P. and W. W. Woessner. 2015. *Applied Groundwater Modeling: Simulation of Flow and Advective Transport*. 2nd Ed. New York: Academic Press.

Barbulescu, A. 2016. *Studies on time series applications in environmental sciences*. New York, NY: Springer.

Bohling, G. 2005. *Introduction to geostatistics and variogram analysis*. Online https://pdfs.semanticscholar.org/ef33/f1ef327b1b8bcf5e424f9f4c90b51fc78ae5.pdf (Last accessed 10 October 2017).

---. 2005. *Kriging*. Online http://people.ku.edu/~gbohling/cpe940/Kriging.pdf (Last accessed 10 October 2017).

Campbell, J. B. and R. H. Wynne. 2011. *Introduction to remote sensing*. New York: Guilford Press.

Getis,A. and B.N. Boots. 1978. *Models of spatial processes: an approach to the study of point, line and area patterns.* Cambridge: Cambridge University Press.

---. 1988. *Point pattern analysis*. London: Sage.

Goovaerts, P. 1997. *Geostatistics for natural resources evaluation*. Cambridge: Oxford University Press.

Groia, J., J. Badley and A. Jones. 2008. *The aftermath of Bre-X: the industry's reaction to the decision and the lessons we all have learned*. Online http://www.groiaco.com/pdf/The_Aftermath_of_Bre-X_Mar_4-08.pdf (Last Accessed 10 October 2017).

Isaaks,E. H. and R. M. Srivastava. 1989. *An introduction to applied geostatistics*. New York: Oxford University Press.

Ledoux, H. and C. Gold. 2005. An efficient natural neighbour interpolation algorithm for geoscientific modelling, in *Developments in Spatial Data Handling: 11th International Symposium on Spatial Data Handling.* Ed. P. F. Fisher. New York: Springer, pp 97-108.

Li, J. and A. D. Heap. 2014. Spatial interpolation methods applied in the environmental sciences: A review, *Environmental Modelling & Software.* 53: 173-189.

Marjoribanks, R. 2010. *Geological methods in mineral exploration and mining*. New York: Springer.

Robinson, T. P. and G. Matternicht. 2006. Testing performance of spatial interpolation techniques for mapping soil properties, *Computers and Electronics in Agriculture*. 50 (2): 97-108.

Shanbeik, S., P. Afzal, P. Moaefvand and M. Qumarsy. 2013. Comparison between ordinary kriging (OK) and inverse distance weighted (IDW) based on estimation error. Case study: Dardevey iron ore deposit, NE Iran, *Arabian Journal of Geosciences.* 7 (9): 3693–3704.

Trauth, M. and E. Sillmann. 2012. *Matlab and design recipes for earth sciences: How to Collect, Process and Present Geoscientific Information*. New York: Springer.

Watson, D. F. and G. M. Philip. 1985. A refinement of inverse distance weighted interpolation, *Geoprocessing.* 2: 315-327.

Wikle, C. K. and N. Cressie. 2011. *Statistics for spatio-temporal data.* Hoboken, NJ: Wiley.

Zimmerman, D., C. Pavlik, A. Ruggles and M. P. Armstrong. 1999. An experimental comparison of Ordinary and Universal Kriging and Invese Distance Weighting, *Mathematical Geology*. 31 (4): 375-390.